

**Water level history of Lake Turkana, Kenya and hydroclimate variability during the African Humid Period**

BY

CHRISTOPHER ANDREW BLOSZIES  
B.A. University of Chicago, 2008

THESIS

Submitted as partial fulfillment of the requirements  
for the degree of Master of Science in Earth and Environmental Sciences  
in the Graduate College of the  
University of Illinois at Chicago, 2014

Chicago, Illinois

Defense Committee:

Steve Forman, Chair and Advisor

Peter Doran

Neil Sturchio

## ACKNOWLEDGEMENTS

I would like to thank Dr. Steve Forman, my research advisor and friend, without whom this thesis would never have seen the light of day. Thanks mate! My deepest thanks go to members of my thesis committee, Dr. Neil Sturchio and Dr. Peter Doran for advice and direction. I am also grateful to Dr. David Wright and his family for providing support in Nairobi, for introducing me to field work in Africa and for providing perspective on this research. Finally, I would like to thank my friends and family.

Also, this study would not have been possible without the cooperation of Dr. Lisa Hildebrand and Dr. John Shea of Stony Brook University, Stony Brook, New York and the Turkana Basin Institute, Turkana, Kenya for providing logistical support in the field. Also, I would like to acknowledge the help of my field assistants Francis Ekai, James Lokuruka and Paul Lomosingo for helping with field labor, providing laughter, and introducing me to the wonderful Turkana people.

Funds for travel to Kenya were made available with the generous support of the University of Illinois at Chicago, with the Provost's Graduate Research Award and the Bodmer International Travel Award. Additionally, my thanks go to Mr. Rob Knourek and the Knourek Environmental Scholarship for financial support.

Radiocarbon analysis was provided by the Accelerator Mass Spectrometry labs at Seoul National University, South Korea, the University of Arizona, USA and the Illinois State Geological Survey.

For Mary. Thank you for your commitment, patience and sense of humor when faced with perceived lethargy and multiple crises of confidence. Thank you for supporting me and putting up with me through an arduous process. I love you.

## TABLE OF CONTENTS

<u>CHAPTER</u>	<u>PAGE</u>
<b>1. INTRODUCTION .....</b>	<b>1</b>
1.1 Paleoclimate of East Africa .....	1
1.2 Climate and Hydrology of the Lake Turkana Basin.....	6
1.3 Previous studies of Lake Turkana water level .....	11
1.4 Objectives of this Study .....	16
1.5 Organization of Thesis .....	18
<b>2. METHODS AND RESULTS .....</b>	<b>19</b>
2.1 Introduction.....	19
2.2 Materials and Methods .....	19
2.2.1 <i>Field Research Area</i> .....	19
2.2.2 <i>Elevation of relict beaches on the Lake Turkana strand plain</i> .....	21
2.2.3 <i>Radiocarbon dating of mollusks from lacustrine sediments</i> .....	21
2.3 Results .....	23
2.3.1 <i>Geomorphology of the Kalokol strandplain</i> .....	23
2.3.2 <i>Sedimentology, stratigraphy and geochronology of the Kalokol strand plain</i> .....	25
2.3.3 <i>Geomorphology of the Lothagam tombolo</i> .....	32
2.3.4 <i>Lothagam sedimentology, stratigraphy and radiocarbon ages</i> .....	33
<b>3. DISCUSSION .....</b>	<b>37</b>
3.1 Introduction.....	37
3.2 Merging previous Lake Turkana records with results from the western strand plain.....	37
3.3 Lake Turkana water level variability.....	43
3.4 On the potential causes of water level variability for Lake Turkana .....	53
3.4.1 <i>Evidence for overflow to Lake Turkana during the African Humid Period</i> .....	54
3.4.2 <i>Linkages between equatorial SSTs and the African Monsoons</i> .....	61
3.4.3 <i>East African hydroclimate for the past 15 ka reflected in water levels for Lake Turkana</i> .....	64
<b>4. CONCLUSIONS .....</b>	<b>72</b>
4.1 Introduction.....	72
4.2 Review of Findings.....	72
4.2.1 <i>15 to 11 ka</i> .....	73
4.2.2 <i>11 to 8 ka</i> .....	73
4.2.3 <i>8 ka to present</i> .....	74
4.3 Future work.....	76
<b>CITED LITERATURE .....</b>	<b>79</b>
<b>VITA.....</b>	<b>92</b>

## LIST OF TABLES

<u>TABLE</u>		<u>PAGE</u>
I	Radiocarbon ages on shell and fish bones from relict beaches, western shore, Lake Turkana Kenya.....	30
II	Previous ages, rank 1 .....	38
III	Optical ages on littoral sands from Mt. Porr (Forman et al., submitted) .....	39
IV	Previous ages, rank 2 .....	40
V	Previous ages, rank 3 .....	41
VI	Ages on archaeological material .....	42

## LIST OF FIGURES

<u>FIGURE</u>	<u>PAGE</u>
1. Overview of Central and East Africa and seasonal positions of major convergence zones .....	3
2. Overview and topography of the Lake Turkana catchment and associated lake dimensions at present and during the AHP .....	8
3. Location map for Lake Turkana and the western strand plain.....	12
4. Previous water level reconstructions for Lake Turkana .....	14
5. Overview of littoral deposits and sample locations for the western strandplain.....	20
6. Depositional facies for stratigraphic sections in the western strandplain and the Lothagam tombolo .....	26
7. Stratigraphy and sedimentology and associated <sup>14</sup> C ages for exposures on the Kalokol strandplain.....	28
8. Stratigraphy and sedimentology and associated <sup>14</sup> C ages for the Lothagam tombolo.....	34
9. Sedimentary features at Lothagam.....	35
10. Reconstruction of Lake Turkana water levels for the past ca. 15 ka .....	44
11. Various $\delta D_{wax}$ chronologies from East Africa .....	47
12. Various terrestrial runoff proxies for East African lakes.....	53
13. Water level chronologies and constraining ages for lakes adjacent to Lake Turkana. ....	56
14. Equatorial sea surface temperature records .....	63

## LIST OF ABBREVIATIONS

AHP	African Humid Period
AMS	accelerator mass spectrometry
BIT	Branched and Isoprenoidal Tetraether
BP	before present
ca.	circa annum
CAB	Congo Air Boundary
$\delta D_{\text{wax}}$	deuterium / hydrogen in leaf waxes
dGPS	differential Global Positioning System
ENSO	El Niño / Southern Oscillation
GHA	Greater Horn of Africa
H1	Heinrich Event 1
ITCZ	Intertropical Convergence Zone
ka	kiloannum
masl	meters above sea level
OSL	optically stimulated luminescence
SRTM	Shuttle Radar Topography Mission
SST	sea surface temperature
YD	Younger Dryas

## SUMMARY

The present chronology of East African paleoclimate suggests the transitions associated with the African Humid Period (AHP) at ca. 15 and 5 ka were binary and reflect abrupt shifts to stable climate states. Previous studies have indicated water levels for Lake Turkana as relatively unchanging at ~88 to 98 m above present level for the AHP, and infer outflow into the White Nile Basin. This interpretation is reinforced by many proxy-inferences for East African hydroclimate, which suggest ubiquitous wet conditions between ca. 11.5 and 6 cal. ka BP. Also, previous studies suggest that peak water levels for Lake Turkana resulted from increased precipitation delivered by elevated monsoonal rainfall and were regionally amplified by overflow from the adjacent Suguta and Chew Bahir basins. This study presents an intensive sedimentologic and stratigraphic investigation of the western strand plain of Lake Turkana and the Lothagam tombolo. Chronologic control for past water level is provided in part by 17 new AMS  $^{14}\text{C}$  ages on freshwater gastropod and bivalve shells taken from these littoral deposits. These results are combined with previous ages that have been systematically vetted and ranked by certainty and form the basis for this reconstruction. Water level for Lake Turkana may have varied by  $\pm 60$  m, potentially reaching the outlet sill elevation (~455 masl) at ca. 11.3, 10.3, 9.0, 6.3 and 5.1 cal. ka. Other possible high stands are indicated at ca. 13.0, 8.4, 7.6 and 7.0 cal. ka, however it is unknown if these lake stands reached the outlet elevation. Inferences on the source of moisture to sustain these many high stands are based on the isotopic data on leaf wax ( $\delta\text{D}_{\text{wax}}$ ) from lakes Tana, Victoria, Challa and Tanganyika, various metrics of precipitation/runoff for East Africa and associated sea surface temperature (SST) records from the Indian and the Atlantic oceans. A single lake level oscillation to >70 m prior to ca. 12.5 cal. ka is associated

## SUMMARY (continued)

with rising SSTs for the Gulf of Guinea and an expanded West African Monsoon, with precipitation delivered by a more eastward convergence of the Congo Air Boundary (CAB). In turn, multiple water level oscillations, possibly to the outlet sill elevation between 11.5 and 8.5 cal. ka are associated with intervals of elevated Atlantic-derived moisture flux to East Africa, and a zonally variable CAB. After ca. 7.5 cal. ka, water level oscillations may be linked to rising SSTs in the Western Indian Ocean, and rainfall delivered by the East African Monsoon. However, between 7.5 and 5 cal. ka, Atlantic moisture is thought to enhance these transgressions with rainfall from the CAB over the Ethiopian Highlands. Evidence from relict beach landforms supports low lake levels associated with Heinrich Event 1, the Younger Dryas, the 8.2 ka meltwater event and mid-Holocene aridity for East Africa after ca. 4.5 cal. ka. These regressions are attributed to intervals of suppressed SSTs for the Eastern Atlantic Ocean, and limited westerly moisture flux to East Africa. A diverse spatial signal of drying between 6.5 and 4.5 cal. ka is associated with a complex decoupling from Atlantic-derived moisture, reflected in variable water levels for Lake Turkana during this interval. Late Holocene and historic lake level changes of less than 20 m principally reflect precipitation variability linked to SSTs in the Western Indian Ocean, which has been implicated in modulating the strength of the East African Monsoon.

## 1. INTRODUCTION

### 1.1 Paleoclimate of East Africa

The mechanisms of climatic transitions in the tropics for the late-Quaternary are complex, non-linear and spatially variable. The sensitivity of such systems to internal (e.g. sea surface temperature variability) and external (e.g. insolation, anthropogenic effects) perturbations remains poorly understood (Toreti et al., 2013). One outstanding question is the nature and timing of monsoonal variability with a changing global climate from glacial to interglacial conditions and for a “super interglacial” with greenhouse induced warming in the 21<sup>st</sup> century. Further, paleoclimatic proxy records derived from lake sediment cores in the Sub-Sahara and in East Africa indicate tens of meters of water level variability in the past 130 ka (Street-Perrott et al., 1989; Gasse, 2000; Garcin et al., 2007; Tierney et al., 2008; Trauth et al., 2010; Foerster et al., 2012; Garcin et al., 2012; Costa et al., 2014) that exceeds hydrologic variability in the historical record (cf. Lamb, 1966; Butzer, 1971; Nicholson, 1988). These wet periods at ca. 120 to 110 ka, 50 to 45 ka and ~15 to 5 ka BP are inferred from proxies of vegetation cover in the Sahara Desert (Castañeda et al., 2007; Foerster et al., 2012). Proxies for rainfall for East Africa and the Greater Horn of Africa (GHA), suggest a shift from a predominantly wet episode, known as the African Humid Period (AHP), to dry conditions post ca. 5.5 ka (Garcin et al., 2009; Tierney et al., 2011a; Berke et al., 2012b; Foerster et al., 2012). The AHP is a period of elevated water balance for North and East Africa between ca. 5.5 ka and 15 ka, with increased vegetation cover (Castañeda et al., 2007; Damsté et al., 2011), surface water availability (Gasse et al., 2008; Verschuren et al., 2009; Blanchet et al., 2013), lake high stands (Street-Perrott et al., 1989), and hydrologic connectivity of presently endorheic East African lakes (Nyamweru, 1989; Garcin et

al., 2009; Johnson and Malala, 2009). The footprint of wet conditions appears widespread, with expansion to a system of interconnected lakes ca. 12 to 4.5 ka BP in eastern and central Sahara (Ritchie et al., 1985; Kuper and Kröpelin, 2006) and high stands for East African lakes like Victoria (Tierney et al., 2011a; Berke et al., 2012a), Tanganyika (Tierney et al., 2008), Challa (Tierney et al., 2011b), Turkana (Garcin et al., 2012), and former lakes Suguta (Garcin et al., 2009) and Chew-Bahir (see Fig. 1; Grove et al., 1975; Foerster et al., 2012). However, there is uncertainty in the temporal and the spatial variability of wet conditions during this period (Costa et al., 2014), which is limited by the resolution and sensitivity of proxy data to infer hydroclimatic changes. Also, the termination of the AHP is less clear, sometime between 4 and 7 ka, and the subsequent onset of arid conditions for Central and East Africa, with the timing of centennial-scale regression(s) uncertain for many lakes in East Africa (Garcin et al., 2009; Garcin et al., 2012; Junginger and Trauth, 2013; Tierney and deMenocal, 2013; Costa et al., 2014).

The assumed primary climate driver for wet conditions during the AHP and associated high water levels for many of the East African Great Lakes (e.g. Tierney et al., 2008; Berke et al., 2012a; Berke et al., 2012b; Garcin et al., 2012; Tierney and deMenocal, 2013), is the gradient between boreal and austral summer insolation which achieved a maximum at ca. 10 ka (deMenocal et al., 2000a; deMenocal et al., 2000b; Gasse, 2000). Further, gradual changes in peak summer insolation are cited as the initial factor in abrupt changes for African climate; the most recent decline in peak summer insolation at 10° N occurred between ca. 10 ka ( $\sim 450 \text{ W/m}^2$ ) and the present ( $\sim 425 \text{ W/m}^2$ ; Berger and Loutre, 1991). However, the abrupt binary shift from wet to dry is inconsistent with the gradual nature of insolation changes at the equator (Berger et al., 2006; Tierney et al., 2011a; Berke et al., 2012b; Garcin et al., 2012). Thus, other forcing

mechanisms may be associated with this shift to aridity including changes in circulation of high latitude oceans (e.g. Gasse et al., 2008; Verschuren et al., 2009; Chase et al., 2010), significant shifts in sources of precipitation with varying strength of the West and the East African monsoons (e.g. Street-Perrott and Roberts, 1983; Lamb et al., 2000; Tierney et al., 2011b) and vegetation-climate feedbacks (e.g. Ganopolski et al., 1998; Braconnot et al., 1999; Liu et al., 2007; Patricola and Cook, 2007; Hély et al., 2009).

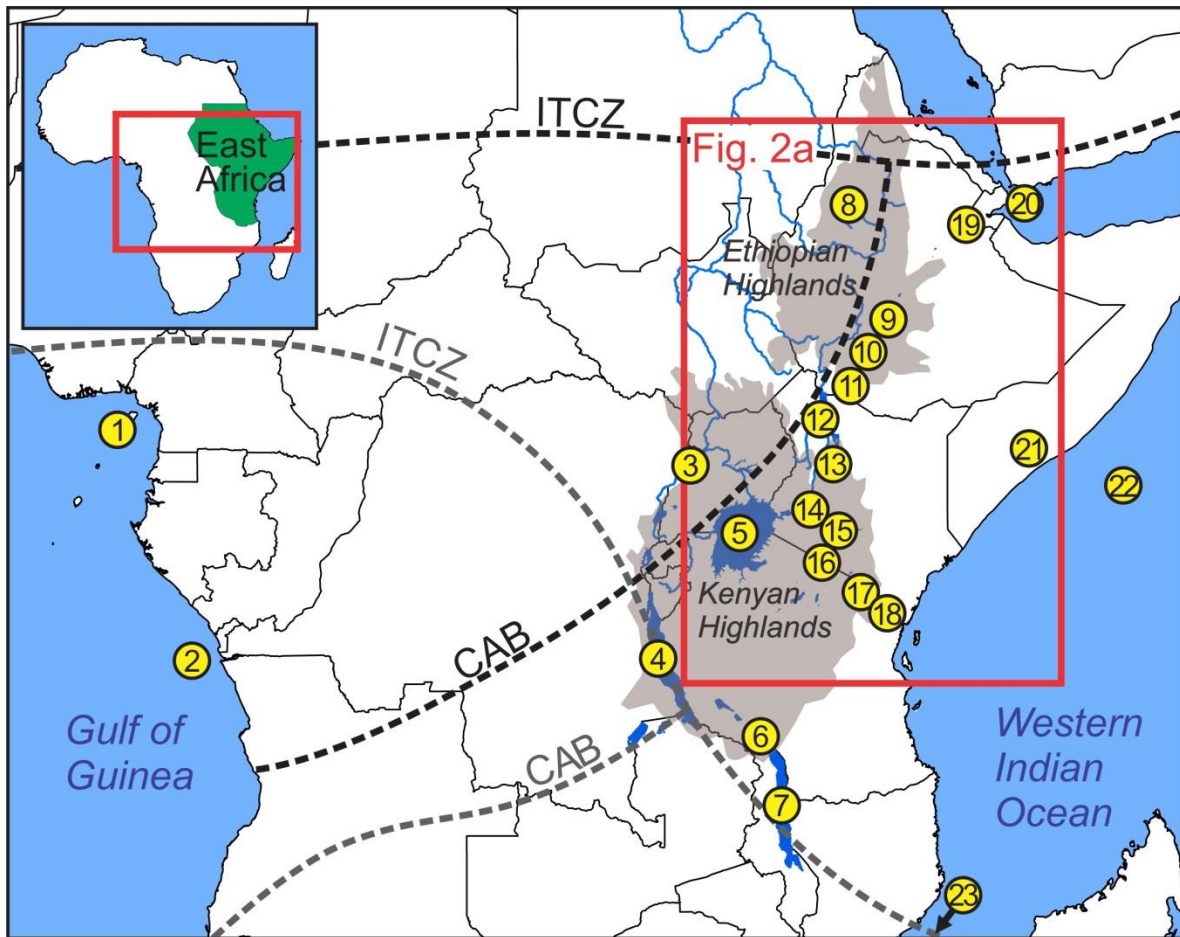


**Figure 1.** Overview of Central and East Africa and seasonal positions of major convergence zones (dashed lines). Position of Intertropical Convergence Zone (ITCZ) and Congo Air Boundary (CAB) for boreal winter (grey) and summer (black) from (Tierney et al., 2011b). The grey shaded areas represents East African topography >1500 masl (SRTM data). Locations of paleoclimate proxies (yellow dots) discussed in the text: (1) Gulf of Guinea SSTs (Weldeab et al., 2007), (2) Congo Basin  $\delta D_{wax}$ , lakes (3) Albert; (4) Tanganyika; (5) Victoria; (6) Masoko; (7) Malawi; (8) Tana; (9) Ziway-Shala; (10) Abaya-Chamo; (11) Chew-Bahir; (12) Turkana, (13) Suguta, (14) Baringo and Bogoria, (15) Nakuru, Elmenteita and Naivasha, (16) Magadi and Natron, (17) Mt. Kilimanjaro ice core (Thompson et al., 2002), lakes (18) Challa, and (19) Abhe, (20) Gulf of Aden  $\delta D_{wax}$ , (21) Mogadishu dunes, (22-23) Western Indian Ocean and Straits of Madagascar SSTs (Bard et al., 1997).

Proxy data and modeling studies for the past 20 ka infer a variable response of biotic and hydrologic systems for the transition into the AHP and the shift toward mid-Holocene aridity (see Fig. 1 for proxy locations). Numerous climatic proxies for East Africa indicate a spatially heterogeneous and temporally diverse response to climate variability associated with global deglaciation (Gasse et al., 2008). Alkenone and coral Mg/Ca records derived for sediment cores from the equatorial Atlantic (Weldeab et al., 2007) and Indian oceans (Bard et al., 1997) infer depressed SSTs associated with Heinrich Event 1 (H1; ca. 18 to 16 ka), and a rise of  $\sim 2^\circ\text{C}$  in the following 2 ka, coeval with an increase in the spatial extent of the East African Monsoon (Gasse, 2000; Gasse et al., 2008). Leaf wax isotopic analyses ( $\delta\text{D}_{\text{wax}}$ ) for a sediment core from the Gulf of Aden indicates the post H1 transition occurred at 14.7 ka, with depletion of 25‰ in  $<0.5$  ka (Tierney and deMenocal, 2013). Hydroclimate proxies ( $\delta\text{D}_{\text{wax}}$  and  $\delta^{13}\text{C}_{\text{wax}}$ ) for sediment record from Lake Tanganyika suggest an onset of wet conditions in  $<0.4$  ka, starting at 15.7 ka,  $\sim 1$  ka earlier than the Gulf of Aden core (Tierney et al., 2010). Lakes Ziway-Shala at ca. 11.2 ka (Gillespie et al., 1983), Lake Turkana between ca. 11.5 and 10.6 ka (Garcin et al., 2012) and paleo-Lake Suguta at ca. 10.9 ka (Garcin et al., 2009; Junginger, 2011) show transgressions associated with the termination of H1.

Interestingly, climate variability associated with the Younger Dryas Chronozone (YD; ca. 12.5 to 11.8 ka) are well expressed across central Africa. Many studies infer drying across equatorial Africa (Schefuß et al., 2005; Weldeab et al., 2005; Garcin et al., 2007; Gasse et al., 2008; Foerster et al., 2012) linked to limited westward penetration of the West African Monsoon (Gasse et al., 2008; Tierney et al., 2011b; Costa et al., 2014) and possible failure of the East African Monsoon (Garcin et al., 2007). Further, reduced monsoonal precipitation during the YD may be linked to suppressed SSTs in the Eastern Atlantic Ocean, with Mg/Ca ratios on forams

suggesting a drop of  $\sim 1$  to  $2^\circ$  C for cores retrieved from the Gulf of Guinea (Weldeab et al., 2005; Weldeab et al., 2007). In turn, several proxies suggest that during the YD the East African Monsoon failed associated with the southward displacement of the mean position of the Intertropical Convergence Zone (ITCZ) at  $\sim 9^\circ$  S (Garcin et al., 2007; Gasse et al., 2008), and perhaps with a penecontemporaneous drops in Indian Ocean SSTs (Bard et al., 1997). Climate models initially forced by insolation and SSTs have reproduced a southward deflection of the ITCZ in response to extra-tropical freshwater influx and coeval dry conditions for sub-tropical regions (Broccoli et al., 2006). This proposed drop in precipitation is reflected in low stands post ca. 12.5 ka for East African lakes like Magadi-Natron (Roberts et al., 1993), Ziway-Shala (Gillespie et al., 1983), and Suguta (Junginger, 2011), and increases of  $\sim 2^\circ$ C in lake surface temperatures for lakes Malawi (Powers et al., 2005), Tanganyika (Tierney et al., 2008), and Victoria (Berke et al., 2012a). Multiple terrestrial and lacustrine proxies also suggest resumption of wet conditions post the YD was abrupt at ca. 11.6 ka and was sustained until ca. 8.5 ka (Foerster et al., 2012; Garcin et al., 2012; Tierney and deMenocal, 2013; Costa et al., 2014).

Climate modeling indicates possible multiple stochastic states between dry and wet conditions between ca. 9 and 4 ka (e.g. Renssen et al., 2003; Renssen et al., 2006). Signals of aridity are observed in various hydroclimate records from sites in the GHA and East Africa between ca. 8.5 and 7.8 ka (Gasse, 2000; Junginger, 2011; Costa et al., 2014), possibly coeval with the 8.2 ka event (Alley et al., 1997). A significant increase in dust flux to the Kilimanjaro ice core record (Thompson et al., 2002), decreases in runoff into Lake Tana (Marshall et al., 2011) and isotopic depletion of  $\delta D_{\text{wax}}$  from lakes Tana (Costa et al., 2014), Challa (Tierney et al., 2011b) and Tanganyika (Tierney et al., 2008), suggest widespread dry conditions.

Aridity appears ubiquitous in East Africa and the GHA post ca. 4.5 ka. However the timing of this transition is variable reflecting differing localities and proxy sensitivities. Analyses of  $\delta D_{\text{wax}}$  from sediment cores indicate appreciable drying between ca. 6 and 4.5 ka for equatorial East African Lakes (e.g. Marshall et al., 2009; Tierney et al., 2010; Tierney et al., 2011b). However,  $\delta D_{\text{wax}}$  records from the Ethiopian Highlands suggest this response may be earlier between ca. 7 and 8 ka, possibly linked to a westward deflection of the Congo Air Boundary (CAB; see below) over the Ethiopian Highlands, potentially driven by reduced flux of Atlantic-derived moisture into the GHA (Costa et al., 2014). Pollen spectra, from sites across equatorial and sub-Saharan Africa often show a smooth transition between states ca. 7 and 4 ka (Kröpelin et al., 2008; Vincens et al., 2010; Amaral et al., 2013). In turn, paleoclimatic proxies from a single archive can yield different indicators of this climate transition; for example, pollen time-series for Lake Tanganyika reveal a gradual climate shift, but  $\delta D_{\text{wax}}$  depict an extremely abrupt hydrological response at ca. 5 ka (Tierney et al., 2010). Thus, the perceived transition from the African Humid Period to late Holocene aridity for some records may be an artifact of chronologic resolution, model assumptions, and the environmental sensitivity of the climate proxy (cf. Ryner et al., 2007; Thomas and Burrough, 2012).

## **1.2 Climate and Hydrology for the Lake Turkana Basin**

The mean annual precipitation in the Turkana Depression is ~200 mm/yr in the 20<sup>th</sup> century (cf. Johnson and Malala, 2009), where >80% occurs between March and November with the biannual passage of the east and the west African monsoons, referred to as the “short” and “long” rains (Avery, 2010). The “long” rains occur from early March to early June and reflect the northward expansion of the ITCZ over East Africa (Fig. 1). The “short” rains are associated with the southward passage of the ITCZ, which may deliver less rainfall than the “long” rains

(Fig. 1), though there is significant interannual variability (Camberlin and Okoola, 2003). These rains usually last from late September to early November, though the onset and termination are variable with rainfall persisting at times into early January (Black et al., 2003; Diro et al., 2011).

Anomalous SSTs in the Western Indian Ocean in the 20<sup>th</sup> and 21<sup>st</sup> centuries may modulate atmospheric convection, the availability of precipitable water for East Africa, and affect the strength and the duration of passage of the East African Monsoon (Goddard and Graham, 1999; Black et al., 2003; Saji and Yamagata, 2003). Warm SSTs (~28 to 29°C) adjacent to East Africa enhance atmospheric convergence and result in increased “short” rain season precipitation across Kenya, Ethiopia and Somalia (Ummenhofer et al., 2009; Becker et al., 2010; Bloszies and Forman, submitted). On balance, cooler SSTs (~ 24 to 25°C) result in a strengthened dry southeasterly Turkana Jet (Kinuthia and Asnani, 1982; Nicholson, 1996), associated with appreciably less vapor transport, often below the threshold for precipitable water (cf. Nicholson, 1996; Nicholson, 2000b; Marchant et al., 2007). Typically, the East African Monsoon in the boreal fall is associated with a relatively cool SSTs in the Western Indian Ocean (~26 to 27°C), with SSTs in the Eastern Indian Ocean comparatively ~2 to 3°C warmer. Another potential significant source of moisture to Lake Turkana is associated with eastward expansion of the West African Monsoon with the zonal advection of Atlantic-derived moisture from the Congo Basin (Nicholson, 2000b; Williams et al., 2012; Costa et al., 2014). In turn, rainfall over the Lake Turkana Basin is associated with a zone of convergence between Indian and Atlantic oceans derived-air masses; an extension of the Congo Air Boundary (see Fig. 1), which is often coincident with a precipitation maximum over central Africa (McGregor and Nieuwolt, 1998; Nicholson, 2000a). The West African Monsoon occurs with the ITCZ passage across west and

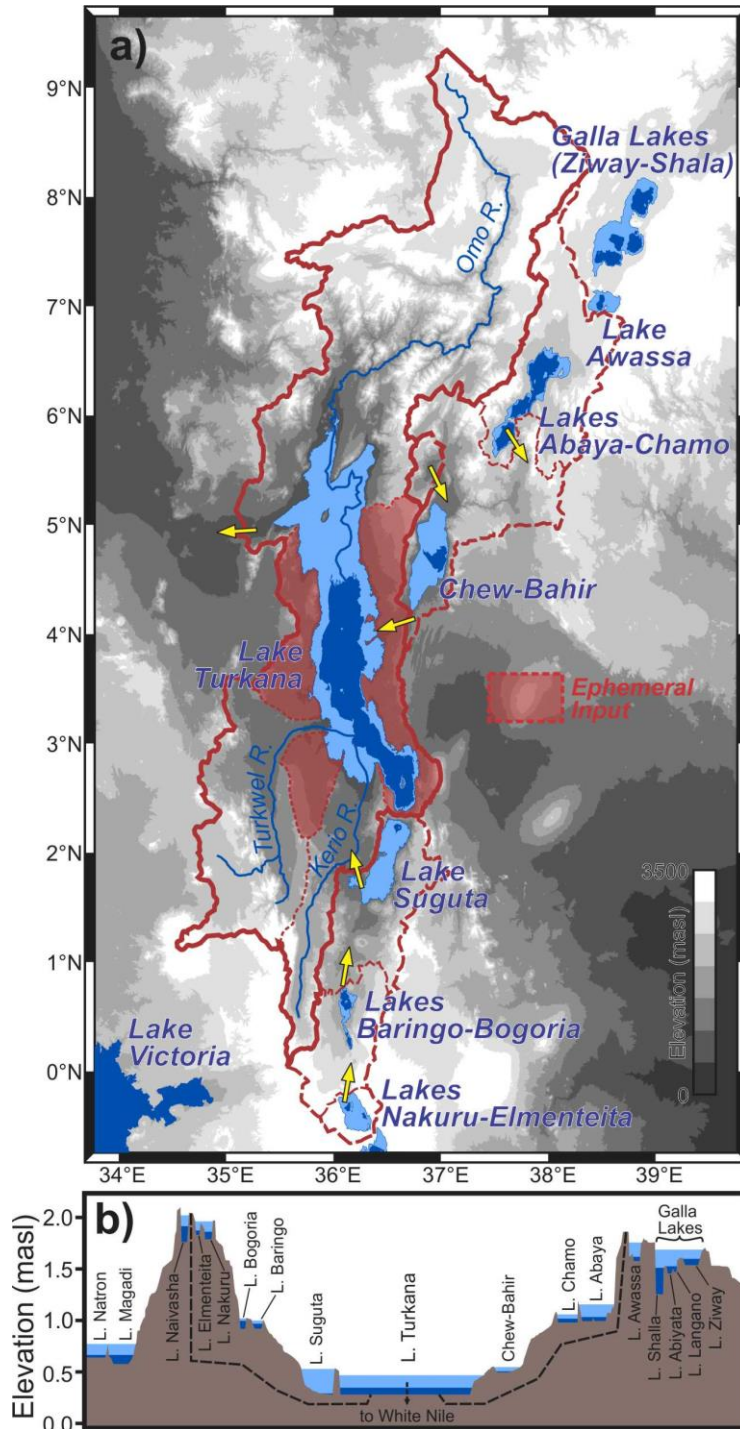


**Figure 2.** Overview and topography of the Lake Turkana catchment and associated lake dimensions at present and during the AHP. **(A)** The current Lake Turkana Basin (solid red line), with Omo, Turkwel and Kerio river sub-basins (dotted red line). Maximum high stands for lakes (light blue), cascading basins (dashed red lines) and locations of basin sills (yellow arrows) from SRTM data and previous studies (Butzer et al., 1972; Grove et al., 1975; Garcin et al., 2009; Foerster et al., 2012; Junginger and Trauth, 2013). Current lake shores from SRTM data and Google Earth (dark blue). **(B)** A cross section of high stand drainage for the AHP, into Lake Turkana, and the White Nile catchment, elevations from Google Earth. Adapted from Junginger and Trauth (2013).

central Africa with precipitation amount modulated apparently by SSTs in the Eastern Indian Ocean (Vizy and Cook, 2001; Giannini et al., 2003; Nicholson, 2008).

The Lake Turkana Basin is located within the East African Rift Valley (Fig. 1). The lake fills the Turkana Depression, an extensional graben formed in the early Miocene within the East African Rift System (Savage and Williamson, 1978), which represents a topographic saddle between the Kenyan and the Ethiopian highlands. Water levels in the 21st century are sustained mostly by discharge from the Omo River, sourced in the Ethiopian Highlands, and the Kerio and Turkwel rivers which drain the Kenyan Highlands. The Omo River catchment ( $\sim 73,000 \text{ km}^2$ ; Fig. 2a) occupies about 50% of the area for the Lake Turkana Basin, and yields  $\sim 90\%$  of the annual water contribution (Avery, 2010), with a modeled discharge of  $526 \pm 132 \text{ m}^3/\text{s}$ , equivalent to  $2.3 \pm 0.6 \text{ m}$  in lake level. Approximately 10% of total discharge is from the Turkwel and Kerio rivers, with a watershed on the northeastern slopes of the Kenyan Highlands (Fig. 2a; Avery, 2010). The remainder of the annual input ( $\sim 10\%$ ) is from direct discharge into Lake Turkana, primarily from ephemeral surface runoff (Fig. 2a). The lake presently has no outlets and the only significant loss of water is by evaporation from the lake surface. The annual estimated evaporation rate is  $2.63 \text{ m}/\text{yr}$ , and is associated with an annual drop in lake level of  $\sim 0.5 \text{ m}$  in the boreal winter (Hopson, 1982; Avery, 2010). The remaining  $\sim 10\%$  of water flow to Lake Turkana is assumed to be from the discharge of the Kerio and Turkwel rivers and ephemeral streams and is equivalent to  $0.13 \text{ m}/\text{yr}$  of lake level (Avery, 2010). The current surface elevation of Lake Turkana of  $362 \text{ masl}$  is derived from satellite altimetry (Velpuri et al., 2012); further discussions of past lake levels will be quantified relative to this zero datum.

Previous research in the Lake Turkana Basin recognize evidence for water levels to rise  $>80 \text{ m}$  above the present lake level in the past ca.  $15 \text{ ka}$  with spill over into the White Nile catchment

(Butzer et al., 1972; Owen et al., 1982; Garcin et al., 2012). The inferred highest outlet elevation for Late Pleistocene/Early Holocene Lake Turkana is at ~455-460 masl, or 95 to 100 m above current lake level; this outlet is located east of the Lotigipi Swamps in the Ilemi Triangle (Fig. 2a). Field surveys in the area of the spill-point observed fluvio-lacustrine sediment facies (e.g. channel-fill and littoral deposits, wave cuts, lake silts) and numerous shells beds at ca. 450 masl, and suggest the area was once covered by slow moving water (Harvey and Grove, 1982). High stands for Lake Turkana in the Late Pleistocene and the Holocene reflect elevated monsoonal precipitation (Junginger and Trauth, 2013; Forman et al., submitted), amplified by additional water input from cascading lake systems to the south and to the northwest (Fig. 2). Studies of water level fluctuations of East African lakes, suggest high stands were episodic prior to ca. 5 ka. At least eight of the presently endorheic lakes may have overflowed at some point during the AHP, which cascade ultimately into Lake Turkana, effectively increasing the catchment surface area of the Lake Turkana Basin from ~148,000 km<sup>2</sup> to ~210,000 km<sup>2</sup>, with much of the additional sub-catchments >1000 masl. Lakes Nakuru and Elmenteita at maximum possible water levels (+180 m above Nakuru, ca. 1940 masl), join to form a single lake which cascades north through the Menengai Crater and into lakes Baringo and Bogoria (Butzer et al., 1972; Dühnforth et al., 2006). The current level of Lake Bogoria (991 masl) is <10 m lower than the sill elevation, with discharge into Lake Bogoria (969 masl); the Lobat Gap (994 masl) represents the sill elevation for Lake Baringo, thus it is possible, yet unclear whether lakes Baringo and Bogoria were previously contiguous (Garcin et al., 2009). The Suguta River flows north from the Lobat Gap to the presently ephemeral Lake Logipi (ca. 275 masl), in the northern Suguta Valley (Junginger and Trauth, 2013). Garcin et al. (2009) took dGPS measurements at this overflow sill and found spillover of paleo-Lake Suguta from the south into the current Kerio River watershed

is possible at >581 masl. In addition, this field survey observed distinct channels underlain by lacustrine silts and clays, which suggests a hydrologic connection was likely (Garcin et al., 2009). At maximum water levels this lake system would add ~23,200 km<sup>2</sup> to the Lake Turkana catchment (Fig. 2; Dühnforth et al., 2006; Garcin et al., 2009; Junginger, 2011). Similarly, lake high stands during the Late-Pleistocene and Holocene for the Chew-Bahir, and lakes Chamo-Abaya potentially linked Lake Turkana to a large hydrologic catchment (~39,000 km<sup>2</sup>) in the central Ethiopian Highlands (Fig. 2). Lakes Abaya (ca. 1180 masl) and Chamo (ca. 1110 masl) are presently 10 m and 15 m below maximum elevation, respectively (Grove et al., 1975; elevation confirmed by DEM). The abandoned outflow from Lake Chamo flows into the Segen River, which in turn flows into the Chew-Bahir Basin (ca. 500 masl; Grove et al., 1975; Foerster et al., 2012). This proposed hydrologic connection between the Chew-Bahir and Lake Turkana is achieved with an increase in water level for paleo-Lake Chew-Bahir to 544 masl (Foerster et al., 2012) and field surveys have observed braided channels and fluvial features flowing toward Lake Turkana (Grove et al., 1975; Foerster et al., 2012).

### **1.3 Previous studies of Lake Turkana water level**

Over the past 50 years, several studies have focused on the geomorphic and stratigraphic record of the strand plain that rises to 100 m above Lake Turkana. Early observations identified low-relief beach features adjacent to the proposed outlet in the Ilemi Triangle near Kibish, Ethiopia (Fig. 3a; Butzer and Thurber, 1969; Butzer et al., 1972; Butzer, 1980). This study inferred water level at ~70 and 90 m between ca. 11.5 to 4 ka, with low stands prior to 11.5 ka and at 10.8, 9.8, 8, 4.4 and post 3.5 ka (Butzer, 1980). The basis for this lake level reconstruction is fifteen <sup>14</sup>C ages on mixed shell assemblages and probably multiple shells of *Unionidae sp.*, *Corbicula sp.* and *Etheria elliptica* (Fig. 4a). Owen et al. (1982) focused on direct <sup>14</sup>C dating of

25 shell samples from the Holocene Galana Boi Formation for a strand plain near the Koobi Fora spit (Fig. 3a). This record also incorporates ages on archeological material, to constrain upper limits for lake levels, and incorporates previously reported ages (Fig. 4b; Butzer and Thurber, 1969; Butzer et al., 1972; and others). This study infers high stands between ca. 11 and 3.8 ka

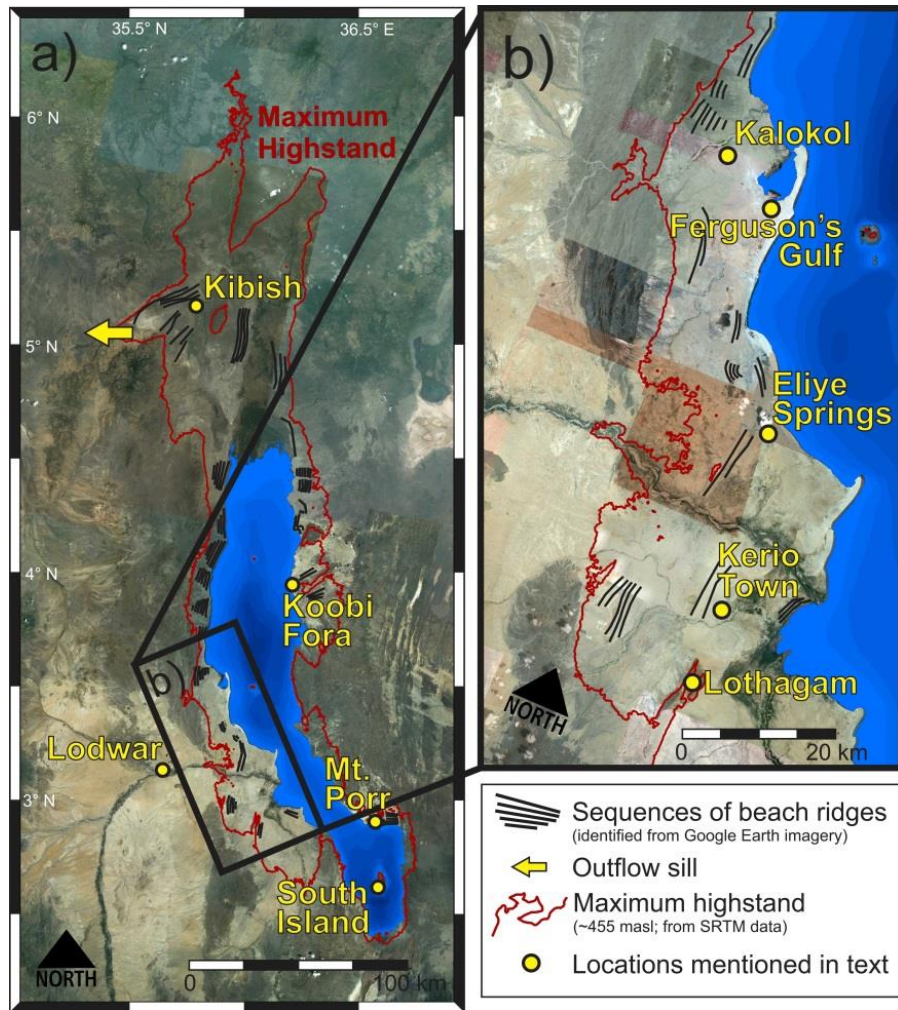


**Figure 3.** Location map for Lake Turkana and the western strand plain. The maximum high stand (red line) is calculated from SRTM data (Farr et al., 2007). (A) Previously sampled strand plains mentioned in text (excepting Lodwar). Outlet sill (yellow arrow) and beach sequences (black lines) identified from Google Earth satellite imagery. (B) The western strand plain with prominent locations referred to in the text.

with potential overflow, interrupted by two distinct low stands at ca. 8 and 4.5 ka. Archeological evidence constrains lake levels to below ~15 m post ca. 2.5 ka and after a high stand of >70 m at ca. 3.9 ka. A 2008 study of the late-Quaternary stratigraphy near Kibish combined and vetted the previous ages from Koobi Fora, Kibish, and Lothagam (see Fig. 3; Brown and Fuller, 2008). This record depicts lake levels >50 m between ca. 13 to 4 ka, with low stands of <30 m at ca. 11.4, 10.6 and 7.9 ka (Fig. 4d; Brown and Fuller, 2008). Inferred high stands are brief, with lake levels greater than the spill elevation at ca. 9.4, 9 and 6.9 ka and sustained high water levels > 75 m until ca. 4 ka (Brown and Fuller, 2008). However, diatom analyses of sediment cores from Lake Turkana indicate a rise in lake level at ca. 6 ka, an abrupt fall at ca. 5 ka and gradual decline post 4.5 ka though the magnitude of these water level changes are unknown (Fig. 4c; Halfman and Johnson, 1988; Johnson et al., 1991; Halfman et al., 1994). Further,  $\delta^{18}\text{O}$  of authigenic calcite from this core suggests qualitatively that lake levels between ca. 3 and 1.2 ka were below present water level (Fig. 4c; Mohammed et al., 1995).

The South Island (Fig. 3a) was the focus of a recent study of relict beaches with  $^{14}\text{C}$  ages on single shell valves. This analysis integrates ages from previous studies of relict strand plains and for the South Island corrects relict beach elevation for regional upwarping (Garcin et al., 2012). The  $^{14}\text{C}$  ages by AMS are from single valves of *Melanoides tuberculata* and *Etheria elliptica* shells with elevation recorded using dGPS-based readings. Sample elevations are adjusted for an uplift rate of ~2 mm/yr, calculated from the elevation and age of the oldest shell in the dataset associated with the maximum high stand (~455 masl). This study extends the lake record by >1 ka and refines the timing and extent of the low stand to ~50 m between ca. 12.6 and 11.7 ka, which is observed in adjacent lake records, and linked to the YD (Fig. 4e; Garcin et al., 2012).

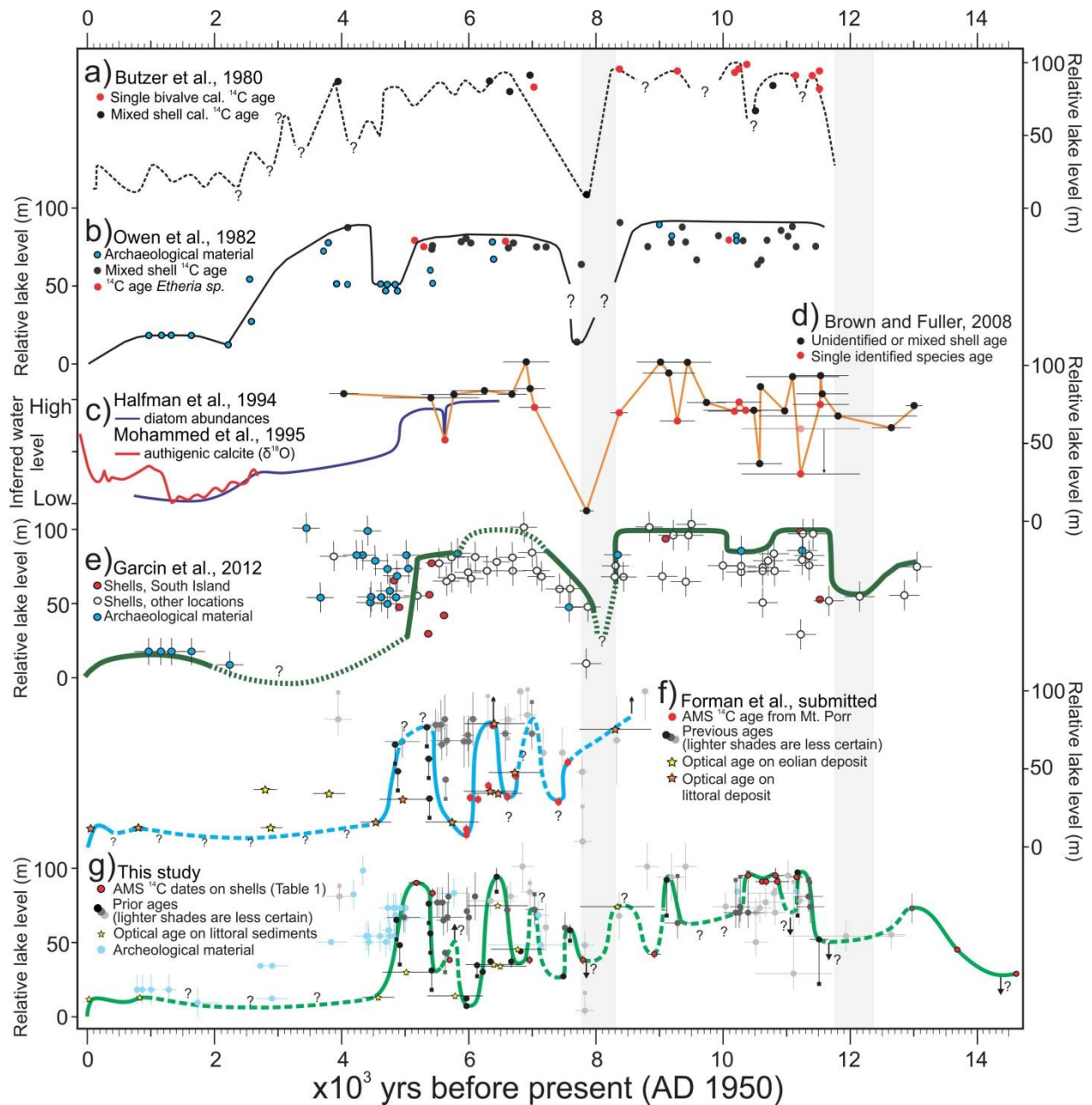


**Figure 4.** Previous water level reconstructions for Lake Turkana: (A) The Kibish strand plain and associated beach features from the Omo Valley (Butzer, 1980), (B) The Koobi Fora area (Owen et al., 1982), (C) Inferred water level from diatom abundances and  $\delta^{18}\text{O}$  analysis of sediment cores (Halfman et al., 1994; Mohammed et al., 1995), (D) Additional sampling from the Kibish area, and other areas around the lake (Brown and Fuller, 2008), (E) the South Island (Garcin et al., 2012). (F) Mt. Porr radiocarbon and optical ages (Forman et al., submitted). (G) This study. All water levels are relative to 362 masl (Velpuri et al., 2012).

Additionally, this record constrains the timing of the regression to late-Holocene and present low water levels, which infers a drop of  $> 60$  m in water level in less than 0.5 ka; the 4 ka high stand is eliminated in this record. A recent reconstruction used optically stimulated luminescence (OSL) dating of littoral sediments and AMS  $^{14}\text{C}$  ages from shells sampled from beach features in the Mt. Porr area (Fig. 3; Forman et al., submitted). Also, this study incorporates  $^{14}\text{C}$  ages on shells from previous studies and ranks the fidelity of these results systematically. This study focuses on the last ca. 9 ka and depicts three water level oscillations of  $>70$  m at ca. 7, 6.4, and 5.4 ka, with low stand conditions post 4.8 ka (Fig. 4f; Forman et al., submitted).

Water level for Lake Turkana has dropped  $\sim 15$  m since AD 1899. A high stand between ca. AD 1850 and 1870 is inferred from the elevation of abandoned deltaic features of the Omo River observed  $\sim 15$  m above the present lake level (Nicholson, 1988). Initial observations by early European explores between AD 1895 and 1902 indicate that lake level was about 20 m higher than today; later gauging from AD 1949 to 1961 (Butzer, 1971) documents the 20<sup>th</sup> century decline in water level. The following the historical low stand of -1 m in AD 1949, water level is bounded between +5 and 0 m (Avery, 2010). Sub-monthly resolved measurements of lake level changes which began in November 1992 reveal a yearly oscillation of  $\sim 0.3$  m, and abrupt transgressions of  $\sim 3$  m in AD 1997 and AD 2007 (Birkett, 1995). Similarly, abrupt rises are inferred in AD 1961 and 1981, reflected in  $\sim 4$  m increases in water level, and coeval with instrumental records of elevated seasonal precipitation for East Africa (Lamb, 1966; Saji et al., 1999).

## 1.4 Objectives of this Study

Well-preserved and minimally vegetated relict beaches occur up to ~100 m from the current shore of Lake Turkana and these landforms are clear geomorphic evidence of changes in lake level. Radiocarbon ages on shells from high elevation beaches indicate a substantially larger water body in the Late Pleistocene to possibly through the middle Holocene compared to today's water level (e.g. Butzer et al., 1972; Butzer, 1980; Harvey and Grove, 1982; Owen et al., 1982; Brown and Fuller, 2008; Garcin et al., 2012; Forman et al., submitted). However, there are troubling disparities among the many reconstructed water levels for Lake Turkana. Central to this thesis is the reconciliation of these discrepancies to establish a lake level chronology which merges previous studies with new data from multiple sampled strand plains of Lake Turkana.

Reconstructions for the YD period are discontinuous and typically reflect inferred low stand conditions, based on limited data (cf. Brown and Fuller, 2008; Garcin et al., 2012). In turn, one study from the Omo River Valley depicts sustained high stand conditions from 11.5 to 8.3 ka (Butzer, 1980); a 2008 study from the same location instead reveals multiple oscillations of > 30 m during the same period (Brown and Fuller, 2008). Also, several previous studies depict a regression from near spillover conditions to <10 m between 8.2 and 7.7 ka, however the timing varies. This regression is not shown in a recent study at Mt. Porr (Forman et al., submitted). Furthermore, interpretations of lake levels for the period between 7.5 and 4 ka are contradictory, and until recently, Lake Turkana was thought to have been near high stand conditions until ca. 3.5 ka (Butzer, 1980; Owen et al., 1982; Brown and Fuller, 2008). A more recent study from South Island reconstructed a rapid fall of ~100 m at ca. 5 ka (Garcin et al., 2012). Finally, Forman et al. (submitted) characterize the period post 7.5 ka as variable, with three oscillations > 70 m, and low lake levels after ca. 5 ka. Therefore, a systematic approach is adopted to

determine the certainty of previous data points in constraining lake level. Together with new data from the Lothagam and Kalokol areas, this dataset constrains a merged lake level history for Lake Turkana which forms the basis for discussions of water level chronology for the past ca. 15 ka. Ultimately, our reconstruction of water level for Lake Turkana will be used to address several questions:

- (1) Did water level for Lake Turkana rapidly recede in response to de-glacial episodes such as H1, the YD and the 8.2 ka North Atlantic cooling event? Cooling in the North Atlantic has been widely implicated in the onset of droughts for Equatorial West and East Africa (Gasse, 2000; Garcin et al., 2007; Gasse et al., 2008; Costa et al., 2014), linked to cool SSTs in adjacent oceanic waters (Bard et al., 1997; Weldeab et al., 2007). However, drought in the Turkana Basin is uncertain for these episodes.
- (2) Apart from possible low stands associated with the 8.2 ka event, was water level high and consistently >80 m during the AHP, from ca. 11.5 to 5.5 ka? Abundant lacustrine and river basin proxies ( $\delta D_{\text{wax}}$ ) suggest this period was universally wet in East Africa (cf. Tierney et al., 2011a; Tierney and deMenocal, 2013), with an increased incursion of Atlantic-derived moisture. However, terrestrial records of surface runoff (Verschuren et al., 2009; Marshall et al., 2011; Foerster et al., 2012), and recent records of water level changes for adjacent lakes (Junginger et al., 2013) characterize this period as profoundly variable.
- (3) What is the timing and nature of the shift from high water levels to present dry conditions associated with the termination of the AHP? Specifically, was there an abrupt and dramatic fall of >90 m in lake level at ca. 5 ka (e.g. Garcin et al., 2012; Forman et al., submitted)? This signal of drying is diversely expressed across sites in East Africa and

specific hydroclimate proxies (Tierney et al., 2011b; Berke et al., 2012a; Forman et al., submitted).

## **1.5 Organization of Thesis**

This thesis is comprised by four chapters. Chapter two describes the field sampling methods, radiocarbon analysis of collected shells and subsequent stratigraphic interpretation in constraining paleo-water levels for Lake Turkana. Chapter three proposes a systematic process for ranking the fidelity of constraining ages and elevations from previous reconstructions of lake level, and presents an amalgamated water level chronology for the past ca. 15 ka. In turn, this section discusses the inferred water level variations from this merged record in context with terrestrial, lacustrine and oceanic paleoclimate proxies from equatorial Africa. Specifically, this chapter debates the causes for water level oscillations, is this related solely to hydroclimate variations, or could an increase in surface hydro-connectivity amplify pluvial events. Chapter four provides a summary of the major conclusions which concern the oceanic and monsoonal controls for water levels for Lake Turkana. Finally, this chapter addresses the potential for future study to refine the hydroclimate variability for the Holocene for the Lake Turkana Basin.

## 2. METHODS AND RESULTS

### 2.1 Introduction

This chapter is divided into two parts which describe the methods and presents the results of a 2012 field study to the western strand plain of Lake Turkana. The first section gives an overview of the western strand plain and the methods to determine the elevation of relict beach landforms. Special consideration is given to the relict Lothagam tombolo, which at elevations above 90 m may provide insight for the timing of lake level high stands. In turn, we review the radiocarbon analysis of sampled lacustrine shells, which provides the age control for this study. The second section explores the sedimentary context of samples and the inferred concomitant lake level, which constrains a chronology of water level changes for the past ca. 15 ka.

### 2.2 Materials and Methods

#### 2.2.1 Field Research Area

The shallow gradient of the western Lake Turkana Basin and the associated relict strand plain is the focus of this study (Fig. 5). This area is broadly delineated as west of the Kerio River, and south of the ephemeral Kalokol Drainage into Ferguson's Gulf, with sequences of relict beaches encountered on the interfluvial flats below the Lothidok Hills. The gradient is variable and ranges from 9.2 m/km adjacent to Kalokol (fig. 5b), to 4.7 m/km near the Turkwel River. Relict beaches are approximately ~100 to 200 m wide, with ~2 to 4m topographic relief (Butzer et al., 1972; Forman et al., submitted). Several beach ridge sequences traced up to 90+ meters above the present shoreline were mapped extensively. The stratigraphy and sedimentology of these littoral deposits were studied and *in situ* lacustrine shells were retrieved for  $^{14}\text{C}$  dating, providing an age on former lake levels. This study focused on relict beaches with elevations between 15 and 40 m, for which there is a paucity of data; this elevation range may constrain previously

hypothesized low stands (Forman et al., submitted). Also, previous investigations indicate at least three high stands of ~90 m, and subsequent falls of >30 m, but the exact timing and magnitude of these events are not well resolved (Owen et al., 1982; Brown and Fuller, 2008; Garcin et al., 2012; Forman et al., submitted). Thus, another clear focus was improving the high stand chronology for Lake Turkana by studying lacustrine sequences between 80 and 105 m above lake level.

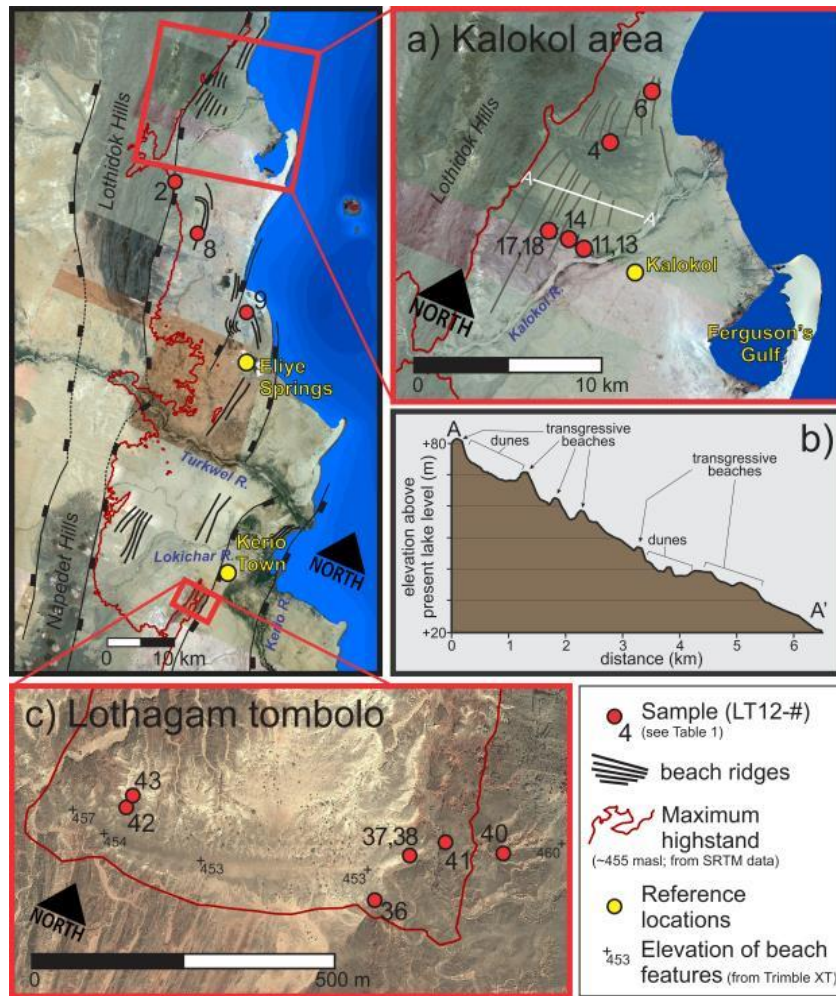


**Figure 5.** Overview of littoral deposits and sample locations for the western strand plain. Major faults, and sampling locations are shown. (A) The Kalokol beach ridge sequence. Sample locations (red dots) and numbers correspond to Table 1. Individual beach ridges in this region were traced up to 2 km and showed no warping or tilting. The A to A' transect is perpendicular to the beach ridges, with elevations from Google Earth. (B) Elevation profile for A to A'. (C) The Lothagam area. Elevation points are from GPS survey (Trimble XT). Satellite imagery from Google Earth.

### 2.2.2 Elevation of relict beaches on the Lake Turkana strand plain

The western strand plain of Lake Turkana extends from 10 to 20 km from the present lakeshore (Fig. 5), and is covered by a sequence of Late Pleistocene to Holocene lacustrine sediments, part of the Galana Boi Formation (Owen et al., 1982; Owen and Renault, 1986). Field research conducted in July and August of 2012 focused on careful mapping of landforms and a detailed sedimentologic assessment of beach deposits. Beach scarps were initially identified using high resolution aerial photography, and samples were recovered from pits dug into beach sediments and sedimentary profiles exposed along cut banks of dry-stream beds. These excavations aid interpretation of contemporaneous lake level based on close examination of *in situ* sediment, and allow for collection of appropriate mollusks for  $^{14}\text{C}$  dating. Elevations were taken using a handheld GPS receiver (Trimble XT) and are post-processed for improved precision using GPS Pathfinder Office 3.10; the final measurement error is approximately  $\pm 2.5$  m.

### 2.2.3 Radiocarbon dating of mollusks from lacustrine sediments

Relict beach ridges around Lake Turkana preserve frequently freshwater mollusks that have been incorporated into littoral gravel and sand (Owen and Renault, 1986; Garcin et al., 2012). In turn, *in situ* sublittoral sand and deeper-water, silt-rich facies often preserve paired bivalves below littoral gravel and sand. There are four primary genera of mollusks identified from relict beaches of Lake Turkana with discrete habitats relative to water depth. Two shallow water species frequently recovered are *Melanooides tuberculata* and *Corbicula fluminalis africana*, which occur at maximum water depths of 2 and 5 m, respectively (Cohen, 1986; Leng et al., 1999; Genner and Michel, 2003; De Kock and Wolmarans, 2007). *Corbicula sp.* is a small (~2 cm) bivalve encountered in water bodies across Africa and is frequently found in fluvial channels

and shallow, turbid water-bodies such as reservoirs (Korniushin, 2004; De Kock and Wolmarans, 2007). *Melanooides tuberculata* is a gastropod which feeds on detritus in muddy portions of a lake or in backshore lagoons in depths <2 m (Genner and Michel, 2003). The other species recovered from Lake Turkana sediments are larger bivalves, the >15-cm-long *Etheria elliptica* and the smaller, and the ~5-to-10-cm long *Unionidae Nitia chefnuexi* (<http://www.mussel-project.net>). *Etheria elliptica* is commonly found in lacustrine muds between 10 and 30 m water depths (Van Bocxlaer and Van Damme, 2009), with *Unionidae sp.* shells typically encountered at depths of <2 m (Abdallah and Barton, 2003).

Our analysis of  $^{14}\text{C}$  ages on mollusks is based on the understanding that shells recovered in littoral facies are reworked from deeper water deposits where these genera lived. Concentrations of genera such as *Corbicula* and *Melanooides* were probably transported *en masse* during storm events, from deeper water depths and deposited with beach gravels and lower shore face sands; thus, in optimal conditions we assume a minimum lag (subdecadal to multidecadal) between death of the organism and its inclusion into beach sediments. We sampled smaller, individual shells or valves to minimize this time lag between mollusk habitat and integration into littoral sediments; shells submitted for radiocarbon analysis were collected systematically from coquinas and have minimal evidence for abrasion and fragmentation, with many bivalves paired, with intact periostracum. We have avoided scrupulously dating sole, highly abraded shells, and unidentifiable shell fragments, which may be reworked from older beach deposits or reflect multiple episodes of reworking.

Radiocarbon ages on shells (Table 1) were determined by accelerator mass spectrometry (AMS). Samples were submitted to the AMS Laboratory at Seoul National University, South Korea (SNU #), the Illinois State Geological Survey, Urbana, Illinois U.S.A. (ISGS #) or to the

Arizona AMS Laboratory at the University of Arizona (AA #). Additionally, several fish bone fragments were submitted to the Arizona AMS Lab (A #), however this result is not included in reconstructions of paleo-lake level, due to the potential for erroneous ages with analysis of bone apatite (cf. Stafford et al., 1990; Collins et al., 2002). All radiocarbon ages have been calendar corrected using Fairbanks et al. (2005), which utilizes a Gaussian probability model calibrated to the tree-ring record and is consistent with previous corrections of  $^{14}\text{C}$  ages (e.g. Forman et al., submitted). Finally, there appears to be no radiocarbon reservoir affect for the Lake Turkana Basin. Biogenic carbonate formed in Lake Turkana appears not to reflect contributions from old carbon from the basin or sediments since the late Holocene. AMS  $^{14}\text{C}$  dating of large ( $> 150 \mu\text{m}$ ) ostracode carapaces extracted from a sediment core from Lake Turkana yielded stratigraphically consistent ages; down core and core top samples yielded ages from 60 to 1200 yr B.P. consistent with variable recovery of core tops (Halfman et al., 1994). In turn, Garcin et al. (2012) dated modern *Melanooides turberculata* which returned  $^{14}\text{C}$  levels which reflect modern atmospheric conditions.

## **2.3 Results**

### *2.3.1 Geomorphology of the Kalokol strand plain*

The relict beach ridges in the Lake Turkana Basin area are exceptionally well preserved and individual strandlines can be traced for  $>10$  km (Fig. 5). These beach ridges directly west of the present shoreline reflect pre-depositional slope, topography, the rate of water level change, and of sediment supply (cf. Thompson and Baedke, 1997). Most of the beach ridges appear to be deposited with initial lake transgression and then subsequent regression; there are noticeable broad, compound relict beaches at  $\sim 80$ ,  $45$ ,  $\sim 40$  to  $38$  and  $<10$  m, potentially reflecting a transgression or a lake still stand (Fig. 5b). These elevations are consistent with previously

studied relict beaches of the Mt. Porr strand plain (Forman et al., submitted), on South Island (Garcin et al., 2012), and other beaches described near the outlet sill (Butzer and Thurber, 1969; Johnson and Malala, 2009).

The relict strand plain nearby the town of Kalokol (Fig. 5a) flanks the western highlands of the Gregory Rift and trends broadly parallel to the dominant axis of rifting ( $\sim N5^{\circ}E$ ; Vétel et al., 2004; McDougall and Brown, 2009). The Lothidok highlands,  $\sim 15$  km to the west of Ferguson's Gulf (Fig. 5), reflect the extensional East African Rift System, with movement along the Lothidok thrust fault (Vétel et al., 2004). Geologic cross-sections perpendicular to the rift axis based on seismic reflection data and geologic maps of the Turkana Basin suggest a single fault block underlies the western strand plain (Vétel et al., 2004; McDougall and Brown, 2009). In turn, the sediments younger than ca. 100 ka which form the Kibish Formation Members III and IV (Owen and Renaut, 1986; Brown and Fuller, 2008; Brown and McDougall, 2011) appear undeformed; the youngest offset formation is older than ca. 100 ka in the lower Kibish Formation (cf. Brown and Fuller, 2008; Gathogo et al., 2008; Brown and McDougall, 2011). Careful scrutiny of remotely sensed images and geomorphic and stratigraphic assessments in the vicinity of these faults document no perceptible vertical offsets of relict beach-ridges. In fact, elevational measurement (derived from SRTM digital elevations) of the crest of single ridges document no measurable altitude changes (within errors) and thus the beach features appear untilted and locally undeformed.

The highest beach ridges studied in the Kalokol sequence are  $\sim 80$  m above the present lake surface, though higher remnant strandlines were observed and traced on satellite imagery. The highest littoral deposits were encountered at  $\sim 89$  m (Fig. 5; sample #2); however erosional scarps (Fig. 6a) observed at  $95 \pm 2$  m are interpreted as wave-cut and associated with washing at the

maximum high stand. There is a distinctive sequence of relict beaches from about 50 to 30 m composed of parallel strandlines trending north-south, with broad (100 to 200 m) crests and a gradient of  $\sim 9.2$  m/km. These strandlines appear to have been deposited with monotonic fall in lake level due to the regular horizontal separation, common gradient, and uniformity of ridges. In contrast, between 40 and 30 m there is a noticeable decrease in gradient to 6 m/km (Fig. 5b) with indistinct strandlines covered by eolian sand, which may reflect a decreased rate in the fall of lake level or stasis. Below 30 m, the slope decreases further to  $\sim 3$  m/km, and large coppice dunes and unconsolidated surface sands indicate a sand sheet may be active closer to the lake shoreline, especially adjacent areas of ephemeral discharge, such as Ferguson's Gulf, and the delta plain for the Turkwel and the Kerio rivers. Also, there is a prominent beach ridge  $< 50$  m wide and  $\sim 2$  m high, anchored by large palm trees and smaller scrub,  $\sim 13$  m above the present lake level. This ridge may reflect the historical high stand of  $\sim 15$  m between AD 1895 and  $\sim 1905$  (Forman et al., submitted). In turn, there is an active beach ridge at the lake margin, capped by linear coastal dunes  $> 8$  m high which extend  $\sim 0.5$  to 2 km from the shoreline, specifically to the south of Ferguson's Gulf.

### 2.2.2 *Sedimentology, stratigraphy and geochronology of the Kalokol strand plain*

The sedimentology of beach ridges for the Kalokol strand plain is well exposed in a series excavations and natural stratigraphic sections (Fig. 6). Underlying many of the littoral deposits at a number of localities are silt-rich deep-water facies below sublittoral sands, which reflects deposition characteristic of lake level transgression. Lacustrine deposits are commonly a silty, very-fine sand to a silty-clay and occur in millimeter-scale planar beds (Fig. 6b). Sublittoral deposits are typically a very well-sorted fine to medium sand with weak or absent bedding, which reflects bioturbation or dewatering (Fig. 6c). The most common depositional facies is a

well sorted, medium to coarse sand that occurs in centimeters to decimeters scale-beds with lenses of 1-to-5 mm-diameter pebbles (Fig. 6d). These beds are inclined  $<10^\circ$  and, include shell concentrations of *Melanooides tuberculata* and *Corbicula fluminalis* and are indicative of upper foreshore environments (Reading, 2009; pp. 175-177). Lower shoreface littoral deposits are comprised of well-sorted fine to medium sands with millimeter-scale planar to sub-planar beds that dip broadly lakeward (Fig. 6e). Sediments interpreted to reflect backshore facies (Fig. 6f) are distinguished by pebble-to-cobble-rich, moderately well sorted coarse sand, probably deposited as wash over during storm events. All Munsell colors are in a dry state.

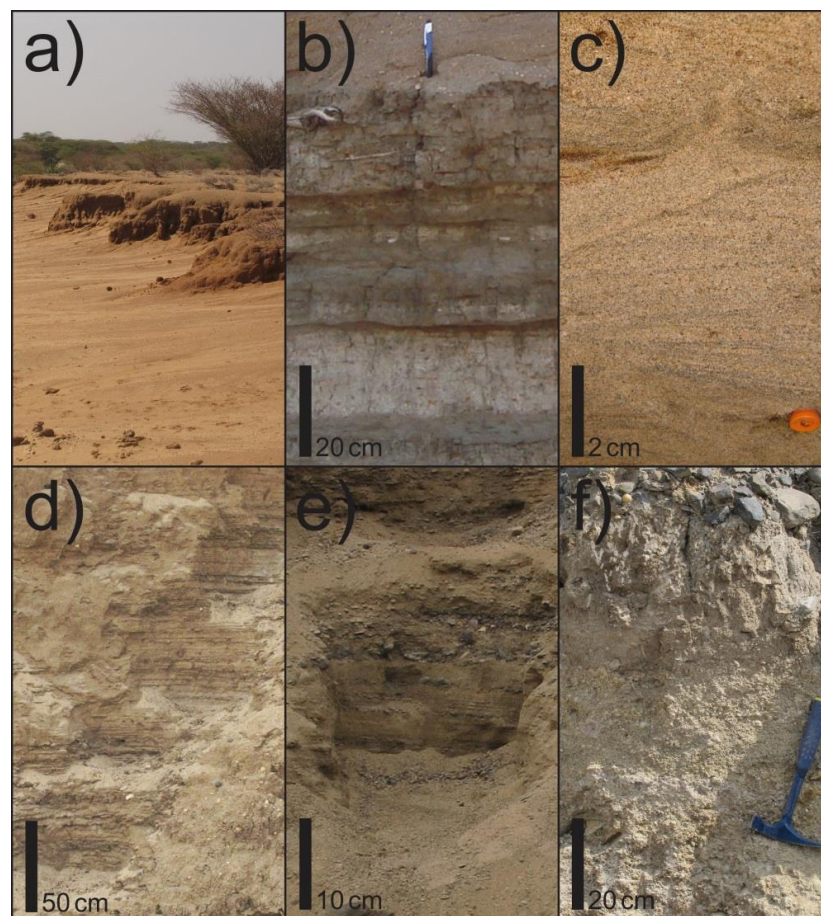


**Figure 6.** Depositional facies for stratigraphic sections in the western strand plain and the Lothagam tombolo. **(A)** Wave-cut notches at 93 m elevation. **(B)** Lacustrine clays and silts, with thin (mm-scale) planar bedding. **(C)** Sublittoral medium to coarse sands. Note dewatering feature apparent in bedding. **(D)** Upper shoreface sands, medium to coarse sands with granular and gravel interbeds. **(E)** Well sorted lower shoreface sands. Interbeds are poorly sorted storm deposits. **(F)** Backshore deposits.

The stratigraphic (Fig. 7) and geochronologic (Table 1) evidence from multiple relict beaches from 89 m to 25 m, on the Kalokol strand plain forms the basis for interpretations of magnitude and timing of oscillations in lake level. The highest beach sediments were encountered at an ephemeral stream bed exposure, at the Ekai Site (89 m), with a basal deposit of >50-cm-thick unit of a very dark grayish-brown (10YR 3/2), well sorted, medium to coarse sand with scattered 1 to 5 cm-diameter rounded pebbles, which reflects an upper foreshore, or backshore environment. This littoral deposit appears to onlap onto adjacent basaltic outcrops. Capping unit 1 is ~1 m thick, moderately sorted, brown (10YR 6/6) medium sand with lens of small pebbles and granules of basalt interpreted as a locally derived colluvial deposit. A single test of *Melanoides tuberculata* taken from littoral sediments in unit 1 gave a  $^{14}\text{C}$  age of  $5.18 \pm 0.12$  cal. ka (SNU12-589).

The Glynnis Site exposes a ~3.5 m section of littoral deposits of various ages within the 81 m beach ridge. The basal unit (1) is extensively pedogenically modified and is a brown (7.5YR 5/4), moderately sorted clay-loam, truncated Btkb horizon, with visible clay cutans and stage 1 filamentous carbonate. Unit 2 is a very well sorted, grayish brown (10YR 5/2) fine sand with discontinuous centimeter-scale horizontal stratification; small sub-millimeter carbonate concretions are common. The top unit (3) is a ~1 m thick, pale brown (10YR 6/3) medium and coarse sand in centimeter-scale beds associated with lower shoreface environment; a single test of *Melanoides tuberculata* from this deposit returned an  $^{14}\text{C}$  age of  $5.43 \pm 0.03$  cal. ka (ISGS-A2782).

The Kalokol strand plain is dissected by multiple ephemeral streams, which provide exposures of relict beach stratigraphy between 50 m and 30 m. The Big Ridge Site is a ~2.5 m vertical section cut into the 45 m beach ridge. The basal unit (1) is a poorly sorted, coarse sand,

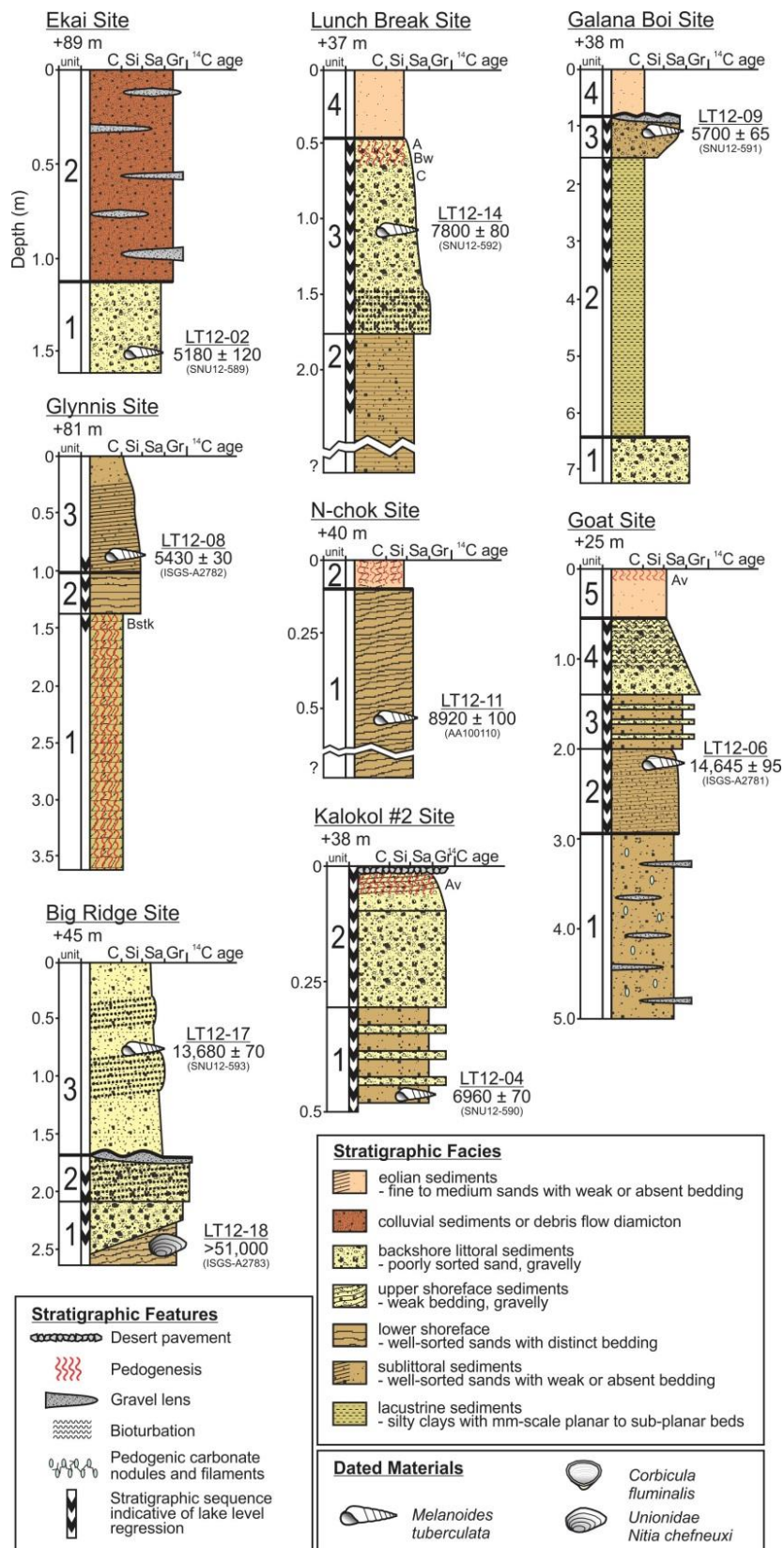


**Figure 7.** Stratigraphy and sedimentology and associated <sup>14</sup>C ages for exposures on the Kalokol strand plain. All elevations are relative to the current water level for Lake Turkana of 362 masl (Velupri et al., 2011).

and crudely stratified, with abundant pebbles and cobbles which reflects upper shoreface deposition. Abundant shells occur in lenses of bedded medium to coarse sands. Unit 2 is a concentration of well-rounded pebbles and cobbles, probably lagged from subjacent unit 1. Unit 3 is a stratified, moderately sorted medium-to-very-coarse sand, with abundant pebbles and a few cobbles reflecting upper shoreface deposition. A valve of *Unionidae Nitia chefnuxi* from Unit 1 yielded a calibrated  $^{14}\text{C}$  age of >51 ka (ISGS-A2783), whereas a test of *Melanooides tuberculata* from Unit 3 returned a  $^{14}\text{C}$  age of  $13.68 \pm 0.07$  cal. ka (SNU12-593).

The Lunch Break Site is a vertical section that exposes littoral deposits in a stream cut-bank ~0.5 km to the east of the Big Ridge Site (Fig. 7). The basal unit 1 is a pale brown (10YR 6/3) massive, slightly silty, well-sorted fine sand with scattered small pebbles reflecting sub-littoral deposition. The overlying unit 2 is a fining upward sequence with stratified pebbly sands in the lower 20 cm and light yellowish brown (10YR6/4) very well sorted, fine to medium sand in the upper 0.5 m; scattered small tests of *Melanooides tuberculata* reflect shore face to back shore deposition. The top of unit 2 has been pedogenically modified with a 20 cm thick brown (10YR5/3) cambic horizon, indicating a period of non-deposition and subaerial exposure. Unconformably overlying this buried soil is a massive, very well sorted, fine-sand (unit 3), probably eolian in origin. This sedimentologic sequence reflects lake transgression and regression, with final burial by a cover sand/sand sheet. A single test of *Melanooides tuberculata* from unit 2, a backshore deposit, yielded a  $^{14}\text{C}$  age of  $7.8 \pm 0.08$  cal. ka (SNU12-592).

An excavation into a relict beach at 40 m elevation, the N-chok Site, exposes a sequence of littoral deposits. The lowermost unit is a brown (10YR5/3), very well-sorted, medium to fine sand with centimeter-scale subhorizontal bedding and some bedding disrupted by dewater structures. This shoreface sand exhibits sub-planar bedding with a down dip  $\sim 10^\circ\text{E}$ , towards the

**Table 1.** Radiocarbon ages on shell and fish bones from relict beaches, western shore, Lake Turkana, Kenya

Field #	Laboratory #	Sample location	Sampled material	$\delta^{13}\text{C}$ (‰)	Laboratory age (yr)	Calendar corrected age (yr) <sup>a</sup>	Depositional environment	Collection elevation (m) <sup>b</sup>	Inferred paleo lake level <sup>b</sup>
LT12-02	SNU12-589	Kolokol	Melanooides	-12.6	4510 ± 60	5180 ± 120	upper foreshore	89.0 ± 2.3	90 ± 2
LT12-04	SNU12-590	Kolokol	Melanooides	-2.69	6100 ± 50	6960 ± 70	upper foreshore	38.0 ± 3.4	38 ± 3
LT12-06	ISGS-A2781	Kolokol	Melanooides	-	12,585 ± 40	14,645 ± 95	upper sublittoral	24.8 ± 2.2	28 ± 2
LT12-08	ISGS-A2782	Kolokol	Melanooides	-	4710 ± 20	5430 ± 30	upper sublittoral	81.0 ± 2.0	83 ± 3
LT12-09	SNU12-591	Kolokol	Melanooides	-5.22	4980 ± 50	5700 ± 65	upper foreshore	37.9 ± 2.3	38 ± 2
LT12-11	AA100110	Kolokol	Melanooides	-1.4	8008 ± 51	8920 ± 100	upper sublittoral	39.5 ± 2	42 ± 3
LT12-14	SNU12-592	Kolokol	Melanooides	-9.55	6970 ± 70	7800 ± 80	upper foreshore	36.7 ± 2.6	38 ± 3
LT12-17	SNU12-593	Kolokol	Melanooides	-2.12	11,830 ± 70	13,680 ± 70	upper foreshore	45.2 ± 2	45 ± 2
LT12-18	ISGS-A2783	Kolokol	Unionidae	-	>51,000	>51,000	lower foreshore	43 ± 2	43 ± 2
LT12-36	SNU12-594	Lothagam	Melanooides	-1.02	9740 ± 70	11,175 ± 75	upper estuarine	93.1 ± 2.7	94 ± 3
LT12-38	A2348	Lothagam	Fish bones	-22.8	5515 ± 30	6300 ± 20	upper foreshore	96.4 ± 2.3	96 ± 2
LT12-40	SNU12-595	Lothagam	Melanooides	-1.96	9390 ± 70	10,610 ± 95	upper foreshore	91.3 ± 2.3	91 ± 2
LT12-41	SNU12-596	Lothagam	Etheria	1.66	9530 ± 60	10,830 ± 140	lacustrine	84.3 ± 3	90-100
LT12-42a	SNU12-597	Lothagam	Melanooides	-2.07	9430 ± 70	10,670 ± 110	upper foreshore	91.3 ± 2.6	91 ± 3
LT12-42b	SNU12-598	Lothagam	Corbicula	-20.22	9540 ± 100	10,850 ± 190	upper foreshore	91.3 ± 2.6	91 ± 3
LT12-43	SNU12-599	Lothagam	Melanooides	1.26	9230 ± 60	10,395 ± 100	sublittoral	92.0 ± 2.2	95 ± 2
LT12-47b	ISGS-A2784	Kalokol	Beach Rock	-	25,110 ± 180	(>) 30,200 ± 290	littoral	144 ± 2	<144

<sup>a</sup>Calendar corrected from <http://radiocarbon.ldeo.columbia.edu/cgi-bin/radcarbcal> (Fairbanks et al., 2005)

<sup>b</sup>Elevation from current lake surface elevation of 362 masl (Velpuri et al., 2011)

present lakeshore. Overlying this littoral sand is a massive, very well-sorted, fine sand, similar to Unit 3 at the Lunch Break Site, which is probably an eolian cover sand. A single *Melanooides tuberculata* shell from ~0.5 m below the beach ridge surface yielded a  $^{14}\text{C}$  age of  $8.92 \pm 0.1$  cal. ka (AA100110). The Kalokol #2 Site also exposes a littoral sequence with abundant shells. This site is characterized by a coarsening upward sequence, with stratified, poorly sorted coarse sand with abundant pebbles transitioning to a moderately well sorted medium to coarse sand; this sequence reflects lower shoreface to backshore deposition. A single *Melanooides tuberculata* shell from the lower shoreface sediments gave a  $^{14}\text{C}$  age of  $6.96 \pm 0.07$  cal. ka (SNU12-590).

At the south margin of the Kalokol strand plain, near Eliye Springs, the Galana Boi Site at 38 m featured steep badlands topography, dissected fluvially, with little vegetative cover. A ~7 m section exposes a variety of lacustrine sediments. The bottom unit (1) is poorly sorted gravel with an overlying ~ 6-m-thick, mica-rich, stratified silt and fine sand (unit 2). The section is capped by a 20 cm thick, poorly sorted, gravelly-sand with abundant shells and in places subsequently buried by very well sorted fine sand which reflects a sand sheet deposit. This

sedimentologic sequence reflects regression with the lower littoral gravels (unit 1), transgression with the deposition of stratified silt and sand (unit 2) and finally transgression with the deposition of unit 3 gravels. A *Melanoides tuberculata* shell from unit 2 gave a  $^{14}\text{C}$  age of  $5.7 \pm 0.07$  cal. ka (SNU12-591) dates the last transgression.

The surface expression of relict beaches between 30 and 10 m elevation is muted with burial by a ubiquitous eolian sand, though littoral deposits are well exposed in stream bank sections. At 25 m, the Goat Site is a ~5 m high, south-facing exposure eroded at the banks of a seasonal river. The basal unit is a ~2 m thick, greyish gray (Gley 1 5/10Y), very well sorted medium sand with lenses of scattered 1 to 3 cm diameter pebbles and reflects sub-littoral deposition. This unit also contains common authigenic carbonate nodules, 1 to 4 cm in diameter; the top contact with Unit 2 is abrupt. Unit 2 is a very well sorted, medium to fine sand with scattered small rounded pebbles, and 1 to 5 millimeter-scale beds with distinctive variations in color from a very dark grey (10YR3/1) to a light yellowish brown (10YR6/4). This unit also contains lenses of coarse sand and pebbles with well-preserved shells and indicative of lower foreshore environments. Unit 3 is composed of medium to coarse sands, with 10 to 20 cm beds of very coarse sands with abundant pebbles and is an upper shoreface deposit. Unit 4 is a fining upward sequence from a very coarse, poorly sorted sand with abundant pebbles to a loose medium sand and reflects backshore deposition with possible bioturbation in the top 60 cm. The capping unit is distinctly eolian: a massive very fine to fine sand with translocated silt. A single *Melanoides tuberculata* shell from unit 2 in the sub-littoral facies yielded a  $^{14}\text{C}$  age of  $14.6 \pm 0.10$  cal. ka (ISGS-A2781; Fig. 7).

### 2.2.3 *Geomorphology of the Lothagam tombolo*

The Lothagam highlands (see Fig. 5) represent an uplifted and tilted fault block, which reflects Mio-Pliocene movement along the Lothagam normal fault (McDougall and Feibel, 1999; McDougall and Brown, 2009). The result is a parallel set of basaltic ridges >140 m above the present lake level, ~10 km to the southwest of the present lakeshore; these highlands form a drainage boundary between the Kerio River to the east and the Lochikar River to the north (see Fig. 5; McDougall and Feibel, 1999; Vétel et al., 2004). Littoral deposits at Lothagam trend broadly east to west (~N80°W) and form a prominent paleo- tombolo (Feibel, 2003). The tombolo is approximately 500 m long, and 200 m wide and the eastern margin widens to >300 m with attachment directly to the basaltic bedrock below Lothagam Hill; the western margin is dissected by ephemeral fluvial discharge which exposes the tombolo stratigraphy. The northern and southern sides of this paleo-tombolo slope away from the ridge with average gradients of 36 m/km and 11 m/km respectively. The elevation of the top of the Lothagam tombolo is consistently  $92 \pm 3$  m (Fig. 5c), and rises slightly to  $96 \pm 2$  m with attachment to the eastern Lothagam ridge; the tombolo potentially reflects a sustained period of littoral deposition at the maximum high stand for Lake Turkana. Similar to other relict beach ridges associated with high stand deposition, a layer of rounded pebbles, 2 to 5 cm in length (see Fig. 9c) covers the upper surface of the tombolo. These basaltic pebbles were observed up to  $102 \pm 3$  m on the talus slope of the eastern ridge of the Lothagam Highlands and potentially reflect a maximum elevation limit for wave washing for lake high stands.

The littoral deposits at Lothagam do not appear to be altered tectonically or warped. The Mio-Pliocene sedimentary bedrock at Lothagam is covered by late Pliocene basaltic flows, which are faulted and tilted >30°W (McDougall and Feibel, 1999; Feibel, 2003); these strata

represent the youngest offset beds (McDougall and Brown, 2009). Whereas recent structural studies have inferred ongoing fault movement along the Lothagam normal fault (see Fig. 5), there appears to be no tilting to the flat surface of the tombolo, and coquinas observed on the southern side of the ridge are flat lying. Absolute elevation changes appear minimal: measured elevations from the tombolo surface of  $92 \pm 3$  m are consistent with an elevation of 94 m for the spill point for Lake Turkana (Harvey and Grove, 1982).

### 2.2.3 *Lothagam sedimentology, stratigraphy and radiocarbon ages*

The stratigraphy of the Lothagam tombolo differs slightly from other sites on the western strand plain and provides insight into sedimentation and at the maximum water level for Lake Turkana (Fig. 8). The depositional structure of the tombolo is relatively consistent across multiple natural exposures: deep water lacustrine silts are 2 to 5 m below medium sublittoral sands, and medium to very-coarse littoral sands, covered by a layer of rounded pebbles. The lacustrine sediments are diatomaceous, typically a silt to very-fine sand, and interbedded with cm-scale beds of granules exposed in the fluvial cut bank at the Paired Bivalve Site (84 m). These facies contain numerous *in situ* paired *Etheria elliptica*, many in vertical position which indicates a thanatocoenosis. A single *Etheria elliptica* valve from this facies yielded the  $^{14}\text{C}$  age of  $10.8 \pm 0.14$  cal. ka (SNU12-596). Based on the habitat requirement of this taxon (Van Bocxlaer and Van Damme, 2009) and associated sedimentologic features, deposition occurred in a deep water environment ( $> 10$  m), with associated lake level  $>90$  m.

At Lothagam, sub-littoral deposits overly lacustrine sediments, and this contact is exposed at ~2 m depth at the Tombolo West Site (Fig. 8). Sub-littoral sediments are composed of a very well sorted fine to medium sand, rich in mafic minerals; thin cm-scale interbeds of granules and

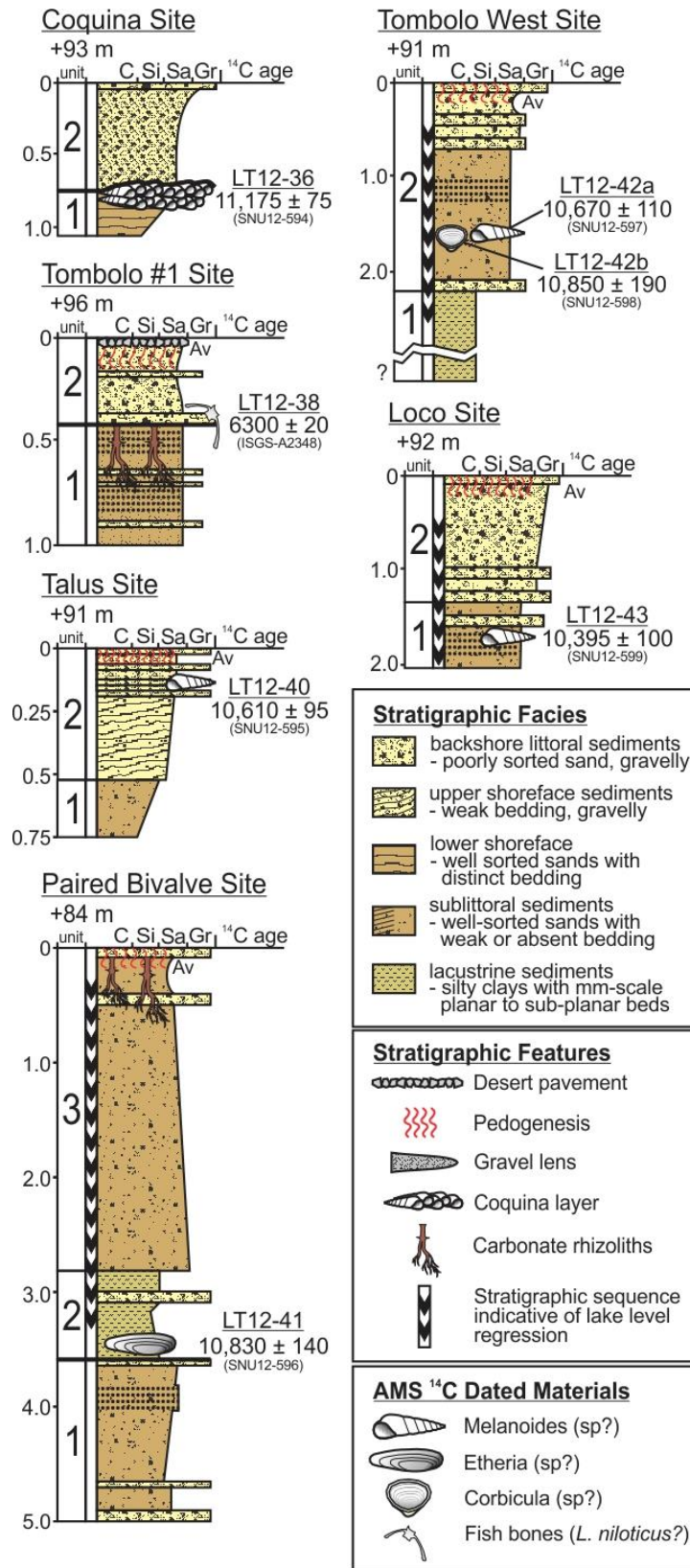


**Figure 8.** Stratigraphy and sedimentology and associated <sup>14</sup>C ages for the Lothagam tombolo. All elevations are relative to the current water level for Lake Turkana of 362 masl (Velupri et al., 2011).

1 to 2 cm pebbles are common in the upper portion of these sands, which may reflect storm deposits as lake level fell. There are prominent carbonate rhizoliths in the top 20 to 40 cm of some sub-littoral and littoral deposits (Fig. 9a) in exposures on the north side of the tombolo, which suggests a period of subaerial exposure with woody vegetation, post regression. Single *Melanooides tuberculata* and *Corbicula fluminalis africana* shells taken from sub-littoral sands, below the interbedded layers returned  $^{14}\text{C}$  ages of  $10.67 \pm 0.11$  cal. ka (SNU12-597) and  $10.85 \pm 0.19$  cal. ka (SNU12-598), respectively. A *Melanooides tuberculata* shell taken from the granular interbed at the adjacent Loco Site (92 m) returned a  $^{14}\text{C}$  age of  $10.4 \pm 0.1$  cal. ka (SNU12-599). At the southerly face of the tombolo, a strongly lithified ~2 to 5 cm thick coquina (Fig. 9b) crops out at 92 m, above the sub-littoral sands, approximately 1 to 2 m below the surface of the

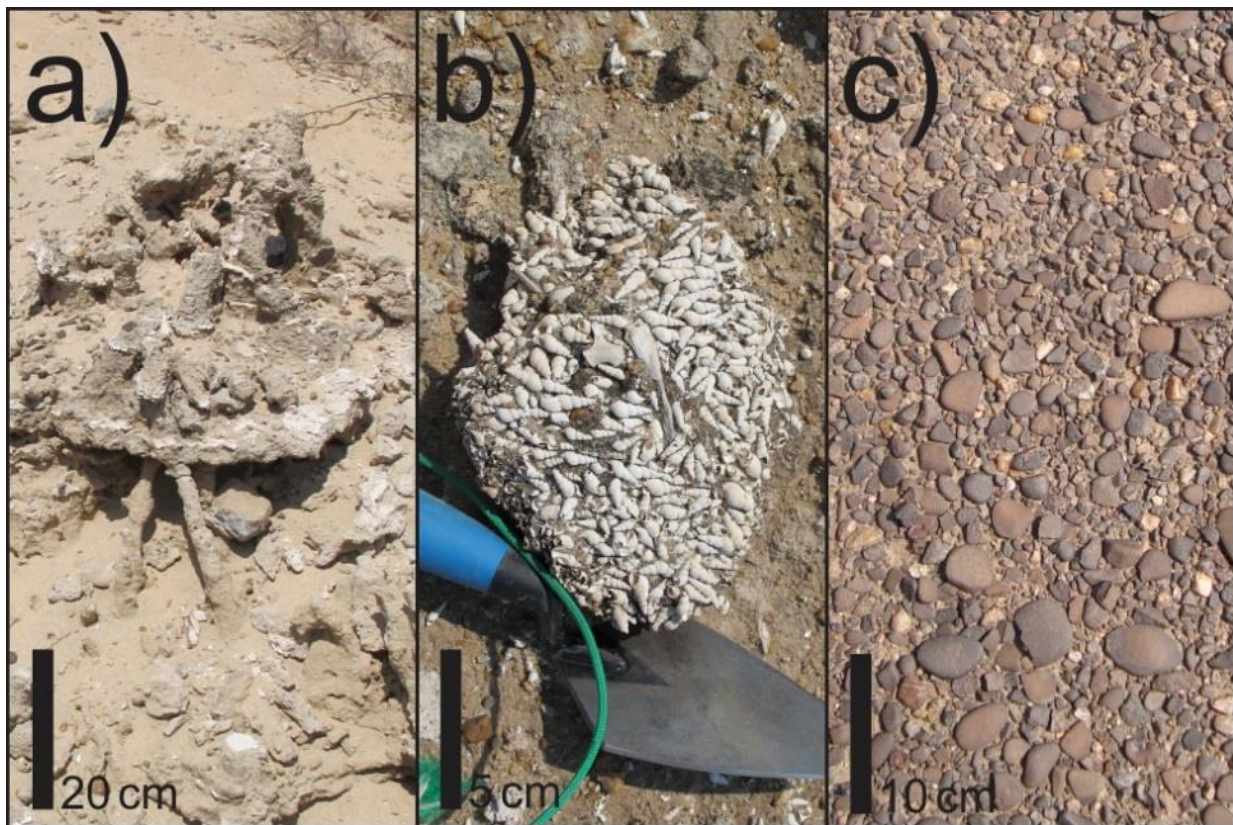


**Figure 9.** Sedimentary features at Lothagam. (A) Carbonate rhizoliths at Lothagam. (B) *Melanooides tuberculata* coquina at Lothagam. (C) Rounded pebbles of tombolo surface.

tombolo. The coquina may reflect a low energy back shore environment on the lee side of the tombolo during a lake high stand. A *Melanooides tuberculata* shell from the coquina produced a  $^{14}\text{C}$  age of  $11.2 \pm 0.08$  cal. ka (SNU12-594).

The upper most deposit across the relict tombolo are moderately well sorted medium to coarse stratified sands with varying quantities of pebbles and cobbles (Figs. 6d and 6e) and reflect shore face environments. Capping the upper shoreface deposits is layer of rounded 2 to 5 cm diameter pebbles, which may reflect a backshore, shingle beach deposit (Fig. 9c). A single *Melanooides tuberculata* shell taken from a gravel layer, ~20 cm below the tombolo surface, at the Talus Site (91 m) gave a  $^{14}\text{C}$  age of  $10.61 \pm 0.1$  cal. ka (SNU12-595). In addition, fish bones (*Lates niloticus?*) taken from imbricated gravels ~0.4 m below the relict tombolo surface on the northern facing Tombolo #1 Site at 96 m, gave an  $^{14}\text{C}$  age of ca. 6.3 cal. ka (ISGS-A2348). We question the fidelity of this radiocarbon age on fish bones due to the hot, arid environment of the Turkana Basin; thus this age is not included in the final inferred lake level reconstruction. However, this evidence does imply sustained water levels at this elevation, and repeated littoral deposition at the transgressive limit.

### 3. DISCUSSION

#### 3.1 Introduction

This chapter contains two sections which presents and interprets a proposed chronology of water level oscillations for Lake Turkana for the past ca. 14.5 ka. The first section evaluates the certitude of prior  $^{14}\text{C}$  ages on lacustrine shells to provide credible age/elevation control on relict beaches. These previous results are merged with data from this study to render a unified dataset which constrains the timing and elevation of penecontemporaneous lake level. This dataset forms the basis for a reconstruction of water levels for Lake Turkana, which depicts more than five oscillations of >70 m prior to ca. 4.5 ka. The second section discusses the potential causes for lake level variability. Possible changes are inferred in moisture sources from the West African and the East African monsoons; fluctuations in the African monsoons may result from changes in SSTs for the Eastern Atlantic and Western Indian oceans (Lamb et al., 2000; Abram et al., 2009; Tierney et al., 2011b; Tierney and deMenocal, 2013). In turn, higher lake level may reflect increased contributions from the Ethiopian and Kenyan Highlands during the AHP (cf. Garcin et al., 2009; Junginger et al., 2013).

#### 3.2 Merging previous Lake Turkana records with results from the western strand plain

The elevation of paleo-lake levels and associated calendar-corrected  $^{14}\text{C}$  ages from the western strand plain is combined with previously reported  $^{14}\text{C}$  ages for lacustrine deposits from other areas surrounding Lake Turkana. However, the reliability of the ages is ranked from 1 to 3, with 1 considered the most reliable with a  $^{14}\text{C}$  age by AMS analysis and associated with a direct elevation measurement (Table 2). Further, optical ages with direct dating of littoral sands are considered possible indicators of contemporary lake level and are considered supportive data for

**Table 2.** Previous ages, rank 1

Sample location	Reference	Sample elevation (m) <sup>a</sup>	Elevation correction & error (m)	Sample <sup>14</sup> C age (yr BP)	Calendar age (yr BP) <sup>b</sup>	Material dated
South Island	Garcin et al., 2012	53	+12 (1)	4330 ± 30	4870 ± 30	<i>Melanoides</i>
South Island	Garcin et al., 2012	36	+12 (1)	4370 ± 35	4920 ± 60	<i>Melanoides</i>
South Island	Garcin et al., 2012	64	+12 (1)	4645 ± 35	5375 ± 55	<i>Melanoides</i>
South Island	Garcin et al., 2012	44	+12 (1)	4680 ± 35	5405 ± 60	<i>Melanoides</i>
South Island	Garcin et al., 2012	19	+12 (1)	4695 ± 35	5420 ± 70	<i>Melanoides</i>
Mt. Porr	Forman et al., submitted	13	-1 (1)	5145 ± 20	5960 ± 15	<i>Corbicula</i>
Mt. Porr	Forman et al., submitted	9	-2 (2)	5220 ± 50	5965 ± 60	<i>Melanoides</i>
Mt. Porr	Forman et al., submitted	30	+4 (3)	5340 ± 50	6135 ± 80	<i>Corbicula</i>
Mt. Porr	Forman et al., submitted	29	-1 (1)	5465 ± 20	6275 ± 15	<i>Corbicula</i>
Mt. Porr	Forman et al., submitted	37	-1 (1)	5560 ± 50	6340 ± 50	<i>Melanoides</i>
Mt. Porr	Forman et al., submitted	75	+18 (8)	5565 ± 20	6440 ± 25	<i>Etheria sp.</i>
Mt. Porr	Forman et al., submitted	30	+6 (4)	5860 ± 60	6670 ± 70	<i>Corbicula</i>
Mt. Porr	Forman et al., submitted	45	-1 (1)	5990 ± 20	6820 ± 35	<i>Melanoides</i>
Mt. Porr	Forman et al., submitted	28	-1 (1)	6600 ± 50	7490 ± 45	<i>Melanoides</i>
Mt. Porr	Forman et al., submitted	55	+3 (4)	6750 ± 25	7600 ± 20	<i>Melanoides</i>
South Island	Garcin et al., 2012	69	+23 (1)	8180 ± 45	9115 ± 75	<i>Melanoides</i>
South Island	Garcin et al., 2012	69	+28 (1)	9740 ± 50	11,180 ± 45	<i>Etheria Elliptica</i>
South Island	Garcin et al., 2012	23	+29 (1)	10,025 ± 55	11,510 ± 150	<i>Melanoides</i>

<sup>a</sup>Elevation from 2008 lake surface elevation of 362 masl (Velpuri et al., 2011).

<sup>b</sup>Calendar corrected from <http://radiocarbon.ldeo.columbia.edu/cgi-bin/radcarbcal>; Fairbanks et al. (2005).

<sup>c</sup>Optical ages expressed in years before 1950

lake level interpretation (Table 3; Forman et al., submitted). A ranking of 2 indicates a conventional <sup>14</sup>C age on large bivalve species of *Etheria sp.* or *Unionidae sp.* (Table 4); probably the most accurate <sup>14</sup>C ages prior to the advent of AMS dating because either a sole valve or 2 to 4 valves were sufficient mass for dating. However, it is difficult to discern if the shells were associated with deep-water facies, sublittoral or reworked into littoral sediments and thus uncertainty remains on the inferred water level. Lastly, a ranking of 3 indicates a conventional <sup>14</sup>C age on bulk mixed shells assemblages with species unidentified and less accurate associated elevation (Table 5). The earliest studies of Butzer et al. (1972), Butzer (1980) and Owen et al. (1982) used conventional <sup>14</sup>C dating, which necessitated the analysis of tens of grams of shell, and thus a potential mixture of shells of various ages. Recent studies of relict beaches in Canadian coastal environments has resolved highly divergent <sup>14</sup>C ages by conventional assays by

**Table 3.** Optical ages on littoral sands from Mt. Porr (Forman et al., submitted)

Elevation & error (m)	Optical age (yr) <sup>a</sup>
10 ± 2	0 ± 45
13 ± 2	830 ± 70
13 ± 2	4580 ± 250
30 ± 2	5020 ± 370
14 ± 2	5790 ± 430
35 ± 2	6395 ± 440
64 ± 2	6450 ± 480
34 ± 2	6500 ± 395
45 ± 2	6800 ± 420
74 ± 2	8340 ± 585

<sup>a</sup>reference year AD 1950

AMS <sup>14</sup>C analysis on a single valve (*Mytilus Edulis*) with a known depth habitat (Lavoie et al., 2012). Thus, we suspect that the spread in ages on relict beaches of similar elevation around Lake Turkana may reflect mixing of shells from older deeper water facies or older beach deposits with penecontemporaneous shells as lake level fell and rose multiple times in the past 15 ka. Thus, <sup>14</sup>C ages with ranks of 1 or 2 are favored, but rank 3 shells are shown as possible lake level constraints. In turn, some of the conventional <sup>14</sup>C ages reported by (Owen et al., 1982) were derived for organic fraction(s) concentrated from bone, which in the hot environment of Lake Turkana was probably preserved poorly and in other contexts yielded erroneous ages (e.g. Stafford et al., 1990; Collins et al., 2002). Subsequent studies have mostly excluded these bone <sup>14</sup>C ages, but have included <sup>14</sup>C ages on mixed shell assemblages, though with larger errors in elevation and in age, with calendar correction (Brown and Fuller, 2008; Garcin et al., 2012).

Lake level post ca. 4.5 ka is largely constrained by the elevational distribution of <sup>14</sup>C-dated archaeological sites around Lake Turkana (Table 6; Butzer et al., 1972; Owen et al., 1982; Garcin et al., 2012; and others). The a priori assumption is that sites were at or close to lake

**Table 4.** Previous ages, rank 2

Sample location	Reference	Sample elevation (m) <sup>a</sup>	Elevation correction & error (m)	Sample <sup>14</sup> C age (yr BP)	Calendar age (yr BP) <sup>c</sup>	Material dated
Koobi Fora	Owen et al., 1982	67	(10)	4380 ± 200	4985 ± 280	<i>Etheria Elliptica</i>
Eliye Springs	Robbins, 1972	77	(10)	4800 ± 100	5540 ± 105	<i>Etheria Elliptica</i>
Nachukui	Garcin et al., 2012	77	(10)	4810 ± 30	5565 ± 40	Oyster (sp?)
Eliye Springs	Stuiver, 1969	65	(10)	4880 ± 100	5615 ± 100	<i>Etheria Elliptica</i>
South Island	Garcin et al., 2012	31	+12 (1)	4910 ± 35	5630 ± 30	Bivalve (sp?)
Koobi Fora	Owen et al., 1982	67	(10)	4940 ± 230	5675 ± 255	<i>Etheria Elliptica</i>
Nachukui	Garcin et al., 2012	81	(16)	4965 ± 40	5685 ± 50	<i>Melanoides</i>
Nachukui	Garcin et al., 2012	71	(16)	5225 ± 80	5980 ± 95	Oyster (sp?)
Nachukui	Garcin et al., 2012	67	(16)	5255 ± 30	6000 ± 45	Oyster (sp?)
Nachukui	Garcin et al., 2012	67	(16)	5260 ± 40	6010 ± 60	Oyster (sp?)
Nachukui	Garcin et al., 2012	81	(16)	5320 ± 35	6105 ± 70	Oyster (sp?)
Kataboi	Garcin et al., 2012	72	(16)	5810 ± 70	6615 ± 85	Oyster (sp?)
Kibish	Butzer et al., 1972	82	-10 <sup>b</sup> (10)	6150 ± 100	7035 ± 135	<i>Unionidae</i>
Eliye Springs	Garcin et al., 2012	60	(16)	6630 ± 45	7515 ± 40	Snail shell (sp?)
Kibish	Butzer et al., 1972	93	-30 <sup>b</sup> (10)	8300 ± 150	9285 ± 190	<i>Etheria Elliptica</i>
Kibish	Butzer et al., 1972	92	-22 <sup>b</sup> (10)	9050 ± 150	10,200 ± 185	<i>Corbicula</i>
Kibish	Butzer et al., 1972	94	-24 <sup>b</sup> (10)	9100 ± 200	10,255 ± 255	<i>Corbicula</i>
Koobi Fora	Owen et al., 1982	74	(10)	9110 ± 130	10,270 ± 145	<i>Etheria Elliptica</i>
Kibish	Butzer et al., 1972	97	-27 <sup>b</sup> (10)	9200 ± 200	10,380 ± 260	<i>Corbicula</i>
Kibish	Butzer et al., 1972	90	-9 <sup>b</sup> (10)	9900 ± 150	11,345 ± 225	<i>Unionidae</i>
Kibish	Butzer et al., 1972	92	-18 <sup>b</sup> (10)	9900 ± 150	11,345 ± 225	<i>Corbicula</i>
Kibish	Brown and Fuller, 2008	73	(10)	11,110 ± 40	12,965 ± 45	Bivalve (sp?)

<sup>a</sup>Elevation from 2008 lake surface elevation of 362 masl (Velpuri et al., 2011).

<sup>b</sup>Elevation correction by Brown and Fuller, 2008

<sup>c</sup>Calendar corrected from <http://radiocarbon.ideo.columbia.edu/cgi-bin/radcarbcal>; Fairbanks et al. (2005).

level. This is a credible inference for sites with bone fishhooks and abundant fish and shell remains, indicating coastal proximity (cf. Robbins, 1984) but, for other sites with evidence of mixed use of aquatic and terrestrial resources the proximity to the shore is unknown (e.g. Wright and Forman, 2011). Thus, the elevational distribution of sites provides a maximum limiting estimate on the subsequent lake levels and with variable uncertainty depending on the archaeological context. Also, the elevation of several <sup>14</sup>C ages on shell reported in recent studies has been re-assessed through GPS-based location on a 16-m-resolution digital elevation model (SRTM; Duren et al., 1998) for strand plains surrounding Lake Turkana, in lieu of direct measurement at the collection site and adds greater uncertainty (cf. Brown and Fuller, 2008; Garcin et al., 2012). This legacy of conventional <sup>14</sup>C ages with larger errors in age (>200 years)

**Table 5.** Previous ages, rank 3

Sample location	Reference	Sample elevation (m) <sup>a</sup>	Elevation correction & error (m)	Sample <sup>14</sup> C age (yr BP)	Calendar age (yr BP) <sup>b</sup>	Material dated
Kibish	Butzer et al., 1972	88	-7 <sup>b</sup> (10)	3650 ± 150	3975 ± 205	Mixed shell
Nachukui	Garcin et al., 2012	77	(10)	4790 ± 30	5545 ± 45	Stromatolite
Kibish	Butzer et al., 1972	86	-8 <sup>b</sup> (10)	5550 ± 350	6340 ± 385	Mixed shell
Kibish	Butzer et al., 1972	79	+2 <sup>b</sup> (10)	5850 ± 100	6660 ± 120	Mixed shell
Lothagam	Robbins, 1972	101	(16)	6010 ± 160	6855 ± 200	Shell (sp?)
Kibish	Butzer et al., 1972	90	-6 <sup>b</sup> (10)	6100 ± 100	6970 ± 135	Mixed shell
Eliye Springs	Garcin et al., 2012	60	(16)	6285 ± 50	7215 ± 55	Bivalve (sp?)
Kibish	Butzer et al., 1972	16	-12 <sup>b</sup> (10)	7000 ± 150	7830 ± 145	Mixed shell
Lothagam	Robbins, 1980	48	(10)	7000 ± 80	7830 ± 85	Shell (sp?)
Lothagam	Butzer et al., 1972	68	(16)	7560 ± 80	8370 ± 60	Shell (sp?)
Lothagam	Robbins, 1972	101	(16)	7960 ± 140	8815 ± 210	Shell (sp?)
Lothagam	Robbins, 1972	94	(16)	8230 ± 180	9190 ± 235	Shell (sp?)
Lothagam	Robbins, 1972	101	(16)	8420 ± 170	9415 ± 180	Shell (sp?)
Koobi Fora	Owen et al., 1982	74	(10)	8920 ± 130	10,040 ± 205	Shell (sp?)
Kibish	Butzer et al., 1972	66	+4 <sup>b</sup> (10)	9300 ± 300	10,520 ± 410	Mixed shell
Koobi Fora	Owen et al., 1982	50	(10)	9315 ± 140	10,520 ± 195	Shell (sp?)
Koobi Fora	Owen et al., 1982	73	(10)	9360 ± 135	10,580 ± 195	Mixed shell
Lowasera	Phillipson, 1977	77	(10)	9420 ± 200	10,675 ± 295	Shell (sp?)
Kibish	Butzer et al., 1972	83	-13 <sup>b</sup> (10)	9500 ± 300	10,800 ± 430	Mixed shell
Kataboi	Garcin et al., 2012	82	(16)	9515 ± 80	10,805 ± 160	Bivalve (sp?)
Koobi Fora	Owen et al., 1982	95	(10)	9660 ± 235	11,025 ± 345	Shell (sp?)
Kibish	Butzer et al., 1972	91	-62 <sup>b</sup> (10)	9700 ± 400	11,100 ± 600	<i>Unionidae</i>
Lothagam	Garcin et al., 2012	78	(16)	9795 ± 100	11,210 ± 100	<i>Melanoides</i>
Koobi Fora	Owen et al., 1982	95	(10)	9940 ± 260	11,445 ± 425	Shell (sp?)
Koobi Fora	Owen et al., 1982	54	(10)	10,280 ± 670	11,935 ± 920	Shell (sp?)
Koobi Fora	Owen et al., 1982	54	(10)	10,720 ± 150	12,645 ± 140	Shell (sp?)

<sup>a</sup>Elevation from 2008 lake surface elevation of 362 masl (Velpuri et al., 2011).

<sup>b</sup>Elevation correction by Brown and Fuller, 2008

<sup>c</sup>Calendar corrected from <http://radiocarbon.ldeo.columbia.edu/cgi-bin/radcarbcal>; Fairbanks et al. (2005).

with some ages derived from mixed assemblage of shells and uncertainty in elevation ( $\sim\pm 10$  to 30 m; Garcin et al., 2012), may obscure centennial-scale fluctuations in lake level. In turn, the *a priori* assumption that relict beaches of equal elevation are correlative across the Turkana Basin is problematic with differential uplift, lithospheric warping, isostasy and fault offsets (cf. Garcin et al., 2012; Melnick et al., 2012).

**Table 6.** Ages on archaeological material

Sample location	Reference	Sample elevation (m) <sup>a</sup>	Lab age	Calendar age (yr BP) <sup>b</sup>	Material dated
Eliye Springs	Lynch and Robbins, 1979; Robbins, 1980	18 ± 10	870 ± 80	785 ± 85	Burned soil
Eliye Springs	Lynch and Robbins, 1979; Robbins, 1980; Robbins, 1984	18 ± 10	950 ± 80	865 ± 85	Charcoal?
Eliye Springs	Robbins, 1980; Robbins, 1984	18 ± 10	1100 ± 80	1005 ± 85	Burned soil
Eliye Springs	Lynch and Robbins, 1979	18 ± 10	1375 ± 125	1285 ± 110	Burned soil?
Eliye Springs	Lynch and Robbins, 1979; Robbins, 1980; Robbins, 1984	9 ± 10	1800 ± 300	1734 ± 339	Charcoal
Mt. Porr	Forman et al., submitted	34 ± 1	2575 ± 20	2725 ± 10	ostrich egg shell
Mt. Porr	Forman et al., submitted	14 ± 1	-	2910 ± 190 <sup>c</sup>	colian fine grained sand
Mt. Porr	Forman et al., submitted	50 ± 1	-	3830 ± 250 <sup>c</sup>	colian fine grained sand
Manemanya	Hildebrand and Grillo, 2012	82 ± 10	3805 ± 20	4185 ± 35	Ostrich eggshell bead
Manemanya	Hildebrand and Grillo, 2012; Hildebrand et al., 2011	82 ± 10	3805 ± 15	4185 ± 30	Ostrich eggshell bead
Kalokol	Hildebrand and Grillo, 2012; Hildebrand et al., 2011	98 ± 10	3890 ± 15	4335 ± 40	Ostrich eggshell bead
Koobi Fora	Owen et al., 1982	54 ± 10	3945 ± 135	4390 ± 195	Charcoal
Koobi Fora	Owen et al., 1982	54 ± 10	3960 ± 60	4415 ± 75	Charcoal
Koobi Fora	Owen et al., 1982	50 ± 10	3970 ± 60	4430 ± 75	Charcoal
Koobi Fora	Owen et al., 1982	54 ± 10	4100 ± 125	4610 ± 180	Humic acid
Jarigole	Hildebrand and Grillo, 2012	73 ± 10	4145 ± 55	4690 ± 110	Ostrich eggshell bead
Koobi Fora	Owen et al., 1982	50 ± 10	4160 ± 110	4695 ± 160	Charcoal
Lothagam	Hildebrand and Grillo, 2012	73 ± 10	4165 ± 20	4730 ± 60	Ostrich eggshell bead
Koobi Fora	Hildebrand and Grillo, 2012	58 ± 10	4180 ± 60	4740 ± 100	Charcoal
Koobi Fora	Ashley et al., 2011	54 ± 10	4180 ± 40	4755 ± 80	Charcoal
Koobi Fora	Ashley et al., 2011	54 ± 10	4180 ± 40	4755 ± 80	Charcoal
Koobi Fora	Ashley et al., 2011	54 ± 10	4240 ± 40	4825 ± 40	Charcoal
Jarigole	Hildebrand and Grillo, 2012	73 ± 10	4250 ± 40	4830 ± 30	Ostrich eggshell bead
Lothagam	Hildebrand and Grillo, 2012; Hildebrand et al., 2011	73 ± 10	4265 ± 15	4840 ± 5	Ostrich eggshell bead
Lothagam	Hildebrand and Grillo, 2012; Hildebrand et al., 2011	68 ± 10	4290 ± 20	4845 ± 10	Charcoal
Lothagam	Hildebrand and Grillo, 2012; Hildebrand et al., 2011	73 ± 10	4385 ± 15	4935 ± 40	Ostrich eggshell bead
Jarigole	Hildebrand and Grillo, 2012	73 ± 10	4380 ± 40	4935 ± 70	Ostrich eggshell bead
Jarigole	Hildebrand and Grillo, 2012	73 ± 10	4400 ± 40	4970 ± 80	Ostrich eggshell bead
Koobi Fora	Owen et al., 1982	66 ± 10	4390 ± 235	5000 ± 325	Charcoal
Lothagam	Butzer et al., 1972; Robbins, 1972; Yamasaki et al., 1972	83 ± 10	5020 ± 220	5765 ± 240	Burned soil?
Lothagam	This study	96 ± 2	5515 ± 30	6300 ± 20	Fish bones
Lothagam	Butzer et al., 1972; Yamasaki et al., 1972	68 ± 10	6200 ± 130	7095 ± 165	Charcoal
Lothagam	Robbin and Lynch, 1978; Robbins, 1980	48 ± 10	6300 ± 800	7135 ± 835	Charcoal
Kolokol	Beyin, 2011	84 ± 10	9060 ± 30	10,220 ± 10	Charcoal
Kolokol	Beyin, 2011	84 ± 10	9785 ± 35	11,210 ± 20	Charcoal

<sup>a</sup>Elevation from 2008 lake surface elevation of 362 masl (Velpuri et al., 2011).

<sup>b</sup>Calendar corrected from <http://radiocarbon.ldeo.columbia.edu/cgi-bin/radcarbeal>; Fairbanks et al. (2005).

<sup>c</sup>Optical ages expressed in years before 1950

Results from the western strand plain, integrated with previously published data from strand plains at Mt. Porr (Forman et al., submitted), South Island (Garcin et al., 2012), Koobi Fora (Owen et al., 1982), and Kibish (Butzer, 1980; Brown and Fuller, 2008) reveal high and low stands for Lake Turkana, which were mostly unrecognized by earlier studies (Fig. 10). These discrepancies in inferred lake level may reflect a sample bias for prior studies (Butzer, 1980; Owen et al., 1982; Brown and Fuller, 2008) which concentrate on lake deposits >50 m, to determine possible spillover into the White Nile catchment. This study, along with recent investigations at Mt. Porr (Forman et al., submitted) and South Island (Garcin et al., 2012)

focused on documenting beaches > 30 m elevation. In turn, the Kalokol strand plain area appears to be unaltered tectonically, at least in the past ca. 100 ka (Vétel et al., 2004; McDougall and Brown, 2009; Brown and McDougall, 2011), and may provide a consistent assessment of elevation for littoral, sublittoral, and deeper-water facies and associated inferences of past lake levels. Also, by elevation, relict beach landforms appear correlative with maximum high stand deposits and washing limits for Lothagam and the Kalokol area. Closely spaced measurements of elevation across the paleo-tombolo at Lothagam document no warping or offset the beach ridge within errors of measurement (ca.  $\pm 1$  m).

### **3.3 Lake Turkana water level variability**

This integrated lake level record for Lake Turkana (Fig. 10) was derived from multiple studies of beach ridge sequences and reveals at least ten centennial-scale oscillations in water level between 15 and 4.5 ka. There are just six radiocarbon ages to constrain the lake level reconstruction between 15 and 11.5 ka which depict a slight regression at ca. 14.5 ka, followed by an apparent oscillation of >50 m. The lake level regression is indicated by the sedimentary sequence of sublittoral sands subjacent to backshore sediments from a relict beach at +25 m dated to 14.6 ka (*Melanoides*; ISGS-A2781). The duration of the transgression up to at least ~80 m appears to be >1.5 ka constrained by AMS  $^{14}\text{C}$  ages on *Melanoides* at 45 (see Table 1); an AMS  $^{14}\text{C}$  age on a bivalve shell indicates a peak age of ca. 13 ka (Brown and Fuller, 2008). Many East African lakes show low stands between 15 and 13 ka, such as lakes Nakuru-Elmenteita (Richardson and Dussinger, 1987), Suguta (Junginger et al., 2013) and Lake Albert (Williams et al., 2006). Also, this peak and subsequent regression to a low at ca. 11.5 ka

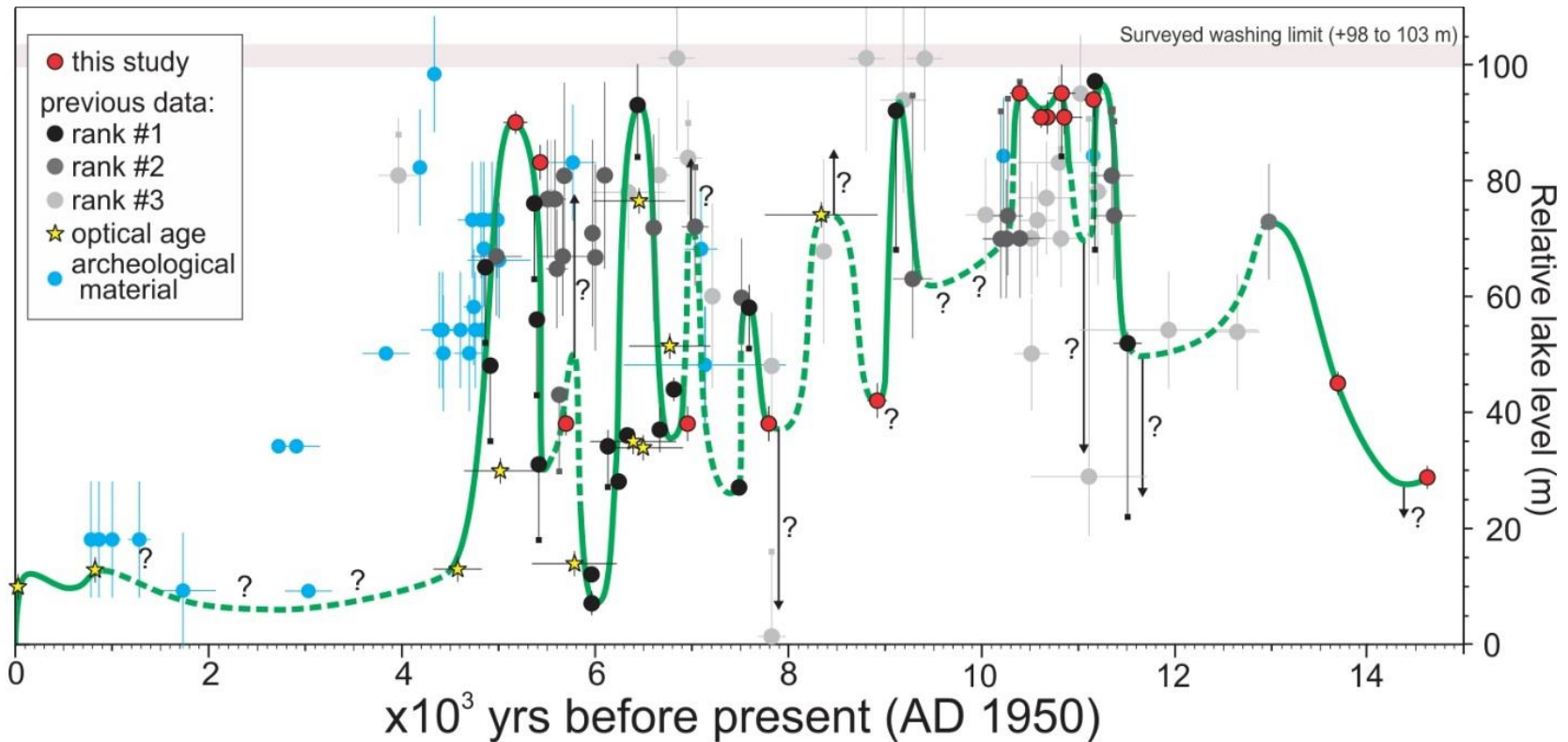


**Figure 10.** Reconstruction of Lake Turkana water levels for the past ca. 15 ka. This reconstruction is based on data from this study (Table 1), and data ranked by certainty. Black - rank 1 radiocarbon ages (Table 2), and yellow stars – OSL ages (Table 3). Dark grey – rank 2 radiocarbon ages (Table 4). Light grey – rank 3 ages (Table 5). Light blue – radiocarbon ages on archaeological material (Table 6). All ages calibrated by Fairbanks et al. (2005), and elevations are relative to the 2008 datum of 362 masl (Velpuri et al., 2012).

to at least 50 m are concordant with previous paleolimnological studies, which suggest a coincident dry period for East Africa linked to the YD. Leaf wax proxies ( $\delta D_{\text{wax}}$ ) from East African lakes Tanganyika, Tana, Victoria and Challa suggest between ca. 12.5 and 11.5 ka was dry (see Fig. 11), with an abrupt and a sustained return of wet conditions directly following the YD (Costa et al., 2014). After this dry period water level rose in Lake Turkana to about 95 m by ca. 11.2 ka constrained by four shell ages from Lothagam, Kibish and the South Island (all of rank 2 or higher). Garcin et al. (2012) hypothesized that there was spillover into the White Nile basin during this high lake stand. A low stand is inferred between ca. 11.2 and 10.8 ka, though constrained by a sole age. This age from a single *Unionidae sp.* shell from Butzer (1980) has an unusually large error (>5%) and the elevation of this shells has been decreased by Brown and Fuller (2008) by 62 m, thus lowest level of this regression at ca. 11 ka is uncertain. Lake level may have fallen by at least 15 m at this time, supported by a  $^{14}\text{C}$  age of  $11.2 \pm 0.02$  ka from an archaeological site in the Kalokol area with human habitation at 84 m (Beyin, 2011; Garcin et al., 2012).

Another high stand to >90 m between ca. 10.8 and 10.3 ka is constrained by five ages from this study (Table 1; Fig. 10). A slight oscillation in water level from 91 m up to >95 m is delimited by  $^{14}\text{C}$  ages of  $10.8 \pm 0.2$  ka and  $10.7 \pm 0.1$  ka on single *Corbicula fluminalis africana* and *Melanooides tuberculata* shells from the same upper foreshore deposit at 91 m; peak water level up to ~100 is indicated by a  $^{14}\text{C}$  age of  $10.8 \pm 0.1$  ka on an *Etheria elliptica* shell taken *in situ* from a lacustrine facies at 84 m. A brief still stand at 91 m is indicated by a  $^{14}\text{C}$  age of  $10.61 \pm 0.095$  ka on a shell from upper foreshore sands. Water level may have transgressed slightly to 95 m, inferred from sublittoral sands at 92 m for which a single shell gave an age of  $10.4 \pm 0.1$  ka. A regression to at least 70 m is indicated following this high stand broadly between 10.4 and

10.2 ka, indicated by three radiocarbon ages from *Corbicula sp.* sampled at Kibish. These shells were sampled originally at a reported elevation of ~95 m (Butzer, 1980), and have been adjusted to 70 m by Brown and Fuller (2008). A calibrated radiocarbon age of ca.  $10.3 \pm 0.2$  ka on a single *Etheria elliptica* shell at 75 m further constrains the timing of this regression (Owen et al., 1982). In addition, the timing of this regression is supported by a calibrated  $^{14}\text{C}$  age of ca. 10.2 ka on buried charcoal from an archaeological site at 84 m (Beyin, 2011). Lacustrine hydroclimatic proxies ( $\delta\text{D}_{\text{wax}}$ ; Fig. 11) indicate a period of wet conditions between 11.5 and ca. 10 ka (cf. Tierney et al., 2010; Tierney et al., 2011b; Berke et al., 2012a; Costa et al., 2014); a record of potassium content for a core from an alluvial fan in the nearby Chew Bahir Basin, a proxy for surface runoff, (Foerster et al., 2012) indicates a period of gradually increasing precipitation.

Reconstructed water level for Lake Turkana records four oscillations of >20 m between ca. 10 and 6.5 ka. A low stand to <65 m is inferred until 9.3 ka, based on a single  $^{14}\text{C}$  age of  $9.3 \pm 0.2$  ka on an *Etheria elliptica* shell, with elevation adjusted from 93 to 63 m (Butzer, 1980; Brown and Fuller, 2008). Garcin et al. (2012) inferred a low stand to ~70 m between 10.7 and 10.0 ka, which is ca. 0.5 to 1 ka prior to the low stand inferred in this reconstruction. Other studies suggest low water levels for Lake Turkana between ca. 10 and 9.3 ka to <65 m (Brown and Fuller, 2008). An AMS  $^{14}\text{C}$  age of  $9.1 \pm 0.1$  ka on a single gastropod (*Melanooides tuberculata*; Table 2) indicates a possible high stand > 90 m, and may reflect another period of spillover at the outlet sill. Regression to low stand to 42 m constrained by an AMS  $^{14}\text{C}$  age of  $8.92 \pm 0.1$  ka on a single gastropod shell (*Melanooides tuberculata*; Table 1; AA100110); these two radiocarbon ages and associated lake level constrain a regression of 50 m in 200 to 400

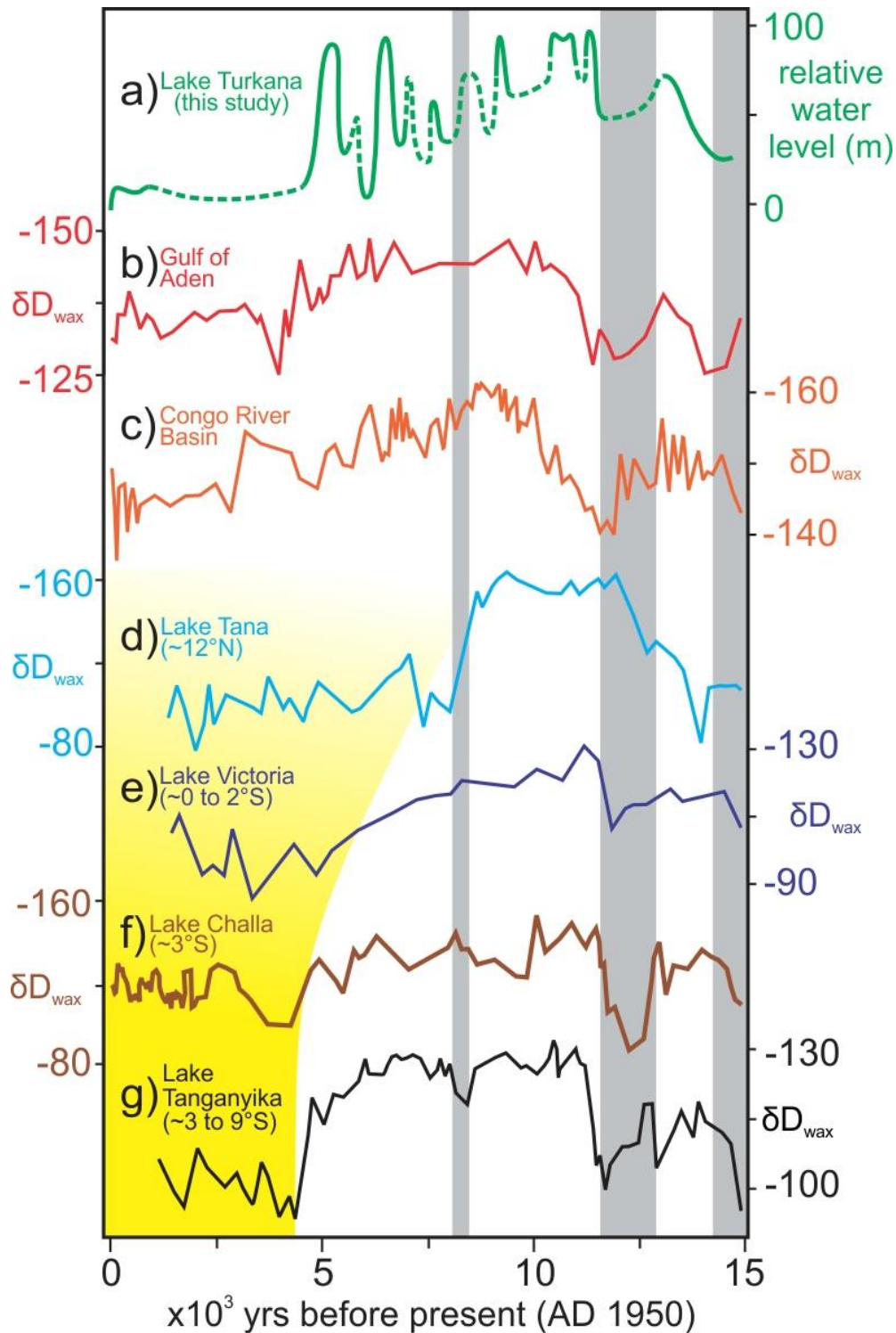


**Figure 11.** Various  $\delta D_{wax}$  chronologies from East Africa. (A) Lake Turkana water levels for comparison. Oceanic cored  $\delta D_{wax}$  records of terrigenous runoff: (B) Gulf of Aden core (Tierney and deMenocal, 2013). (C) Congo River delta core (Schefuß et al., 2005). Lacustrine  $\delta D_{wax}$  records (D) Lake Tana (Costa et al., 2014). (E) Lake Victoria (Berke et al., 2012). (F) Lake Challa (Tierney et al., 2011). (G) Lake Tanganyika (Tierney et al., 2010).

years. A single OSL age of  $8.3 \pm 0.6$  ka indicates a  $\sim 35$  m transgression inferred to at least 74 m at ca. 8.3 ka. In addition, a conventional  $^{14}\text{C}$  age of  $8.4 \pm 0.1$  ka on an unidentified shell at 68 m at Lothagam supports this peak (Butzer et al., 1972), though this age is of low certainty (Table 5).

This reconstruction infers a low stand  $< 38$  m at ca. 7.8 ka, which may be associated with drought in East Africa linked to the 8.2 ka event (Alley et al., 1997). This low stand at least 42 m is constrained by a sole  $^{14}\text{C}$  age of  $7.8 \pm 0.18$  ka (SNU12-593) on a *Melanoides tuberculata* shell (Table 1). In turn, water level may have regressed by as much as 70 m, suggested by a conventional  $^{14}\text{C}$  age of  $7.8 \pm 0.8$  ka on mixed shell (Table 5), from a beach near Kibish at 16 m (Butzer, 1980), adjusted to 4 m elevation by Brown and Fuller (2008). Water level regressions of  $>30$  m are indicated between ca. 8.3 and 8 ka at lakes Ziway-Shala, Suguta, and Abhe (Gasse and Van Campo, 1994), with abrupt drying indicated at Lake Tana (Marshall et al., 2011; Costa et al., 2014). A significant dust spike at  $\sim 8.3$  ka observed in ice cores from Mt. Kilimanjaro suggest adjacent lakes may have been low or desiccated during this period (Thompson et al., 2002). In turn, the Chew Bahir sediment core records a decrease in moisture from 8.1 to 7.5 ka (Foerster et al., 2012). A distinct, but brief low stand is indicated at Lake Tana, at the source of the Blue Nile in Ethiopia, prior to ca. 7.4, linked to abrupt regressions with the 8.2 ka event (Marshall et al., 2011). In addition, the  $\delta\text{D}_{\text{wax}}$  record from a sediment core of Lake Tana records abrupt enrichment of 70‰ between ca. 8.2 and 7.8 ka linked to the onset of drought for the Greater Horn of Africa (Fig. 11d; Costa et al., 2014). Surprisingly,  $\delta\text{D}_{\text{wax}}$  records for lakes Victoria and Challa show no significant isotopic changes, which may reflect the multi-century sampling interval of  $\sim 250$  years (Berke et al., 2012a) and  $\sim 300$  yrs (Tierney et al., 2011b), respectively.

Water level rose to > 60 m between 7.8 and 6.6 ka with two oscillations at ca. 7.6 and 7.0 ka, which may have occurred within <500 years. The oldest of the two transgressions is constrained by  $^{14}\text{C}$  ages of ca. 7.6 ka and 7.5 ka on a single gastropod (*Melanoides sp.*) from 58 m at Mt. Porr (Forman et al., submitted) and a snail shell at 60 m at Eliye Springs (Garcin et al., 2012), which provide minimum elevation for this inferred high stand. Subsequently lake level fell to at least 27 m by  $7.5 \pm 0.1$  ka, based on a single  $^{14}\text{C}$  age on a gastropod (*Melanoides sp.*) from Mt. Porr (Forman et al., submitted). A rise in lake level to at least 72 m is constrained by a single conventional  $^{14}\text{C}$  age of  $7.0 \pm 0.1$  ka on a *Unionidae sp.* shell from a relict beach at 82 m (Butzer, 1980), and adjusted to 72 m by Brown and Fuller (2008). Also, a calibrated  $^{14}\text{C}$  age of  $7.0 \pm 0.1$  ka on mixed shells collected at 84 m suggests this oscillation may have been greater, yet this age is of low certainty (Table 5). A low stand between ca. 6.9 and 6.5 ka to ~35 m is well constrained by three  $^{14}\text{C}$  ages, with additional associated optical ages. The duration of this low stand is constrained by two AMS  $^{14}\text{C}$  ages of  $6.96 \pm 0.07$  ka and  $6.75 \pm 0.03$  ka on single *Melanoides tuberculata* shells at 38 m (SNU12-591; Table 1), and another AMS  $^{14}\text{C}$  age of on a *Corbicula sp.* at 30 m from Mt. Porr (Forman et al., submitted). Surface runoff in the Ethiopian Highlands suggest between 7.5 and 6.8 ka was generally wet, as indicated by elevated titanium concentration in a lacustrine sediment core from Lake Tana (Marshall et al., 2011) and lower potassium levels in a sediment core from an alluvial fan in the Chew Bahir (Foerster et al., 2012). Similarly, a low stand for Lake Tana persisted from 8.2 ka until ca. 7.2 ka with an abrupt transgression indicated at 7 ka (Marshall et al., 2011). Other lacustrine records from lakes Abbe (Gasse, 2000) and Ziway-Shala (Gillespie et al., 1983) in the northern Ethiopian Rift Valley infer a low stand at ca. 8 ka, though it is not well dated, and a transgression to near peak water levels by ca. 7 ka. A sediment core record from Lake Ashenge, also on the northern Ethiopia Plateau

indicates a pronounced low stand associated with eolian erosion and a hiatus in this record, just prior to 7.6 ka (Marshall et al., 2009).

An rise to at least +95 m at ca. 6.3 ka is depicted in previous reconstructions of water level, and is constrained by multiple  $^{14}\text{C}$  ages with high certainty (Tables 2 and 4). This transgression is supported by a conventional  $^{14}\text{C}$  age of  $6.6 \pm 0.1$  ka from an oyster sampled by Garcin et al. (2012) at 72 m from near Kataboi. Peak water levels  $>85$  m are inferred from an AMS  $^{14}\text{C}$  age of ca. 6.4 ka on an *Etheria elliptica* at 75 m taken *in situ* from sediments associated with deep water deposition ( $>15$  m). An optical age of  $6.4 \pm 0.5$  ka on these lower sublittoral sands supports this peak (Forman et al., submitted). Butzer (1980) depicts a slight oscillation of  $<10$  m between ca. 6.9 and 6.2 ka, which is inferred in the reconstruction of Garcin et al. (2012), which widens this possible high stand to between 7.0 and 5.8 ka, with possible spillover to the Nile River outlet. Lake level to  $<28$  m is constrained by  $^{14}\text{C}$  ages of ca. 6.3 ka at 36 m on a *Melanoides tuberculata* shell and 6.3 ka at 28 m on a *Corbicula sp.* shell (Forman et al., submitted). A water level of 12 m is indicated by an AMS  $^{14}\text{C}$  age of ca. 6.0 ka on a *Melanoides tuberculata* at 7 m from Mt. Porr (Forman et al., submitted). Further, upper sublittoral deposits at 14 m that yielded an optical age of  $5.8 \pm 0.4$  ka which reinforces the timing of this low stand and may reflect the lowest water level prior to historical records (cf. Butzer, 1980). This fall in water level is also inferred by Garcin et al. (2012), with a reconstructed regression of  $\sim 15$  m from the maximum high stand elevation at ca. 6 ka. In contrast, earlier studies of relict beaches record stable, high ( $> 60$  m) lake levels for this period, though based on  $^{14}\text{C}$  dating of shells of mixed species, and uncertain stratigraphic context (see Fig. 4; Butzer, 1980; Owen et al., 1982; Robbins, 1984) and are based on less secure ages. The potassium levels from the Chew Bahir Basin gradually increase between 6 and 5 ka, indicating an apparent progressive transition to aridity for the catchment immediately

northeast of Lake Turkana (Fig. 12b; Foerster et al., 2012). Farther south, seismic stratigraphic data and a terrestrial runoff proxy (BIT index) for a sediment record from Lake Challa indicate a drop in lake level at ca. 6 ka (Fig. 12d), though the magnitude is unconstrained (Verschuren et al., 2009).

A potentially major oscillation may have occurred between ca. 5.9 and 5.5 ka, but is constrained by less certain ages, with elevation assessed by digital elevation models ( $\pm 16$  m error; Table 2). Material from an archaeological site at Lothagam (+83 m) returned a  $^{14}\text{C}$  age of  $5.8 \pm 0.2$  ka, which places a maximum constraining elevation for this transgression (Butzer et al., 1972). A more probable elevation is at  $\sim 65$  m, with two conventional  $^{14}\text{C}$  ages on a single *Melanoides tuberculata* shell ( $5.7 \pm 0.05$  ka; Garcin et al., 2012) and an *Etheria elliptica* shell ( $5.7 \pm 0.26$  ka; Owen et al., 1982) providing chronological control.

The integrated strand plain record (Fig. 10) depicts water levels rising and falling  $>80$  m between ca. 5.5 and 4.5 ka, which is the last major oscillation prior to the onset of late Holocene ca. 4.5 to 4.0 ka ago. Further, this oscillation may represent the last maximum transgression for Lake Turkana, with possible spillover. The transgression is constrained by three AMS  $^{14}\text{C}$  ages from the South Island, which infer a rapid rise from 31 m at  $5.4 \pm 0.1$  ka to 56 m at  $5.4 \pm 0.1$  ka, with rapid rise to 76 m at  $5.4 \pm 0.1$  ka (Garcin et al., 2012); these elevations have been raised by 12 m to account for tectonic subsidence (cf. Melnick et al., 2012). A final high stand is indicated by backshore deposits at 90 m, supported by a sole AMS  $^{14}\text{C}$  age of  $5.18 \pm 0.12$  ka on a single *Melanoides tuberculata* shell. The regression in water level from this high stand is constrained by a conventional  $^{14}\text{C}$  age of  $4.985 \pm 0.28$  ka on a bivalve shell (*Etheria elliptica*) at 67 m from Koobi Fora (Owen et al., 1982) and two AMS  $^{14}\text{C}$  ages of  $4.92 \pm 0.035$  ka at 48 m and  $4.87 \pm 0.03$  ka at 65 m from the South Island (Garcin et al., 2012). Numerous radiocarbon ages mostly

on ostrich eggshell beads and charcoal from archaeological sites, associated with human habitation support a water level < 66 m post ca. 5 ka and <54 m after ca. 4.8 ka (Table 6). In turn, analyses of diatoms from a sediment core from Lake Turkana detect a drop in lake levels after 4.7 ka, but of unknown magnitude (see Fig. 4c; Halfman et al., 1994).

Geomorphic and archaeological evidence from the Mt. Porr strand plain constrains lake level below 13 m between ca. 4.6 ka and AD 1888, the start of historical records of lake level. Low water levels <13 m are inferred from an optical age of  $4.6 \pm 0.3$  ka from Mt. Porr taken from a regression beach (Forman et al., submitted). A peak to >80 m at ca. 3.9 m is inferred in past reconstructions (Butzer, 1980; Owen et al., 1982; Brown and Fuller, 2008), however in recent studies the sole radiocarbon age constraining this peak is treated as spurious (Garcin et al., 2012; Forman et al., submitted). In turn, an optical age of  $2.91 \pm 0.19$  ka on eolian sediments supports a lake level at 14 m (Wright and Forman, 2011).

Forman et al. (submitted) reports an optical age of  $2.9 \pm 0.19$  ka from surface eolian sands underlying archaeological sites (Table 6) at 14 m which indicates lake level remained below this level for the rest of the Holocene to preserve the artefact-rich surface deposits on the site (cf. Wright and Forman, 2011). In turn, charcoal samples taken from archaeological sites on relict beaches from Eliye Springs at +10 and +20 m are dated to 1.7 and 0.9 ka (Table 6), respectively (Robbins, 1984). A prominent berm at ~13 m may mark a recent (historical) high stand, and may coincide with the ~15 m regression observed in the historical record from +15 to 20 m water level in ca. AD 1900 to near present levels by AD 1950 (Butzer, 1971; Johnson and Malala, 2009). A well dated sequence (+9m) at the Mt. Porr strand plain revealed a surface beach deposit ca. <100 years old, which buried a ca. 0.83 ka littoral deposit with a prominent Av horizon, indicating surface exposure (Forman et al., submitted).

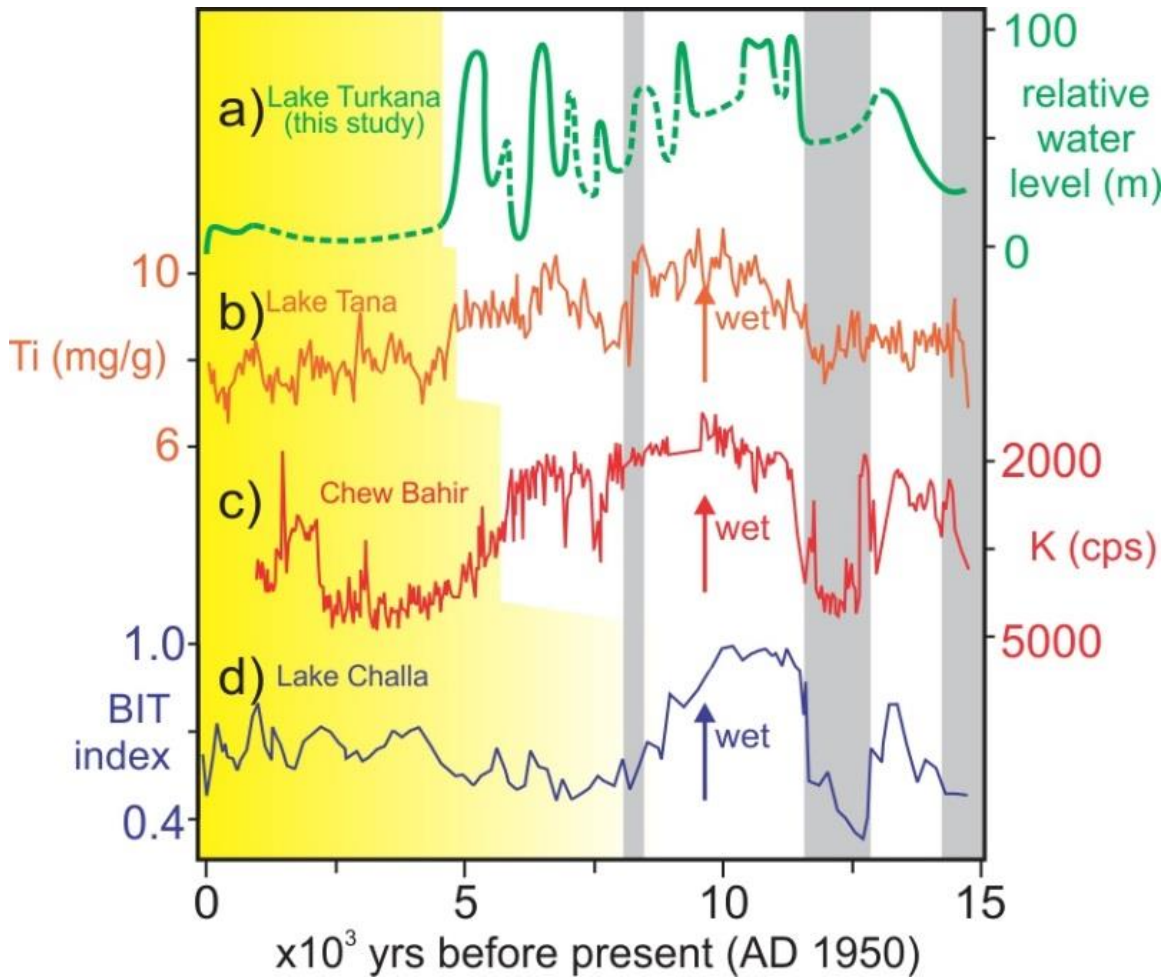


**Figure 12.** Various terrestrial runoff proxies for East African lakes. (A) Lake Turkana water levels for comparison. (B) Lake Tana titanium concentration (Marshall et al., 2011). (C) Chew Bahir potassium record (Foerster et al., 2012). (D) Lake Challa BIT index (Verschuren et al., 2009).

### 3.4 On the potential causes of water level variability for Lake Turkana

The half precessional-cycle of equatorial insolation has been implicated for the transition into the AHP, and the abrupt onset of mid-Holocene aridity (e.g. Gasse and Van Campo, 1994; deMenocal et al., 2000a; Gasse, 2000; Clement et al., 2001; Berger et al., 2006; Verschuren et al., 2009). However, other hydrologic and climatic factors are pertinent to Lake Turkana as probable contributory drivers for the multiple centennial-scale, >30 m fluctuations in water level during the AHP. The volume of water input into Lake Turkana may be amplified by increases in

the basin surface area up to 142% of the present size, with overflow from Lake Suguta into the Kerio River (Garcin et al., 2009; Garcin et al., 2012; Junginger et al., 2013) and possible discharge from an ephemeral lake in the Chew Bahir Basin (Grove et al., 1975; Foerster et al., 2012). Water levels in these former lakes were augmented with input from cascading system of lakes above ~1000 masl, which incorporate regions with present precipitation >1500 mm/yr (Sombroek et al., 1982). In turn, many of the lake level oscillations inferred for Lake Turkana appear consistent with metrics of moisture variability in other basins in East Africa (e.g. Tierney et al., 2011b; Foerster et al., 2012; Costa et al., 2014; and others), with inferred significant changes to the strength and extent of the West and East African monsoons linked to changes in SSTs over the past ca. 15 ka. Recent studies of East African hydroclimate variability have implicated the location and energy of the convergence of moisture flux from the Atlantic and Indian oceans, reflected in the longitudinal position of the Congo Air Boundary as a primary control for droughts and pluvials for East Africa (Tierney et al., 2011b; Junginger et al., 2013; Costa et al., 2014).

#### *3.4.1 Evidence for overflow to Lake Turkana during the African Humid Period*

Increased westerly incursion of Atlantic-derived moisture into East Africa is associated with wet conditions for the Ethiopian and Kenyan highlands between 15 and 5 ka, and reflects in a more eastward position of the Congo Air Boundary. There is abundant evidence for high stands associated with the AHP for endorheic East African lakes Albert (Beuning et al., 1997), Naivasha (Washbourn-Kamau, 1975) and Natron-Magadi (Roberts et al., 1993) and Ethiopian lakes Tana (Marshall et al., 2011) and Abhe (Gasse and Van Campo, 1994). For many lakes with catchments adjacent to the present Lake Turkana Basin, sustained high stands are inferred from ca. 14.5 to 12.2 ka, 11.5 to 8.5 ka, and 7.5 to ~5 ka and there is compelling evidence for periods

of overflow (Grove et al., 1975; Gillespie et al., 1983; Garcin et al., 2009; Foerster et al., 2012; Junginger et al., 2013), however the timing for discharge is uncertain. The timing of spillover and the ultimate source of discharge to Lake Turkana (e.g. Ethiopian or Kenyan highlands) is critical to understanding the spatial precipitation patterns for East Africa over the past ca. 14.5 ka.

Two principal drainage systems, comprised of a total of eight presently closed basin lakes, are thought to have overflowed into the Lake Turkana catchment at periods during the late-Pleistocene and Holocene (Butzer et al., 1972; Grove et al., 1975; Garcin et al., 2009; Foerster et al., 2012; Garcin et al., 2012; Forman et al., submitted). The Ethiopian system is comprised of lakes Abaya-Chamo and Chew Bahir. Water level variations for Lake Abaya-Chamo are inferred based on the well-dated lake level reconstruction of nearby Lake Ziway-Shala (<100 km; Fig. 13a; Gillespie et al., 1983). Presently, the water level for the Lake Abaya is <20 m below the spill elevation into Lake Chamo which is within <30 m of the spill point with discharge into the Chew Bahir (Grove et al., 1975). In turn, the Ziway-Shala system is presently ~120 m below the spill elevation, thus it is reasonable to assume even minor increases in water levels for these lakes may have resulted in considerable discharge for the Abaya-Chamo system. In turn, a sediment core from an alluvial fan in the Chew Bahir Basin (Fig. 12c) suggests a variable wet-dry history for the past ca. 15 ka (Foerster et al., 2012), from which possible overflow is inferred. Discharge from the Kenyan system, which includes lakes Suguta, Baringo-Bogoria, and Nakuru-Elmenteita, is better understood. Diatom species abundance, determined from multiple lacustrine cores from Lake Nakuru-Elmenteita provides a water level chronology (Fig. 13e; Richardson and Richardson, 1972; Richardson and Dussinger, 1987), and infers overflow to Lake Bogoria.

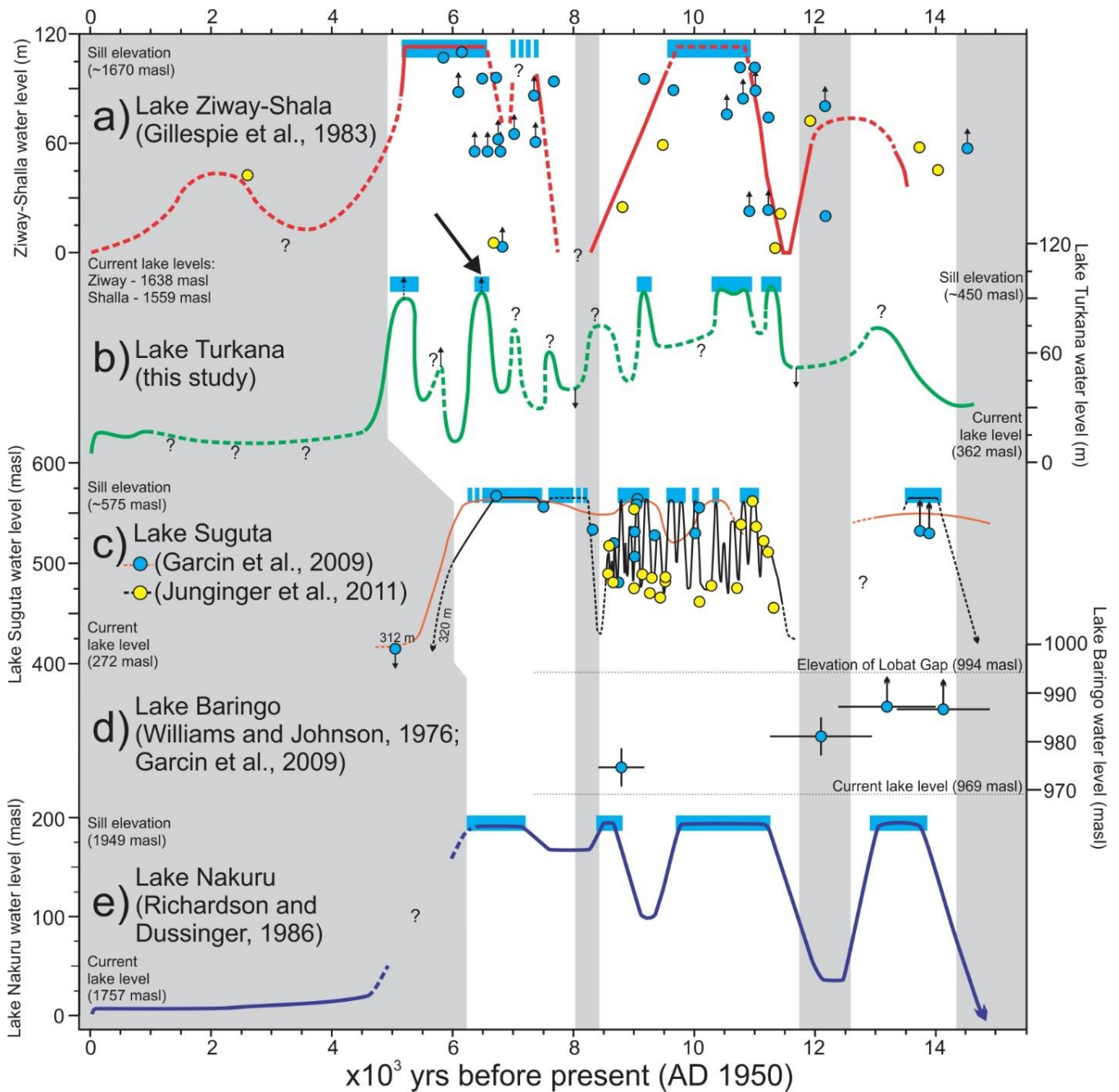


**Figure 13.** Water level chronologies and constraining ages for lakes adjacent to Lake Turkana. **(A)** Lake Ziway-Shala (Gillespie et al., 1983). **(B)** Lake Turkana water levels for comparison. Note solid black arrow, which reflects possible spillover from Lake Chew Bahir, with  $^{14}\text{C}$  age from *Etheria elliptica* shells. **(C)** Lake Suguta water levels, with  $^{14}\text{C}$  ages corrected for a  $\sim 1.9$  ka carbon reservoir effect (Garcin et al., 2009; Junginger et al., 2013). **(D)** Radiocarbon ages on shells from Lake Baringo (Williams and Johnson, 1976). **(E)** Lake Nakuru water level chronology based on diatom assemblages (Richardson and Dussinger, 1987). Blue shaded areas reflect periods of spillover. All ages calibrated by Fairbanks et al. (2005).

Also, some littoral deposits from Lake Baringo-Bogoria have been studied, and four  $^{14}\text{C}$  ages on shells constrain water levels prior to ca. 8.5 ka (Fig. 13d; Williams and Johnson, 1976). Water level variations in Lake Suguta are well constrained, by the study of littoral deposits and by hydrologic modelling (Fig. 13c), which depict intermittent overflow between ca. 14 and 6 ka (Garcin et al., 2009; Junginger et al., 2013). Thus, the timing of spill-over into Lake Turkana can be inferred which may inform interpretations for variability of the CAB and the East and West African monsoons.

High stands are inferred for both Ethiopian and Kenyan lakes post Heinrich Event 1 (H1), with assumed spillover reflected in a transgression to >70 m at 13 ka for Lake Turkana. Lakes Nakuru-Elmenteita were high between ca. 13.8 and 12.8 ka (Richardson and Dussinger, 1987), and two  $^{14}\text{C}$  ages on bulk *Melanoides tuberculata* constrain Lake Baringo near the spill elevation for the same period (Williams and Johnson, 1976). Garcin et al. (2009) observed littoral deposits which were inferred to reflect the maximum high stand for Lake Suguta and two AMS  $^{14}\text{C}$  ages of ca. 13.8 and 13.6 ka on *Melanoides tuberculata* from these deposits may reflect spillover. Lakes in the Ethiopian system may have transgressed later, at ca. 13 ka, which appears asynchronous with lakes in Kenya. Lake Ziway-Shala may have reached a transgressive limit at ca. 12.7 ka (Fig. 13a; Gillespie et al., 1983). The Chew Bahir core (Fig. 12c) depicts a slight wet period at ca. 13.6 and an abrupt, more profound pluvial at 12.7 ka (Foerster et al., 2012). In turn, the  $\delta\text{D}_{\text{wax}}$  record (Fig. 11) suggests this interval was one of progressive depletion for super-equatorial sites (Tierney and deMenocal, 2013; Costa et al., 2014) and sub-equatorial sites indicate no change to slight enrichment (Schefuß et al., 2005; Tierney et al., 2010; Tierney et al., 2011b; Berke et al., 2012a), which may indicate increasing incursion of Atlantic-derived air into the Ethiopian Highlands closer to ca. 12.7 ka with an eastward migration of the CAB.

Water level oscillations between ca. 11.7 and 8.5 ka for Lake Turkana may have been augmented with discharge from the Ethiopian and Kenyan lake systems, which reflects what may be the wettest conditions for East Africa in the past ca. 15 ka (Verschuren et al., 2009; Berke et al., 2012a; Foerster et al., 2012). However, a recent reconstruction of water levels for Lake Suguta (Fig. 13c) shows approximately fifteen oscillations of >50 m between ca. 11.5 and 8.5, and eight episodes of spillover at broadly 0.2 ka intervals from ca. 10.7 to 9.1 ka (Junginger et al., 2013). Water level oscillations for Lake Turkana to >90 m occurred at ca. 11.3, 10 and 9.1 ka; the latter two high stands may have been influenced by discharge from the Kenyan lake system (Figs. 14c and 14e). Water level between ca. 10.1 and 9.4 ka for Lake Turkana is inferred however additional high stands during this interval may result from discharge from Lake Suguta. In turn, water level for Lake Turkana is inferred >60 m between 11.4 and 9 ka and periodic spillover from Lake Suguta may have helped maintain this sustained water volume. The lacustrine  $\delta D_{\text{wax}}$  records (Figs. 11d and 11g) depict abrupt depletion at ca. 11.5 ka and sustained until 8.5 ka which suggests a continual contribution of Atlantic-derived air to East Africa. This signal has been interpreted as an eastward migration of the CAB over the Ethiopian Highlands and parts of Kenya, with periods of elevated rainfall delivered to the Kenyan Highlands by a contracted East African Monsoon (Junginger et al., 2013; Costa et al., 2014). In addition, abrupt  $\delta^{18}\text{O}$  enrichment of a speleothem from Oman (~23° N) at ca. 9.6 ka, suggests a southern deflection of the ITCZ prior, and may explain elevated precipitation for the Ethiopian Highlands (Fleitmann et al., 2003).

Water level for Lake Turkana oscillated up to >70 m three times following a low stand at ca. 8 ka, associated with widespread drought for East Africa (Costa et al., 2014). A transgression for Lake Turkana up to 60 m at ca. 7.5 ka may reflect overflow from the Ethiopian lake system, with

possible overflow from Lake Suguta. An increase in water levels of ~120 m for Lake Ziway-Shala occurred between 7.5 to 7 ka (Gillespie et al., 1983) and a pronounced increase in precipitation for the Chew Bahir basin suggests overflow for this interval (Foerster et al., 2012). Also, a gradual increase terrigenous runoff into Lake Tana is indicated between ca. 8 and 6.7 ka, and indicates progressive increases in rainfall for the Ethiopian Highlands (Fig. 12b; Marshall et al., 2011). Water level is inferred to overtop the sill elevation for Lake Suguta between ca. 8 and 7.4 ka (Fig. 13c), yet Lake Nakuru-Elmenteita is inferred to be low (Fig. 13e; Richardson and Dussinger, 1987) which suggests wet conditions were isolated north of the Kenyan Highlands. Another oscillation for Lake Turkana up to >70 m at ca. 7.0 ka may reflect increased input from the Kenyan lake system. This peak is coincident with an inferred high stand for Lake Nakuru-Elmenteita between ca. 7 and 6.2 ka (Richardson and Dussinger, 1987), and discharge from Lake Suguta (Garcin et al., 2009; Junginger et al., 2013). A low stand for Lake Turkana to <40 m between ca. 6.8 and 6.6 ka, may be in response to a brief drought in Ethiopia, with slight regression in water level for lakes Ziway-Shala (Gillespie et al., 1983) and Abhe (Gasse and Van Campo, 1994), and drying indicated at Chew Bahir (Foerster et al., 2012). The prominent oscillation of water level to >90 m at ca. 6.4 ka for Lake Turkana appears coincident with the termination of a proposed outflow period from ca. 8.3 to 6.5 ka in the revised record from Lake Suguta (Junginger et al., 2013). High lake stands are also inferred between ca. 6.5 and 6 ka ago for Lakes Abbe (Gasse and Van Campo, 1994) and Ziway-Shala (Gillespie et al., 1983), which may indicate overflow from Lakes Abaya-Chamo into Lake Chew Bahir and into Lake Turkana. Grove et al. (1975) identified large quantities of *in situ* paired *Etheria elliptica*, which gave a  $^{14}\text{C}$  age of  $6.45 \pm 0.12$  cal. ka BP, in sediments associated with the wave washing at the transgressive limit for Lake Chew Bahir (see Fig. 13; solid black arrow); consistent with a period of elevated

discharge into the Chew Bahir basin (Foerster et al., 2012). The spatial distribution of high stands and possible pattern of spillover is consistent with the interpretation of progressive increase in East African Monsoon precipitation over the Ethiopian Highlands (Costa et al., 2014; Forman et al., submitted). In turn, the Kenyan Highlands are thought to have received continual moisture flux from Atlantic sources, reflected in the depleted  $\delta D_{wax}$  signal for sub-equatorial East African sites (Berke et al., 2012a; Tierney and deMenocal, 2013).

The final oscillation for Lake Turkana to >90 m at 5.1 ka may reflect contributions from Ethiopian lakes. Indicated water levels for Lake Nakuru-Elmenteita appear near present low stand levels by ca. 5.5 ka (Richardson and Dussinger, 1987); a hydrologic balance model suggests high water for Lake Suguta may have persisted to ca. 5.4 at the very latest water levels, which precludes contribution from the Kenyan Highlands to the 5.1 ka peak. In turn, high water level for Lake Ziway-Shala is indicated until ca. 5.1 ka, however the duration of this peak is inferred (Gillespie et al., 1983). Also, sedimentary concentrations of potassium from the Chew Bahir core indicate an abrupt resumption of wet conditions at ca. 5.1 ka (Foerster et al., 2012). Elevated titanium content in Lake Tana sediments suggest this wet period abruptly ended ca. 4.9 ka (Marshall et al., 2011). Costa et al. (2014) interpreted abrupt  $\delta D_{wax}$  depletions at Lake Tana until ca. 5 ka to reflect a period of eastward migration for the CAB with a return of Atlantic-derived moisture for the Ethiopian Highlands. Present day low stands for Lake Ziway-Shala and the onset of aridity for the Chew Bahir at ca. 5 ka reflect the last inferred period of spillover into Lake Turkana, and the migration of the CAB to west of the East African Highlands.

### *3.4.2 Linkages between equatorial SSTs and the African Monsoons*

The contribution of Atlantic-derived or recycled moisture to rainfall for East Africa has been broadly inferred from  $\delta D_{wax}$  records revealed from sediment cores from lakes Tana (Fig. 11d;

Costa et al., 2014), Challa (Fig. 11f; Tierney et al., 2011b) and Tanganyika (Fig. 11g; Tierney et al., 2010; Tierney and deMenocal, 2013). Others interpret this signal in nearby Lake Victoria (Fig. 11e) not as a moisture source, but a proxy for total rainfall volume principally from the East African Monsoon, with exclusive moisture derivation from the Western Indian Ocean (Berke et al., 2012a). Broadly, the  $\delta D_{wax}$  chronology (Fig. 11) suggests profound climate variability between ca. 15 and 11 ka, linked to de-glacial events in the North Atlantic Ocean (Heinrich Event 1 and the Younger Dryas), and followed by an abrupt and sustained increase in precipitation for East Africa between ca. 11 and 5.5 ka (Fig. 11), with eastward migration of the CAB. This wet period appears uninterrupted, except for a minor dry event linked to the 8.2 ka meltwater event in the North Atlantic (Alley et al., 1997). Elevated moisture flux derived from Atlantic Ocean is repeatedly implicated in high stands for East African lakes during the AHP (Tierney et al., 2011b). In turn, enrichment of  $\delta D_{wax}$  between ca. 6 and 5 ka is interpreted as a decoupling of Atlantic moisture with westward migration of the CAB (Junginger et al., 2013; Costa et al., 2014) resulting in widespread mid-Holocene drying and low stands for East African lakes.

There is compelling evidence that SSTs in the Equatorial Atlantic Ocean modulated the intensity of the West African Monsoon for much of the Pleistocene (Scheffuß et al., 2003; Weldeab et al., 2007). Similar controls have been inferred for the past ca. 15 ka from  $\delta D_{wax}$  and  $\delta^{13}C_{wax}$  proxies (Scheffuß et al., 2005; Collins et al., 2013) and from a combined analysis of terrestrial and marine proxies from sediment cores from off the west coast of Africa (Marret et al., 2006). Well-dated sediment records from lakes Bosumtwi (Shanahan et al., 2006) and Tanganyika (Tierney et al., 2010) also document substantial hydrologic changes between ca. 15 and 4 ka. These studies of marine and lacustrine archives infer an increased flux of Atlantic-

derived moisture to West and Central Africa between ca. 15 to 6 ka, with a transition between ca. 4 and 3 ka to dry conditions.

Interestingly, abrupt cessation of this flux is inferred at ca. 14.5 with H1, at ca. 12 ka with the YD and between 8.5 to 7.5 ka, linked to the 8.2 ka meltwater event and associated with abrupt cooling in the North Atlantic Ocean (Alley et al., 1997). Resulting evidence of drying is observed in East Africa like widespread lake low stands (Gasse, 2000; Weldeab et al., 2005; Garcin et al., 2012; Junginger et al., 2013), enrichment of  $\delta D_{\text{wax}}$  records (Tierney and deMenocal, 2013; Costa et al., 2014), reduced surface runoff (Marshall et al., 2011; Berke et al., 2012a; Foerster et al., 2012) and a dust spike in the Kilimanjaro ice cores at ca. 8 ka (Thompson et al., 2002), though this record is not well dated. These intervals of drying appear synchronous with low stands for Lake Turkana (Fig. 10). In addition, droughts post ca. 8 ka in Africa have been associated with decreased SSTs in the Equatorial Atlantic Ocean, primarily deduced from  $\delta^{18}\text{O}$  values and changes in Mg/Ca ratios of foraminifera (Weldeab et al., 2005; Weldeab et al., 2007). Significant drought periods are inferred at ca. 7.5 to 8.7 ka, 6.5 to 5.7 ka and 4.4 to 2.5 ka, which are broadly consistent with low lake stands for many lakes in East Africa (Weldeab et al., 2005) and this record of water levels for Lake Turkana (Fig. 10). Mechanistic explanation for depressed precipitation for East Africa and drought involves a zonally contracted Western African Monsoon and a westward deflection of the CAB (Nicholson, 2000b; Tierney et al., 2011b; Costa et al., 2014).

An additional source of increased moisture flux to East Africa is linked to relatively warm SSTs in the Western Indian Ocean and cool SSTs for the Eastern Indian Ocean, reflected in the convective strength of the East African Monsoon and westerly deflection of the Congo Air

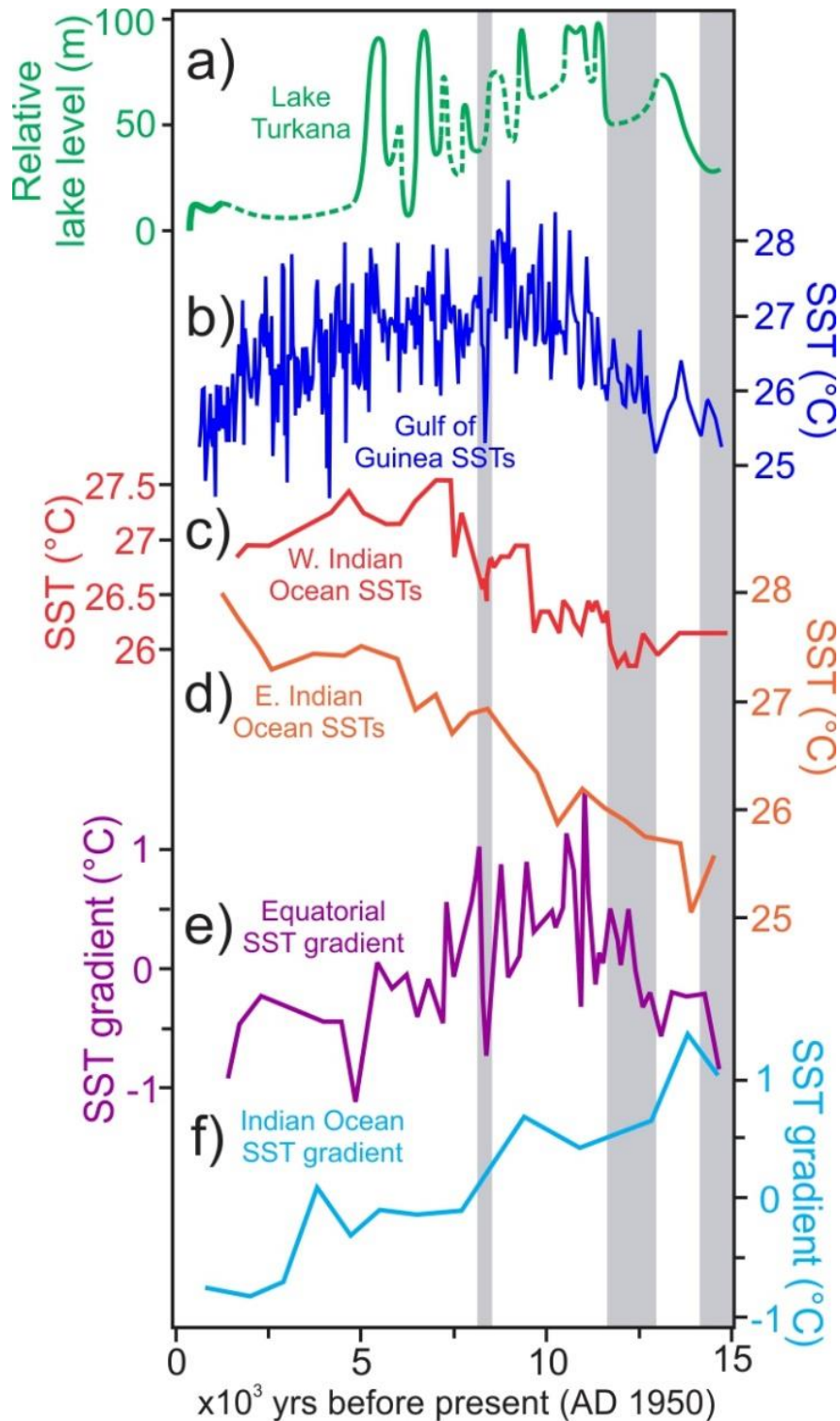


**Figure 14.** Equatorial sea surface temperature records. **(A)** Lake Turkana water levels for comparison. **(B)** Gulf of Guinea SSTs, from Mg/Ca ratios on planktonic forams (Weldeab et al., 2007). **(C)** Western Indian Ocean SST record, based on alkenones (Bard et al., 1997). **(D)** Eastern Indian Ocean SST record, from Mg/Ca ratios on planktonic forams (Mohtadi et al., 2010). **(E)** Cross-continental SST gradient for equatorial Africa, reconstructed by subtracting (C) from (B). **(F)** zonal Indian Ocean SST gradient, reconstructed by subtracting (D) from (C), from Berke et al. (2012).

Boundary (Tierney et al., 2011b; Junginger et al., 2013; Costa et al., 2014). Elevated precipitation during the “short rains”, linked to warm SSTs adjacent to East Africa, is implicated in recent transgressions for many East African lakes (Becker et al., 2010; Bloszies and Forman, submitted), thus it is reasonable to infer a possible connection between elevated adjacent SSTs and high stands in the Holocene and late-Pleistocene (Marchant et al., 2007; Tierney et al., 2011b; Berke et al., 2012a; Forman et al., submitted). A zonal SST gradient for the past ca. 15 ka (Fig. 14f), reconstructed by subtracting SSTs for the Eastern Indian Ocean (Mg/Ca on planktonic forams; Fig. 14d; Mohtadi et al., 2010) from inferred SSTs (alkenones; Bard et al., 1997) for the western Indian Ocean, suggests a peak positive gradient of  $\sim 1^\circ \text{C}$  at ca. 15 ka declining to zero by 5 ka; this progressive switch in SST gradient is interpreted to reflect a progressive weakening of the East African Monsoon, with the onset of drying at ca. 5 ka (Berke et al., 2012a). However, this calculated SST gradient change is small, within the margin error for paleo-thermometry (Bard et al., 1997; Mohtadi et al., 2010), and considerably less than west to east temperature differences associated with historic SSTs variability (e.g. Saji et al., 1999; Ihara et al., 2008; Ummenhofer et al., 2009). The switch in the SST gradient at ca. 5 ka appears synchronous with a bifurcation in periodicities of paleo-ENSO between ca. 7 to 4 ka, identified in analysis of terrigenous content in a freeze-core from Lake Pallcacocha in the western equatorial Andes (Moy et al., 2002); this muted variability prior to ca. 5 ka, in the early Holocene, has been linked to a reduced west to east zonal SST gradient and a weakening of the Pacific Walker Circulation (Rodbell et al., 1999).

### *3.4.2 East African hydroclimate for the past 15 ka reflected in water levels for Lake Turkana*

This reconstruction depicts variable water levels for Lake Turkana between ca. 14.5 and 4.5 ka (Fig. 10) which are interpreted to reflect differential moisture contributions from the Atlantic

and Indian oceans. This linkage is deduced from the numerous and broadly synchronous  $\delta D_{\text{wax}}$  records (Fig. 11), various proxies for precipitation and surface runoff (Fig. 12) and equatorial SSTs proxies for the Eastern Atlantic Ocean (Fig. 14b; Weldeab et al., 2007) and Indian Ocean (Figs. 14c and 14d; Bard et al., 1997; Mohtadi et al., 2010).

A transgression to >70 m is depicted for Lake Turkana at between ca. 14.4 and 13 ka, and may reflect moisture contribution from Atlantic and Indian-derived sources. Ocean surface temperatures rebounded by  $\sim 1^\circ \text{C}$  for the Eastern Atlantic (Weldeab et al., 2007) and western Indian oceans (Bard et al., 1997) directly following H1, at ca. 14.5 ka. An abrupt 20‰  $\delta D_{\text{wax}}$  depletion is revealed post ca. 14.5, in a sediment core from the Gulf of Aden, which indicates a resumption of the East African Monsoon in <500 yrs (Tierney and deMenocal, 2013). Further, a  $\delta D_{\text{wax}}$  depletion of 10‰ is observed from ca. 15 to 14.5 ka in a sediment core from the Congo River delta, which is interpreted to reflect an increase in West African Monsoon rainfall (Schefuß et al., 2005). Also, surface runoff proxies broadly infer wet conditions post ca. 15 ka (Verschuren et al., 2009; Marshall et al., 2011; Foerster et al., 2012). However, lacustrine  $\delta D_{\text{wax}}$  records from East Africa are discordant between ca. 15 and 13 ka. Sediments for lakes Victoria (Berke et al., 2012a), Challa (Tierney et al., 2011b) and Tanganyika (Tierney et al., 2010) reflect no change in depleted  $\delta D_{\text{wax}}$  ( $\sim 120\text{‰}$ ), which suggests sustained precipitation, with possible Atlantic-derived moisture. In turn, Lake Tana sediments record a sustained  $\sim 50\text{‰}$  depletion for Lake Tana between ca. 14 and 13 ka (Costa et al., 2014). This asynchronistic depletion may signal the presence of Atlantic-derived moisture over the Kenyan Highlands but not over far eastern Africa. Precipitation may have increased with gradually increased advection into the Ethiopian Highlands post 14 ka. Wet conditions are reflected in high stands for Ethiopian lakes

at ca. 13.5 ka, and an inferred spillover from the lakes Chamo, Abaya and Chew Bahir into the Lake Turkana Basin.

The Younger Dryas period appears in multiple lacustrine and oceanic proxies as ubiquitously dry for sites across equatorial Africa (cf. Schefuß et al., 2005; Berke et al., 2012a; Tierney and deMenocal, 2013). Water level for Lake Turkana during the YD appears to have fell by >25 m, to below 50 m. Between ca. 12.8 and 12.5 ka, SSTs for the Gulf of Guinea cooled to ~25° C (Weldeab et al., 2007). In turn, this cool SST interval appears ~1 ka longer for the Western Indian Ocean, with surface temperature of 26° C to 11.5 ka (Bard et al., 1997). A metric of SST gradient across equatorial Africa (Fig. 14e), determined by subtracting inferred SSTs for the Western Indian Ocean (Bard et al., 1997) from Gulf of Guinea SSTs (Weldeab et al., 2007), shows a shift during the YD, with SSTs warming to ~1° C higher in the Atlantic Ocean. Proxies for surface water runoff depict this period as dry for lakes Challa (Verschuren et al., 2009), Tana (Marshall et al., 2011) and Chew Bahir (Foerster et al., 2012). Also, the  $\delta D_{wax}$  analysis of sediments for many East African lakes like Challa and Tanganyika show rapid enrichment during the YD, which indicates drought and increased Indian Ocean moisture (Tierney et al., 2010; Tierney et al., 2011b). Conversely, Lake Tana sediments depict pronounced depletion (>40‰) between 12.5 and 11.8 ka (Costa et al., 2014), which indicates the Ethiopian Highlands received continual Atlantic moisture. This discrepancy suggests the CAB may have been altered during the YD, with convergence over the Ethiopian Highlands and migration west of the Kenyan Highlands.

There is compelling evidence after the YD between ca. 11.6 to 9 ka that precipitation and lake levels increased which may be associated with increased flux of moisture from Atlantic-derived sources (Tierney et al., 2011b). On average,  $\delta D_{wax}$  appears depleted post 11.5 ka (Fig.

11) and the rapid transition from an enriched state during the YD is reflected in proxies for terrestrial runoff (Fig. 12), which suggest an abrupt return of wet conditions between ca. 11.5 and 11.4 ka. In the Western Indian Ocean, SSTs rebounded abruptly by  $\sim 0.5^\circ\text{C}$  at 11.5 ka (Bard et al., 1997), and a high stand to  $>95$  at 11.2 ka for Lake Turkana may be linked to the resumption of the East African Monsoon (Garcin et al., 2007). Lacustrine  $\delta D_{\text{wax}}$  proxies between 11 and 8.5 ka for East Africa suggest sustained depletion, which may reflect a constant westerly flux of moisture (Tierney et al., 2011b). Ocean surface temperatures for the Gulf of Guinea increased  $\sim 2.5^\circ\text{C}$  following the YD to a peak of  $28.5^\circ\text{C}$  at ca. 9 ka (Weldeab et al., 2005), which suggests a progressive increase in the strength and westward penetration of the West African Monsoon (Garcin et al., 2007). However, Mg/Ca ratios for planktonic foraminifera from Gulf of Guinea sediments depict fluctuating SSTs for this interval (Weldeab et al., 2007). This variability appears to have influenced the severity and westward extent of the West African Monsoon, captured by a  $\delta D_{\text{wax}}$  record of sediments from Congo River delta (Schefuß et al., 2005). In turn, SSTs for the Western Indian Ocean appear consistently between  $27$  and  $26.5^\circ\text{C}$  (Bard et al., 1997). The reconstructed SST gradient between the Atlantic and Indian oceans shows a SST difference  $> 0.75^\circ\text{C}$  at ca. 10.5, 9.2 and 8.5 ka (Fig. 14e), which appears concomitant with high stands for Lake Turkana, and indicate eastward deflections of the CAB.

Suppressed SSTs for the Atlantic Ocean are implicated in a spatially and temporally extended arid period from 8.7 to ca. 7.5 ka, which reflects a significant deviation in a period of “stable” wet conditions for East Africa and the GHA (Weldeab et al., 2007; Marshall et al., 2011; Junginger et al., 2013; Costa et al., 2014). Equatorial SSTs for the Eastern Atlantic Ocean cooled by 2 to  $3^\circ\text{C}$  (Weldeab et al., 2007), and SSTs in the Western Indian Ocean fell  $\sim 0.5^\circ\text{C}$  (Bard et al., 1997), linked to the 8.2 ka meltwater event (Alley et al., 1997); this reflects an abrupt

decrease in the SST gradient (Fig. 14e), potentially linked to a weak CAB. Low water levels are recorded synchronously for lakes Ziway-Shala (Gillespie et al., 1983), Abhe (Gasse and Van Campo, 1994) and Bosumtwi (Shanahan et al., 2006) in West Africa at ca. 8 ka, and appear attendant with proxy inferences for reduced water runoff into Lake Challa (Verschuren et al., 2009) and the Chew Bahir Basin (Foerster et al., 2012), post ca. 8.5 ka. However, the  $\delta D_{\text{wax}}$  signal for this period is spatially diverse. There appears to be no abrupt depletion for lakes Challa (Tierney et al., 2011b) and Victoria (Berke et al., 2012a), yet this may reflect a ~300 yr sampling resolution of lacustrine sediments. A high resolution  $\delta D_{\text{wax}}$  record from Lake Tanganyika shows a 10 to 15‰ enrichment between ca. 8.5 and 8 ka (Fig. 11g; Tierney et al., 2010). Also, at Lake Tana this transition is abrupt, with ~60‰ enrichment between ca. 8.5 and 8 ka, with  $\delta D_{\text{wax}}$  levels to -80‰ which reflects present levels (Costa et al., 2014). Water levels are inferred to fall to <40 m for Lake Turkana, which is a minimum estimate for regression associated with the 8.2 ka meltwater event.

A brief high stand inferred at ca. 7 ka may be associated with amongst the highest measured postglacial SSTs (Bard et al., 1997) in the western Indian Ocean (Fig. 14c), with an enhanced East African Monsoon. The  $\delta D_{\text{wax}}$  record from Lake Tana shows a brief depletion of 30‰ at 7 ka. In turn, depleted  $\delta D_{\text{wax}}$  values from Lake Challa at ca. 7 ka indicate a persistence of Atlantic-derived air (Tierney et al., 2011b), though the record from Lake Victoria shows a progressive enrichment of  $\delta D_{\text{wax}}$  between 8 and 5 ka and thus possibly a lessening influence of Atlantic-derived moisture (Berke et al., 2012a). The  $\delta D_{\text{wax}}$  record from Lake Tana suggests an abrupt cessation of Atlantic-derived air at ca. 8 ka (Costa et al., 2014), yet titanium content, a proxy for surface runoff suggest wet conditions persisted in Ethiopia for another 3 ka (Marshall et al., 2011). Another oscillation to at least 70 m and centered at ca. 6.4 ka may be coincident with high

postglacial SSTs between 6.7 and 6.2 ka in the western Indian Ocean (Fig. 14c; Bard et al., 1997). This apparent concurrence of elevated SSTs may indicate expansion of the Indian Ocean Warm Pool and intensification of the East African Monsoon. Further, enhanced rainfall/runoff in the Western Indian Ocean is indicated between ca. 6.6 and 6.4 ka, from analysis of  $\delta D_{\text{wax}}$  from a sediment core in the Gulf of Aden (Fig. 11b; Tierney and deMenocal, 2013). Also, the ca. 6.4 ka high stand also appears coeval with elevated post-glacial SSTs in the eastern Equatorial Atlantic Ocean SSTs (Fig. 14b; Weldeab et al., 2005) and reinforces the likelihood of the flux of Atlantic-derived-moisture into East Africa. This lake level high may be coeval with a significant decrease (1- 3 ‰) in  $\delta^{18}\text{O}$  values at ca. 6.3 ka for a stalagmite from southern Oman, which likely reflects the southern displacement of the mean latitudinal position of the summer ITCZ for the Saudi Peninsula to  $\sim 23^\circ \text{N}$  (Fleitmann et al., 2003). This compression of the ITCZ may have intensified precipitation in the Turkana Basin. An ensemble mean of 17 atmospheric general circulation models and 11 coupled ocean–atmosphere general circulation for ca. 6 ka ago shows a notable increased precipitation in the northern East African Rift Valley with an ITCZ shift, in response to insolation and SST forcings (Zhao and Harrison, 2012).

Lake level precipitously fell by over 70 m reaching a record low stand by ca. 6 ka which is associated with a regression in SSTs of  $\sim 0.5^\circ \text{C}$  in the western Indian Ocean (Bard et al., 1997) when compared to SSTs ca. 6.5 to 7.0 ka. This period has been previously associated with a declining influence of Atlantic-derived precipitation (cf. Tierney et al., 2011b), and a westward deflection of the CAB (Costa et al., 2014), which is consistent with a drop in SSTs of  $\sim 1^\circ \text{C}$  for ca. 0.8 ka in the Eastern Atlantic Ocean (Weldeab et al., 2005). Additionally, this period is associated with desiccation of lakes Suguta (Junginger et al., 2013) and Nakuru (Richardson and Dussinger, 1987). An inferred transgression for Lake Turkana to  $>50 \text{ m}$ , at 5.8 ka may be linked

to elevated East African Monsoon precipitation, with brief wet conditions indicated by the Gulf of Aden core (Fig. 11b; Tierney and deMenocal, 2013), and runoff proxies from the Chew Bahir (Fig. 12c; Foerster et al., 2012). In turn, a brief increase in SSTs for the Gulf of Guinea to  $\sim 28^{\circ}\text{C}$  at ca. 5.8 ka (Weldeab et al., 2007) suggests increased precipitation associated with a brief eastward deflection of the CAB. The final high stand to  $>90\text{ m}$  at 5.2 ka occurs with a rise of  $\sim 1^{\circ}\text{C}$  for Gulf of Guinea surface temperatures (Weldeab et al., 2007) and peak SSTs to  $\sim 27.5^{\circ}\text{C}$  for the Western Indian Ocean (Bard et al., 1997). A slight  $\delta D_{\text{wax}}$  depletion (Fig. 11d) and indications of elevated runoff (Fig. 12b) at Lake Tana coincide with this peak (Marshall et al., 2011; Costa et al., 2014). In turn, cooler SSTs prevailed in the eastern Indian Ocean (Abram et al., 2009), and warmer SSTs in the western Indian Ocean (Bard et al., 1997), which indicates a strengthened East African Monsoon and encourages increased convergence of the CAB (Costa et al., 2014).

The zonal gradient between equatorial SSTs in the eastern Atlantic and western Indian oceans dropped precipitously after ca. 4.9 ka (Fig. 14e), largely reflecting drops of  $\sim 1.5^{\circ}\text{C}$  in SSTs for the Gulf of Guinea to near present values (Weldeab et al., 2007). A spatial contraction of the Western African Monsoon, a cessation of westerly moisture flux, with a coeval increase in easterly wind shear, may have caused a zonal shift of the CAB to west of the Kenyan and Ethiopian highlands (Costa et al., 2014) and is blamed for the onset of abrupt drought in East Africa (Tierney et al., 2011b). Water balance models for Lake Suguta (Junginger and Trauth, 2013) and probabilistic models based on  $\delta D_{\text{wax}}$  records from lakes Challa and Tanganyika and the Gulf Aden (Tierney and deMenocal, 2013) suggest this transition could have dried East Africa within  $<500$  years, with timing consistent with the ultimate regression for Lake Turkana (Garcin et al., 2012; Forman et al., submitted; this study). At Lake Tanganyika,  $\delta D_{\text{wax}}$

enrichment at ca. 4.8 ka is abrupt (Tierney and deMenocal, 2013) and coeval with a ~100 m regression for Lake Turkana.

Late Holocene water level changes for Lake Turkana and other lakes in East Africa may be principally controlled by the hydroclimatology associated with SSTs variations in the western Indian Ocean post ca. 5 ka , rather than variable moisture flux from Atlantic-derived sources (cf. Abram et al., 2009; Tierney et al., 2013). The persistence of a warm pool adjacent to East Africa is associated with a strengthened East African Monsoon and heightened precipitation, particularly in the southern part of the Turkana Basin (Tierney et al., 2013; Bloszies and Forman, submitted; Forman et al., submitted). Thus, late Holocene water variability reflects a change in volume contributions from the northern and the southern areas of the Lake Turkana Basin. Model results show an increase precipitation in the catchments of the Kerio and Turkwel rivers, rather than flow from the Omo River and may have been an important factor in late Holocene lake level variability (cf. Tierney et al., 2013; Bloszies and Forman, submitted). This potential change in source for lake level fluctuations is particularly poignant because of irrigation, diversion projects, and droughts in the past 20 years have resulted in profoundly reduced relative discharge from the Kerio and Turkwel rivers into Lake Turkana (Avery, 2010).

## 4. Conclusions

### 4.1 Introduction

This chapter is divided in three major sections. The first section summarizes the water level variations for Lake Turkana for the past 15 ka, and the primary methods for the determination of this chronology. The second section summarizes the hydroclimate inferences which are invoked to explain the >80 m oscillations depicted in our reconstructed lake level history. Further, we summarize the contribution of moisture derived from the Atlantic and the Indian oceans to the West and East African monsoons, respectively, and the inferred position of the Congo Air Boundary for specific periods in the past ca. 15 ka: from 15 to 12 ka, between 12 and 8.5 ka, and post 8.5 ka. The third and final section describes areas for potential future research in the Lake Turkana Basin.

### 4.2 Review of findings

An intensive study of relict beaches up to the maximum water level for Lake Turkana reveals up to ten major lake level oscillations greater than 30 m between ca. 14.5 and 4.5 ka. Geomorphic, sedimentological and stratigraphic observations from lacustrine sequences provide elevational constraints on past lake levels. Radiocarbon dating of carefully selected shells with minimal re-transportation from littoral sediments constrains the chronology for lake level changes. In turn, this reconstruction of water level for Lake Turkana has systematically vetted prior constraining ages, which have been ranked by certainty. Previously studied strand plains include Mt. Porr (Forman et al., submitted), South Island (Garcin et al., 2012), Koobi Fora (Owen et al., 1982) and Kibish (Butzer, 1980; Brown and Fuller, 2008). Material from archeological sites with human habitation also provide a maximum constraint for concomitant lake level (Robbins, 1984; Ashley et al., 2011; Beyin, 2011; Hildebrand et al., 2011).

#### 4.2.1 15 to 11 ka

This study reveals increased variability in water level for Lake Turkana post ca. 15 ka, which is a period that has been previously depicted as relatively stable and wet (deMenocal et al., 2000a; Gasse, 2000; Garcin et al., 2012; Tierney and deMenocal, 2013). Water level rose by >45 m between ca. 14.5 and 13 ka to a high stand of at least 72 m, which is linked to an abrupt return of wet conditions post Heinrich Event 1 (H1). Further, this transgression is associated with a rise in SSTs for the Gulf of Guinea and an energized and spatially extended West African Monsoon. Surface temperatures also rose progressively for the Western Indian Ocean, linked to a westward flux of moisture and elevated precipitation over the Kenyan Highlands delivered by the Congo Air Boundary (CAB). Further, this high stand may be associated with wet conditions inferred for the Kenyan lake system, with possible overflow into Lake Turkana. From ca. 13 to 11.4 ka, water level fell to <50 m, coeval with the Younger Dryas Chronozone. Drought during the YD is thought to be widespread for East Africa, and linked to a contracted West and East African monsoon, with suppressed equatorial SSTs indicated for the Gulf of Guinea (Weldeab et al., 2007) and the Western Indian Ocean (Bard et al., 1997).

#### 4.2.2 11 to 8 ka

Peak water level >90 m for Lake Turkana from 11.2 to 10.3 ka was interrupted by a low stand to <70 m at ca. 11 ka. This high stand may reflect resumption of the flux of Atlantic-derived moisture into East Africa (CAB), with elevated precipitation delivered with convection over the Kenyan and Ethiopian highlands. Also, high water level for Lake Turkana during this interval is augmented by overflow from lakes in the Kenyan and Ethiopian highlands, with discharge into the White Nile catchment. A low stand at ~65 m is inferred between ca. 10.3 and 9.3 ka. In turn, between ca. 9 and 8 ka water level for Lake Turkana broadly regressed,

punctuated by two oscillations to >90 m at 9 ka and to ~75 m at 8.4 ka. These high stands are linked to elevated SSTs in the Gulf of Guinea relative to the Western Indian Ocean, which may indicate eastward deflection of the CAB. In turn, low water level inferred to below 40 m from ca. 8.3 to 7.8 ka, reflects widespread drying indicated for East Africa post ca. 8.5 ka, and may be associated with the 8.2 ka meltwater event (Alley et al., 1997). Further, between ca. 11 and 8 ka, SSTs for Gulf of Guinea were suppressed, which supports a contraction of the West African Monsoon and westward deflection of the CAB (cf. Marshall et al., 2011; Tierney et al., 2011b; Costa et al., 2014).

#### *4.2.3 8 ka to present*

A water level oscillation for Lake Turkana to at least 60 m at 7.5 ka may be associated with increased SSTs for the Western Indian Ocean, and elevated rainfall over the Ethiopian Highlands from the East African Monsoon. Possible divergent proxy signals for Lake Tana, Ethiopia suggest increasing runoff following ca. 8 ka, concomitant with abrupt  $\delta D_{\text{wax}}$  enrichment (e.g. Marshall et al., 2011; Costa et al., 2014). These signals support a CAB west of the Ethiopian Highlands, and elevated rainfall from the East African Monsoon; this interpretation is consistent with suppressed SSTs for the Gulf of Guinea, and elevated SSTs for the Western Indian Ocean between ca. 8 and 7.4 ka. Interestingly, south of the equator, the CAB may have deflected eastward, with depleted  $\delta D_{\text{wax}}$  for lakes Victoria (Berke et al., 2012a), Challa (Tierney et al., 2011b) and Tanganyika (Tierney et al., 2010), despite possible drying indicated for Lake Challa (Verschuren et al., 2009).

Between ca. 7.6 and 6 ka, water level for Lake Turkana is inferred to at least 70 m at ca. 7 ka and to >90 m at ca. 6.4 ka, potentially amplified by overflow from the Kenyan and Ethiopian lake systems. These oscillations are interpreted to reflect periodic eastward deflection of the

CAB over the Ethiopian Highlands, with moisture advection from the Atlantic Ocean for the Kenyan Highlands. Further, these oscillations are coincident with the warmest ( $>27.5^{\circ}\text{C}$ ) post-glacial SSTs for the Western Indian Ocean, which supports strengthened East African Monsoon rainfall inferred for areas to the South of Lake Turkana; discharge from the Kenyan lake system into Lake Turkana is likely. In turn, a low stand to below 35 m between ca. 6.8 and 6.6 ka may be associated with lower SSTs in the Gulf of Guinea, with coeval drying indicated for the Chew Bahir Basin.

A water level regression between ca. 6.3 and 6.0 ka to a low stand  $<10\text{ m}$  by ca. 6.0 ka reflects the low lake level during the African Humid Period, and may reflect drying for the Kenyan Highlands. This interval is coincident with the desiccation of Lakes Suguta and the isolation of Lake Nakuru from Lake Elmenteita, which may reflect suppressed SSTs for the Western Indian and Eastern Atlantic oceans.

Two transgressions to above 40 m for Lake Turkana are inferred between ca. 6 and 4.6 ka, with water level to at least 50 m at ca. 5.8 ka, and  $>90\text{ m}$  at ca. 5.1 ka. The earlier water level oscillation is associated with a brief SST warming for the Gulf of Guinea, reflected in  $\delta\text{D}_{\text{wax}}$  depletion for lakes Challa and Tanganyika, and suggests an eastward deflection of the CAB. In turn, the latter transgression to  $>90\text{ m}$  may reflect spatial expansion of the West and East African monsoons with near-synchronous warming of surface waters for the Eastern Atlantic and Western Indian Ocean. Lake level fell precipitously to below 20 m by ca. 4.6 ka and subsequent transgressions appear to have not risen above this level for the remainder of the Holocene.

The abrupt transition to late-Holocene aridity appears to reflect a decoupling with Atlantic-moisture flux as previously thought (cf. Tierney et al., 2011b; Forman et al., submitted).

However, this transition appears asynchronous for East Africa and highly variable between ca. 6 and 4.5 ka, which is inconsistent with a previously proposed hydroclimate bifurcation for Africa at 5 ka (cf. deMenocal et al., 2000a). The high amplitude centennial-scale oscillations of Lake Turkana ca. 6 and 5 ka reflect brief pulses of Atlantic-derived moisture, which effectively ended ca. 5 ka (cf. Junginger et al., 2013; Tierney and deMenocal, 2013). Post 4.5 ka, hydroclimate variability for East Africa may be dominated by the Indian Ocean and associated easterly moisture flux, with migration of the CAB to the west. There were two modest high stands for Lake Turkana in the past ca. 1 ka, between ~ 12 and 20 m with one centered at 830 yr BP and the latest <100 yr BP, the latter is consistent with the historic record of lake level variability (cf. Butzer, 1971; Bloszies and Forman, submitted). Late Holocene and historic lake level changes of < 20 m in amplitude principally reflect precipitation variability linked to SSTs in the Western Indian Ocean, which has been implicated in modulating the strength of the East African Monsoon.

#### **4.4 Future work**

Many recent studies have documented hydroclimate variability for East Africa between 15 and 5 ka, associated with the AHP. This study attempts to characterize the hydrologic variability for Lake Turkana, which integrates precipitation to the Ethiopian and Kenyan highlands delivered by the East and West African monsoons. However, further research is required to quantify the ultimate source of moisture and hydroclimate dynamics associated with water level oscillations for Lake Turkana. Several key areas of future work include:

- 1) Analyses of the stable isotopic content of lake and oceanic sediments for many sites in East Africa provide unique insight into the variability and source of precipitation during the late-Quaternary (e.g. Schefuß et al., 2005; Berke et al., 2012a; Tierney and

deMenocal, 2013). Attempts to recover lake bed sediments for Lake Turkana have been problematic and the oldest recovered cores date to a maximum age of ca. 6 ka (Halfman et al., 1994; Mohammed et al., 1995; Berke et al., 2012b). Thus, isotopic analysis ( $\delta^{18}\text{O}$  and  $\delta^{13}\text{C}$ ) of lacustrine shells recovered from the western strand plain during this field season at Lake Turkana may yield a stable isotopic record which may span >15 ka.

Finally, a stable isotope record, when combined with associated water level constraints (site sedimentology, age/elevation, etc.), may provide insight on the isotopic content of water for Lake Turkana.

- 2) Hydrological models have been conducted previously for Lake Turkana with primary focus on seasonal and historical hydroclimate variability (Cerling, 1986; Ricko et al., 2011; Velpuri et al., 2012). In turn, several recent studies have investigated the basin constraints for profound hydrologic variability for lakes Suguta (Borchardt and Trauth, 2012; Junginger and Trauth, 2013) and Nakuru (Dühnforth et al., 2006). A hydrologic model for Lake Turkana would greatly benefit the understanding of abrupt water level changes documented in this study. This model would propose hydrologic constraints for the Lake Turkana Basin, and evaluate probable rates of water level transgression and regression. Finally, this model would incorporate scenarios for potential overflow from the Ethiopian and Kenyan highlands and evaluate the potential for discharge of Lake Turkana into the White Nile catchment.
- 3) The record of water level changes for Lake Turkana for the past ca. 15 ka is discontinuous, with many significant temporal gaps in our chronology. Further field study is required to fill these breaks in the reconstructed record. Specific sites for further study may improve resolution; these sites include the northwest shoreline of Lake

Turkana, and additional study of the western strand plain. In turn, periods of spillover of Lake Turkana into the White Nile catchment are unclear, and largely inferred from sampling of littoral sediments associated with maximum lake levels. A field investigation at the basin sill in the Ilemi Triangle would greatly improve the understanding of the nature and timing of spillover. Finally, utilization of optical dating of fluvial features may compliment  $^{14}\text{C}$  dating of shells from littoral and fluvial deposits.

- 4) Finally, this study presents a qualitative argument for two systems of interconnected lakes ultimately discharging into the Turkana Basin at periods during the last 15 ka. Field surveys of the Lake Suguta and Chew-Bahir basin sills, with sampling of material for  $^{14}\text{C}$  and OSL dating would quantify these periods and help assess frequency and fidelity of these proposed hydro-connections.

## CITED LITERATURE

- Abdallah, A.M., Barton, D.R., 2003. Environmental Factors Controlling the Distributions of Benthic Invertebrates on Rocky Shores of Lake Malawi, Africa. *Journal of Great Lakes Research* 29, Supplement 2, 202-215.
- Abram, N.J., McGregor, H.V., Gagan, M.K., Hantoro, W.S., Suwargadi, B.W., 2009. Oscillations in the southern extent of the Indo-Pacific Warm Pool during the mid-Holocene. *Quaternary Science Reviews* 28, 2794-2803.
- Alley, R.B., Mayewski, P.A., Sowers, T., Stuiver, M., Taylor, K., Clark, P.U., 1997. Holocene climatic instability: A prominent, widespread event 8200 yr ago. *Geology* 25, 483-486.
- Amaral, P., Vincens, A., Guiot, J., Buchet, G., Deschamps, P., Doumnang, J.-C., Sylvestre, F., 2013. Palynological evidence for gradual vegetation and climate changes during the African Humid Period termination at 13° N from a Mega-Lake Chad sedimentary sequence. *Climate of the Past* 9, 223-241.
- Ashley, G.M., Ndiema, E.K., Spencer, J.Q.G., Harris, J.W.K., Kiura, P.W., 2011. Paleoenvironmental context of archaeological sites, implications for subsistence strategies under Holocene climate change, northern Kenya. *Geoarchaeology* 26, 809-837.
- Avery, S., 2010. Hydrological impacts of Ethiopia's Omo basin on Kenya's lake Turkana water levels and fisheries. African Development Bank, Tunis, p. 146.
- Bard, E., Rostek, F., Sonzogni, C., 1997. Interhemispheric synchrony of the last deglaciation inferred from alkenone palaeothermometry. *Nature* 385, 707-710.
- Becker, M., Llovel, W., Cazenave, A., Güntner, A., Crétaux, J.-F., 2010. Recent hydrological behavior of the East African great lakes region inferred from GRACE, satellite altimetry and rainfall observations. *Comptes Rendus Geoscience* 342, 223-233.
- Berger, A., Loutre, M.-F., 1991. Insolation values for the climate of the last 10 million years. *Quaternary Science Reviews* 10, 297-317.
- Berger, A., Loutre, M., Mélice, J., 2006. Equatorial insolation: from precession harmonics to eccentricity frequencies. *Climate of the Past* 2, 131-136.
- Berke, M.A., Johnson, T.C., Werne, J.P., Grice, K., Schouten, S., Sinninghe Damsté, J.S., 2012a. Molecular records of climate variability and vegetation response since the Late Pleistocene in the Lake Victoria basin, East Africa. *Quaternary Science Reviews* 55, 59-74.

- Berke, M.A., Johnson, T.C., Werne, J.P., Schouten, S., Sinninghe Damsté, J.S., 2012b. A mid-Holocene thermal maximum at the end of the African Humid Period. *Earth and Planetary Science Letters* 351–352, 95-104.
- Beuning, K.R., Talbot, M.R., Kelts, K., 1997. A revised 30,000-year paleoclimatic and paleohydrologic history of Lake Albert, East Africa. *Palaeogeography, Palaeoclimatology, Palaeoecology* 136, 259-279.
- Beyin, A., 2011. Recent archaeological survey and excavation around the Greater Kalokol Area, west side of Lake Turkana: preliminary findings. *Nyame Akuma* 75, 40-50.
- Birkett, C.M., 1995. The contribution of TOPEX/POSEIDON to the global monitoring of climatically sensitive lakes. *Journal of Geophysical Research-Oceans* 100, 25179-25204.
- Black, E., Slingo, J., Sperber, K.R., 2003. An Observational Study of the Relationship between Excessively Strong Short Rains in Coastal East Africa and Indian Ocean SST. *Monthly Weather Review* 131, 74-94.
- Blanchet, C.L., Tjallingii, R., Frank, M., Lorenzen, J., Reitz, A., Brown, K., Feseker, T., Brückmann, W., 2013. High-and low-latitude forcing of the Nile River regime during the Holocene inferred from laminated sediments of the Nile deep-sea fan. *Earth and Planetary Science Letters* 364, 98-110.
- Bloszies, C.A., Forman, S.L., submitted. Potential relation between equatorial sea surface temperatures and historic water level variability for Lake Turkana, Kenya. *Journal of Hydrology*.
- Borchardt, S., Trauth, M.H., 2012. Remotely-sensed evapotranspiration estimates for an improved hydrological modeling of the early Holocene mega-lake Suguta, northern Kenya Rift. *Palaeogeography, Palaeoclimatology, Palaeoecology* 361, 14-20.
- Braconnot, P., Joussaume, S., Marti, O., De Noblet, N., 1999. Synergistic feedbacks from ocean and vegetation on the African Monsoon response to Mid-Holocene insolation. *Geophysical Research Letters* 26, 2481-2484.
- Broccoli, A.J., Dahl, K.A., Stouffer, R.J., 2006. Response of the ITCZ to Northern Hemisphere cooling. *Geophysical Research Letters* 33, L01702.
- Brown, F.H., Fuller, C.R., 2008. Stratigraphy and tephra of the Kibish Formation, southwestern Ethiopia. *Journal of Human Evolution* 55, 366-403.
- Brown, F.H., Mcdougall, I., 2011. Geochronology of the Turkana depression of northern Kenya and southern Ethiopia. *Evolutionary Anthropology: Issues, News, and Reviews* 20, 217-227.

- Butzer, K., 1980. The Holocene lake plain of North Rudolph, East Africa. *Physical Geography* 1, 42-58.
- Butzer, K.W., 1971. Recent history of an Ethiopian delta: the Omo River and the level of Lake Rudolf. University of Chicago, Dept. of Geography, Chicago.
- Butzer, K.W., Isaac, G.L., Richardson, J.L., Washbourn-Kamau, C., 1972. Radiocarbon Dating of East African Lake Levels. *Science* 175, 1069-1076.
- Butzer, K.W., Thurber, D.L., 1969. Some late Cenozoic sedimentary formations of the Lower Omo Basin. *Nature* 222, 1138-1143.
- Camberlin, P., Okoola, R.E., 2003. The onset and cessation of the "long rains" in eastern Africa and their interannual variability. *Theoretical and Applied Climatology* 75, 43-54.
- Castañeda, I.S., Werne, J.P., Johnson, T.C., 2007. Wet and arid phases in the southeast African tropics since the Last Glacial Maximum. *Geology* 35, 823-826.
- Cerling, T.E., 1986. A mass-balance approach to basin sedimentation: Constraints on the recent history of the Turkana Basin. *Palaeogeography, palaeoclimatology, palaeoecology* 54, 63-86.
- Chase, B.M., Meadows, M.E., Carr, A.S., Reimer, P.J., 2010. Evidence for progressive Holocene aridification in southern Africa recorded in Namibian hyrax middens: implications for African Monsoon dynamics and the African Humid Period. *Quaternary Research* 74, 36-45.
- Clement, A.C., Cane, M.A., Seager, R., 2001. An orbitally driven tropical source for abrupt climate change. *Journal of Climate* 14.
- Cohen, A.S., 1986. Distribution and faunal associations of benthic invertebrates at Lake Turkana, Kenya. *Hydrobiologia* 141, 179-197.
- Collins, J.A., Schefuß, E., Mulitza, S., Prange, M., Werner, M., Tharammal, T., Paul, A., Wefer, G., 2013. Estimating the hydrogen isotopic composition of past precipitation using leaf-waxes from western Africa. *Quaternary Science Reviews* 65, 88-101.
- Collins, M.J., Nielsen-Marsh, C.M., Hiller, J., Smith, C., Roberts, J., Prigodich, R., Wess, T., Csapo, J., Millard, A.R., Turner-Walker, G., 2002. The survival of organic matter in bone: a review. *Archaeometry* 44, 383-394.
- Costa, K., Russell, J., Konecky, B., Lamb, H., 2014. Isotopic reconstruction of the African Humid Period and Congo Air Boundary migration at Lake Tana, Ethiopia. *Quaternary Science Reviews* 83, 58-67.
- Damsté, J.S.S., Verschuren, D., Ossebaar, J., Blokker, J., van Houten, R., van der Meer, M.T., Plessen, B., Schouten, S., 2011. A 25,000-year record of climate-induced changes in lowland

vegetation of eastern equatorial Africa revealed by the stable carbon-isotopic composition of fossil plant leaf waxes. *Earth and Planetary Science Letters* 302, 236-246.

- De Kock, K., Wolmarans, C., 2007. Distribution and habitats of *Corbicula fluminalis africana* (Mollusca: Bivalvia) in South Africa. *Water Sa* 33, 709-716.
- deMenocal, P., Ortiz, J., Guilderson, T., Adkins, J., Sarnthein, M., Baker, L., Yarusinsky, M., 2000a. Abrupt onset and termination of the African Humid Period:: rapid climate responses to gradual insolation forcing. *Quaternary Science Reviews* 19, 347-361.
- deMenocal, P., Ortiz, J., Guilderson, T., Sarnthein, M., 2000b. Coherent high-and low-latitude climate variability during the Holocene warm period. *Science* 288, 2198-2202.
- Diro, G., Grimes, D.I.F., Black, E., 2011. Teleconnections between Ethiopian summer rainfall and sea surface temperature: part I—observation and modelling. *Climate dynamics* 37, 103-119.
- Dühnforth, M., Bergner, A.G., Trauth, M.H., 2006. Early Holocene water budget of the Nakuru-Elmenteita basin, central Kenya Rift. *Journal of Paleolimnology* 36, 281-294.
- Duren, R.M., Wong, E., Breckenridge, B., Shaffer, S.J., Duncan, C., Tubbs, E.F., Salomon, P.M., 1998. Metrology, attitude, and orbit determination for spaceborne interferometric synthetic aperture radar, *Aerospace/Defense Sensing and Controls. International Society for Optics and Photonics*, pp. 51-60.
- Fairbanks, R.G., Mortlock, R.A., Chiu, T.C., Cao, L., Kaplan, A., Guilderson, T.P., Fairbanks, T.W., Bloom, A.L., Grootes, P.M., Nadeau, M.J., 2005. Radiocarbon calibration curve spanning 0 to 50,000 years BP based on paired  $^{230}\text{Th}$  /  $^{234}\text{U}$  /  $^{238}\text{U}$  and  $^{14}\text{C}$  dates on pristine corals. *Quaternary Science Reviews* 24, 1781-1796.
- Farr, T.G., Rosen, P.A., Caro, E., Crippen, R., Duren, R., Hensley, S., Kobrick, M., Paller, M., Rodriguez, E., Roth, L., 2007. The shuttle radar topography mission. *Reviews of geophysics* 45.
- Feibel, C.S., 2003. Stratigraphy and depositional history of the Lothagam sequence. . Columbia University Press, New York, pp. 17-29.
- Fleitmann, D., Burns, S.J., Mudelsee, M., Neff, U., Kramers, J., Mangini, A., Matter, A., 2003. Holocene forcing of the Indian monsoon recorded in a stalagmite from southern Oman. *Science* 300, 1737-1739.
- Foerster, V., Junginger, A., Langkamp, O., Gebu, T., Asrat, A., Umer, M., Lamb, H.F., Wennrich, V., Rethemeyer, J., Nowaczyk, N., Trauth, M.H., Schaebitz, F., 2012. Climatic change recorded in the sediments of the Chew Bahir basin, southern Ethiopia, during the last 45,000 years. *Quaternary International* 274, 25-37.

- Forman, S.L., Wright, D.K., Bloszies, C.A., Pierson, J., Gomez-Mazzocco, J., submitted. Variations in water level for Lake Turkana in the past 8500 years near Mt. Porr, Kenya and the transition from the African Humid Period to Holocene aridity. *Quaternary Science Reviews*.
- Ganopolski, A., Kubatzki, C., Claussen, M., Brovkin, V., Petoukhov, V., 1998. The influence of vegetation-atmosphere-ocean interaction on climate during the mid-Holocene. *Science* 280, 1916-1919.
- Garcin, Y., Junginger, A., Melnick, D., Olago, D.O., Strecker, M.R., Trauth, M.H., 2009. Late Pleistocene–Holocene rise and collapse of Lake Suguta, northern Kenya Rift. *Quaternary Science Reviews* 28, 911-925.
- Garcin, Y., Melnick, D., Strecker, M.R., Olago, D., Tiercelin, J.-J., 2012. East African mid-Holocene wet–dry transition recorded in palaeo-shorelines of Lake Turkana, northern Kenya Rift. *Earth and Planetary Science Letters* 331–332, 322-334.
- Garcin, Y., Vincens, A., Williamson, D., Buchet, G., Guiot, J., 2007. Abrupt resumption of the African Monsoon at the Younger Dryas—Holocene climatic transition. *Quaternary Science Reviews* 26, 690-704.
- Gasse, F., 2000. Hydrological changes in the African tropics since the Last Glacial Maximum. *Quaternary Science Reviews* 19, 189-211.
- Gasse, F., Chalié, F., Vincens, A., Williams, M.A., Williamson, D., 2008. Climatic patterns in equatorial and southern Africa from 30,000 to 10,000 years ago reconstructed from terrestrial and near-shore proxy data. *Quaternary Science Reviews* 27, 2316-2340.
- Gasse, F., Van Campo, E., 1994. Abrupt post-glacial climate events in West Asia and North Africa monsoon domains. *Earth and Planetary Science Letters* 126, 435-456.
- Gathogo, P.N., Brown, F.H., McDougall, I., 2008. Stratigraphy of the Koobi Fora Formation (Pliocene and Pleistocene) in the Loiyangalani region of northern Kenya. *Journal of African Earth Sciences* 51, 277-297.
- Genner, M.J., Michel, E., 2003. Fine-scale habitat associations of soft-sediment gastropods at Cape Maclear, Lake Malawi. *Journal of Molluscan Studies* 69, 325-328.
- Giannini, A., Saravanan, R., Chang, P., 2003. Oceanic forcing of Sahel rainfall on interannual to interdecadal time scales. *Science* 302, 1027-1030.
- Gillespie, R., Street-Perrott, F.A., Switsur, R., 1983. Post-glacial arid episodes in Ethiopia have implications for climate prediction.

- Goddard, L., Graham, N.E., 1999. Importance of the Indian Ocean for simulating rainfall. *Journal of Geophysical Research* 104, 19,099-019,116.
- Grove, A., Street, F.A., Goudie, A., 1975. Former lake levels and climatic change in the Rift Valley of southern Ethiopia. *Geographical Journal*, 177-194.
- Halfman, J.D., Johnson, T.C., 1988. High-resolution record of cyclic climatic change during the past 4 ka from Lake Turkana, Kenya. *Geology* 16, 496-500.
- Halfman, J.D., Johnson, T.C., Finney, B.P., 1994. New AMS dates, stratigraphic correlations and decadal climatic cycles for the past 4 ka at Lake Turkana, Kenya. *Palaeogeography, Palaeoclimatology, Palaeoecology* 111, 83-98.
- Harvey, C.P.D., Grove, A.T., 1982. A Prehistoric Source of the Nile. *The Geographical Journal* 148, 327-336.
- Hély, C., Braconnot, P., Watrin, J., Zheng, W., 2009. Climate and vegetation: Simulating the African humid period. *Comptes Rendus Geoscience* 341, 671-688.
- Hildebrand, E.A., Shea, J.J., Grillo, K.M., 2011. Four middle Holocene pillar sites in West Turkana, Kenya. *Journal of Field Archaeology* 36, 181-200.
- Hopson, A.J., 1982. Lake Turkana: a report on the findings of the Lake Turkana Project, 1972-1975. Overseas Development Administration London.
- Ihara, C., Kushnir, Y., Cane, M.A., 2008. Warming Trend of the Indian Ocean SST and Indian Ocean Dipole from 1880 to 2004\*. *Journal of Climate* 21, 2035-2046.
- Johnson, T., Halfman, J., Showers, W., 1991. Paleoclimate of the past 4000 years at Lake Turkana, Kenya, based on the isotopic composition of authigenic calcite. *Palaeogeography, Palaeoclimatology, Palaeoecology* 85, 189-198.
- Johnson, T.C., Malala, J.O., 2009. Lake Turkana and its link to the Nile. *The Nile*, 287-304.
- Junginger, A., 2011. East African climate variability on different time scales: the Suguta Valley in the African-Asian Monsoon Domain. PhD Thesis, University of Potsdam, Potsdam, p. 153 pp.
- Junginger, A., Roller, S., Olaka, L.A., Trauth, M.H., 2013. The effects of solar irradiation changes on the migration of the Congo Air Boundary and water levels of paleo-Lake Suguta, Northern Kenya Rift, during the African Humid Period (15–5ka BP). *Palaeogeography, Palaeoclimatology, Palaeoecology*.

- Junginger, A., Trauth, M.H., 2013. Hydrological constraints of paleo-Lake Suguta in the Northern Kenya Rift during the African Humid Period (15–5ka BP). *Global and Planetary Change* 111, 174-188.
- Kinuthia, J., Asnani, G., 1982. A newly found jet in North Kenya (Turkana Channel). *Monthly Weather Review* 110, 1722-1728.
- Korniushin, A.V., 2004. A revision of some Asian and African freshwater clams assigned to *Corbicula fluminalis* (Müller, 1774) (Mollusca: Bivalvia: Corbiculidae), with a review of anatomical characters and reproductive features based on museum collections. *Hydrobiologia* 529, 251-270.
- Kröpelin, S., Verschuren, D., Lézine, A.-M., Eggermont, H., Cocquyt, C., Francus, P., Cazet, J.-P., Fagot, M., Rumes, B., Russell, J., 2008. Climate-driven ecosystem succession in the Sahara: the past 6000 years. *Science* 320, 765-768.
- Kuper, R., Kröpelin, S., 2006. Climate-controlled Holocene occupation in the Sahara: motor of Africa's evolution. *Science* 313, 803-807.
- Lamb, A.L., Leng, M.J., Lamb, H.F., Mohammed, M.U., 2000. A 9000-year oxygen and carbon isotope record of hydrological change in a small Ethiopian crater lake. *The Holocene* 10, 167-177.
- Lamb, H.H., 1966. Climate in the 1960's Changes in the World's Wind Circulation Reflected in Prevailing Temperatures, Rainfall Patterns and the Levels of the African Lakes. *The Geographical Journal* 132, 183-212.
- Lavoie, C., Allard, M., Duhamel, D., 2012. Deglaciation landforms and C-14 chronology of the Lac Guillaume-Delisle area, eastern Hudson Bay: A report on field evidence. *Geomorphology* 159–160, 142-155.
- Leng, M.J., Lamb, A.L., Lamb, H.F., Telford, R.J., 1999. Palaeoclimatic implications of isotopic data from modern and early Holocene shells of the freshwater snail *Melanoides tuberculata*, from lakes in the Ethiopian Rift Valley. *Journal of Paleolimnology* 21, 97-106.
- Liu, Z., Wang, Y., Gallimore, R., Gasse, F., Johnson, T., DeMenocal, P., Adkins, J., Notaro, M., Prentice, I., Kutzbach, J., 2007. Simulating the transient evolution and abrupt change of Northern Africa atmosphere–ocean–terrestrial ecosystem in the Holocene. *Quaternary Science Reviews* 26, 1818-1837.
- Marchant, R., Mumbi, C., Behera, S., Yamagata, T., 2007. The Indian Ocean dipole—the unsung driver of climatic variability in East Africa. *African Journal of Ecology* 45, 4-16.
- Marret, F., Maley, J., Scourse, J., 2006. Climatic instability in west equatorial Africa during the Mid-and Late Holocene. *Quaternary International* 150, 71-81.

- Marshall, M.H., Lamb, H.F., Davies, S.J., Leng, M.J., Kubsa, Z., Umer, M., Bryant, C., 2009. Climatic change in northern Ethiopia during the past 17,000 years: a diatom and stable isotope record from Lake Ashenge. *Palaeogeography, Palaeoclimatology, Palaeoecology* 279, 114-127.
- Marshall, M.H., Lamb, H.F., Huws, D., Davies, S.J., Bates, R., Bloemendal, J., Boyle, J., Leng, M.J., Umer, M., Bryant, C., 2011. Late Pleistocene and Holocene drought events at Lake Tana, the source of the Blue Nile. *Global and Planetary Change* 78, 147-161.
- McDougall, I., Brown, F.H., 2009. Timing of volcanism and evolution of the northern Kenya Rift. *Geological Magazine* 146, 34-47.
- McDougall, I., Feibel, C.S., 1999. Numerical age control for the Miocene-Pliocene succession at Lothagam, a hominoid-bearing sequence in the northern Kenya Rift. *Journal of the Geological Society* 156, 731-745.
- McGregor, G.R., Nieuwolt, S., 1998. *Tropical climatology: an introduction to the climates of the low latitudes*. John Wiley & Sons Ltd.
- Melnick, D., Garcin, Y., Quinteros, J., Strecker, M.R., Olago, D., Tiercelin, J.J., 2012. Steady rifting in northern Kenya inferred from deformed Holocene lake shorelines of the Suguta and Turkana basins. *Earth and Planetary Science Letters*.
- Mohammed, M.U., Bonnefille, R., Johnson, T.C., 1995. Pollen and isotopic records in Late Holocene sediments from Lake Turkana, Kenya. *Palaeogeography, Palaeoclimatology, Palaeoecology* 119, 371-383.
- Mohtadi, M., Lückge, A., Steinke, S., Groeneveld, J., Hebbeln, D., Westphal, N., 2010. Late Pleistocene surface and thermocline conditions of the eastern tropical Indian Ocean. *Quaternary Science Reviews* 29, 887-896.
- Moy, C.M., Seltzer, G.O., Rodbell, D.T., Anderson, D.M., 2002. Variability of El Niño/Southern Oscillation activity at millennial timescales during the Holocene epoch. *Nature* 420, 162-165.
- Nicholson, S., 2000a. Land surface processes and Sahel climate. *Reviews of Geophysics* 38, 117-139.
- Nicholson, S.E., 1988. Historical fluctuations of Lake Victoria and other lakes in the northern Rift Valley of East Africa. *Monographiae Biologicae*, 7-36.
- Nicholson, S.E., 1996. A review of climate dynamics and climate variability in eastern Africa. The limnology, climatology and paleoclimatology of the East African lakes, 25-56.
- Nicholson, S.E., 2000b. The nature of rainfall variability over Africa on time scales of decades to millenia. *Global and planetary change* 26, 137-158.

- Nicholson, S.E., 2008. The intensity, location and structure of the tropical rainbelt over west Africa as factors in interannual variability. *International Journal of Climatology* 28, 1775-1785.
- Nyamweru, C., 1989. New Evidence for the Former Extent of the Nile Drainage System. *The Geographical Journal* 155, 179-188.
- Owen, R.B., Barthelme, J.W., Renaut, R.W., Vincens, A., 1982. Palaeolimnology and archaeology of Holocene deposits north-east of Lake Turkana, Kenya. *Nature* 298, 523-529.
- Owen, R.B., Renaut, R.W., 1986. Sedimentology, stratigraphy and palaeoenvironments of the Holocene Galana Boi Formation, NE Lake Turkana, Kenya. Geological Society, London, Special Publications 25, 311-322.
- Patricola, C., Cook, K., 2007. Dynamics of the West African monsoon under mid-Holocene precessional forcing: regional climate model simulations. *Journal of climate* 20, 694-716.
- Powers, L.A., Johnson, T.C., Werne, J.P., Castañeda, I.S., Hopmans, E.C., Sinninghe Damsté, J.S., Schouten, S., 2005. Large temperature variability in the southern African tropics since the Last Glacial Maximum. *Geophysical Research Letters* 32.
- Reading, H.G., 2009. *Sedimentary environments: processes, facies and stratigraphy*. John Wiley & Sons.
- Renssen, H., Brovkin, V., Fichefet, T., Goosse, H., 2003. Holocene climate instability during the termination of the African Humid Period. *Geophysical Research Letters* 30.
- Renssen, H., Brovkin, V., Fichefet, T., Goosse, H., 2006. Simulation of the Holocene climate evolution in Northern Africa: the termination of the African Humid Period. *Quaternary International* 150, 95-102.
- Richardson, J., Dussinger, R., 1987. Paleolimnology of mid-elevation lakes in the Kenya Rift Valley, *Paleolimnology IV*. Springer, pp. 167-174.
- Richardson, J.L., Richardson, A., 1972. History of an African rift lake and its climatic implications. *Ecological monographs*, 499-534.
- Ricko, M., Carton, J.A., Birkett, C., 2011. Climatic effects on lake basins. Part I: modeling tropical lake levels. *Journal of Climate* 24, 2983-2999.
- Ritchie, J., Eyles, C., Haynes, C.V., 1985. Sediment and pollen evidence for an early to mid-Holocene humid period in the eastern Sahara. *Nature* 314, 352-355.

- Robbins, L., 1984. Late prehistoric and aquatic adaptations west of Lake Turkana, Kenya., In: Clark, J.D., Brandt, S.A. (Eds.), *From hunters to farmers: the causes and consequences of food production in Africa*. University of California Press, Berkeley, pp. pp. 206-211.
- Roberts, N., Taieb, M., Barker, P., Damnati, B., Icole, M., Williamson, D., 1993. Timing of the Younger Dryas event in East Africa from lake-level changes.
- Rodbell, D.T., Seltzer, G.O., Anderson, D.M., Abbott, M.B., Enfield, D.B., Newman, J.H., 1999. An ~15,000-Year Record of El Niño-Driven Alluviation in Southwestern Ecuador. *Science* 283, 516-520.
- Ryner, M., Gasse, F., Rumes, B., Verschuren, D., 2007. Climatic and hydrological instability in semi-arid equatorial East Africa during the late Glacial to Holocene transition: a multi-proxy reconstruction of aquatic ecosystem response in northern Tanzania. *Palaeogeography, Palaeoclimatology, Palaeoecology* 248, 440-458.
- Saji, N., Yamagata, T., 2003. Possible impacts of Indian Ocean dipole mode events on global climate. *Climate Research* 25, 151-169.
- Saji, N.H., Goswami, B.N., Vinayachandran, P.N., Yamagata, T., 1999. A dipole mode in the tropical Indian Ocean. *Nature* 401, 360-363.
- Savage, R.J.G., Williamson, P.G., 1978. The early history of the Turkana Depression. *Geological Society, London, Special Publications* 6, 375-394.
- Schefuß, E., Schouten, S., Jansen, J.F., Damsté, J.S.S., 2003. African vegetation controlled by tropical sea surface temperatures in the mid-Pleistocene period. *Nature* 422, 418-421.
- Schefuß, E., Schouten, S., Schneider, R.R., 2005. Climatic controls on central African hydrology during the past 20,000 years. *Nature* 437, 1003-1006.
- Shanahan, T.M., Overpeck, J.T., Wheeler, C.W., Beck, J.W., Pigati, J.S., Talbot, M.R., Scholz, C.A., Peck, J., King, J.W., 2006. Paleoclimatic variations in West Africa from a record of late Pleistocene and Holocene lake level stands of Lake Bosumtwi, Ghana. *Palaeogeography, Palaeoclimatology, Palaeoecology* 242, 287-302.
- Sombroek, W.G., Braun, H., Pouw, B.J.A., 1982. Exploratory soil map and agro-climatic zone map of Kenya, 1980. Scale 1: 1,000,000. Kenya Soil Survey.
- Stafford, T.W., Hare, P.E., Currie, L., Jull, A.T., Donahue, D., 1990. Accuracy of North American human skeleton ages. *Quaternary Research* 34, 111-120.
- Street-Perrott, F., Marchand, D., Roberts, N., Harrison, S., 1989. Global lake-level variations from 18,000 to 0 years ago: A palaeoclimate analysis. Oxford Univ.(UK). Geography School.

- Street-Perrott, F.A., Roberts, N., 1983. Fluctuations in closed-basin lakes as an indicator of past atmospheric circulation patterns, *Variations in the global water budget*. Springer, pp. 331-345.
- Thomas, D.S.G., Burrough, S.L., 2012. Interpreting geoproxies of late Quaternary climate change in African drylands: Implications for understanding environmental change and early human behaviour. *Quaternary International* 253, 5-17.
- Thompson, L.G., Mosley-Thompson, E., Davis, M.E., Henderson, K.A., Brecher, H.H., Zagorodnov, V.S., Mashiotta, T.A., Lin, P.N., Mikhalenko, V.N., Hardy, D.R., Beer, J., 2002. Kilimanjaro ice core records: Evidence of Holocene climate change in tropical Africa. *Science* 298, 589-593.
- Thompson, T.A., Baedke, S.J., 1997. Strand-plain evidence for late Holocene lake-level variations in Lake Michigan. *Geological Society of America Bulletin* 109, 666-682.
- Tierney, J.E., deMenocal, P.B., 2013. Abrupt Shifts in Horn of Africa Hydroclimate Since the Last Glacial Maximum. *Science* 342, 843-846.
- Tierney, J.E., Lewis, S.C., Cook, B.I., LeGrande, A.N., Schmidt, G.A., 2011a. Model, proxy and isotopic perspectives on the East African Humid Period. *Earth and Planetary Science Letters* 307, 103-112.
- Tierney, J.E., Russell, J.M., Huang, Y., 2010. A molecular perspective on Late Quaternary climate and vegetation change in the Lake Tanganyika basin, East Africa. *Quaternary Science Reviews* 29, 787-800.
- Tierney, J.E., Russell, J.M., Huang, Y., Damsté, J.S.S., Hopmans, E.C., Cohen, A.S., 2008. Northern Hemisphere Controls on Tropical Southeast African Climate During the Past 60,000 Years. *Science* 322, 252-255.
- Tierney, J.E., Russell, J.M., Sinninghe Damsté, J.S., Huang, Y., Verschuren, D., 2011b. Late Quaternary behavior of the East African monsoon and the importance of the Congo Air Boundary. *Quaternary Science Reviews* 30, 798-807.
- Tierney, J.E., Smerdon, J.E., Anchukaitis, K.J., Seager, R., 2013. Multidecadal variability in East African hydroclimate controlled by the Indian Ocean. *Nature* 493, 389-392.
- Toreti, A., Naveau, P., Zampieri, M., Schindler, A., Scoccimarro, E., Xoplaki, E., Dijkstra, H.A., Gualdi, S., Luterbacher, J., 2013. Projections of global changes in precipitation extremes from Coupled Model Intercomparison Project Phase 5 models. *Geophysical Research Letters* 40, 4887-4892.
- Trauth, M.H., Maslin, M.A., Deino, A.L., Junginger, A., Lesoloyia, M., Odada, E.O., Olago, D.O., Olaka, L.A., Strecker, M.R., Tiedemann, R., 2010. Human evolution in a variable

- environment: the amplifier lakes of Eastern Africa. *Quaternary Science Reviews* 29, 2981-2988.
- Ummenhofer, C.C., Sen Gupta, A., England, M.H., Reason, C.J., 2009. Contributions of Indian Ocean sea surface temperatures to enhanced East African rainfall. *Journal of Climate* 22, 993-1013.
- Van Bocxlaer, B., Van Damme, D., 2009. Palaeobiology and evolution of the Late Cenozoic freshwater molluscs of the Turkana Basin: Iridinidae Swainson, 1840 and Etheriidae Deshayes, 1830 (Bivalvia: Etherioidea). *Journal of Systematic Palaeontology* 7, 129-161.
- Velpuri, N.M., Senay, G.B., Asante, K.O., 2012. A multi-source satellite data approach for modelling Lake Turkana water level: calibration and validation using satellite altimetry data. *Hydrol. Earth Syst. Sci.* 16, 1-18.
- Verschuren, D., Damsté, J.S.S., Moernaut, J., Kristen, I., Blaauw, M., Fagot, M., Haug, G.H., Van Geel, B., De Batist, M., Barker, P., 2009. Half-precessional dynamics of monsoon rainfall near the East African Equator. *Nature* 462, 637-641.
- Vétel, W., Le Gall, B., Johnson, T.C., 2004. Recent tectonics in the Turkana Rift (North Kenya): an integrated approach from drainage network, satellite imagery and reflection seismic analyses. *Basin Research* 16, 165-181.
- Vincens, A., Buchet, G., Servant, M., 2010. Vegetation response to the "African Humid Period" termination in Central Cameroon (7° N)—new pollen insight from Lake Mbalang. *Climate of the Past* 6, 281-294.
- Vizy, E.K., Cook, K.H., 2001. Mechanisms by which Gulf of Guinea and eastern North Atlantic sea surface temperature anomalies can influence African rainfall. *Journal of Climate* 14, 795-821.
- Washbourn-Kamau, C.K., 1975. Late Quaternary shorelines of Lake Naivasha, Kenya. *AZANIA: Journal of the British Institute in Eastern Africa* 10, 77-92.
- Weldeab, S., Lea, D.W., Schneider, R.R., Andersen, N., 2007. 155,000 years of West African monsoon and ocean thermal evolution. *Science* 316, 1303-1307.
- Weldeab, S., Schneider, R.R., Kölling, M., Wefer, G., 2005. Holocene African droughts relate to eastern equatorial Atlantic cooling. *Geology* 33, 981-984.
- Williams, A.P., Funk, C., Michaelsen, J., Rauscher, S.A., Robertson, I., Wils, T.H., Koprowski, M., Eshetu, Z., Loader, N.J., 2012. Recent summer precipitation trends in the Greater Horn of Africa and the emerging role of Indian Ocean sea surface temperature. *Climate Dynamics*, 1-22.

- Williams, M., Talbot, M., Aharon, P., Abdl Salaam, Y., Williams, F., Inge Brendeland, K., 2006. Abrupt return of the summer monsoon 15,000 years ago: new supporting evidence from the lower White Nile valley and Lake Albert. *Quaternary Science Reviews* 25, 2651-2665.
- Williams, R., Johnson, A., 1976. Birmingham University radiocarbon dates X. *Radiocarbon* 18, 249-267.
- Wright, D.K., Forman, S.L., 2011. Holocene Occupation of the Mount Porr Strand Plain in Southern Lake Turkana, Kenya. *Nyame Akuma*, 47-62.
- Zhao, Y., Harrison, S., 2012. Mid-Holocene monsoons: a multi-model analysis of the inter-hemispheric differences in the responses to orbital forcing and ocean feedbacks. *Climate dynamics* 39, 1457-1487.

## VITA

### NAME

**CHRISTOPHER A. BLOSZIES**

### EDUCATION

*B.A. in Economics*, University of Chicago, Chicago, Illinois, 2008

*M.S. in Earth and Environmental Sciences*, University of Illinois at Chicago, Chicago, Illinois, 2014

### TEACHING ASSISTANT

Earth Systems, Sedimentary Environments, Field Work in Missouri, Environmental Geomorphology

### PROFESSIONAL SOCIETIES

Geological Society of America (Since Sept. 2012)

American Geophysical Union (Since Jan. 2013)

### AWARDS

Knourek Environmental Scholarship (UIC)

Bodmer International Travel Award (UIC)

Provost Award for Graduate Study (UIC)

Outstanding Teaching Assistant, Academic year 2012-2013 (UIC)

### PUBLICATIONS

**Bloszies, CA**, Forman, SL, Wright, DK. In prep. *Rapid changes in water level for Lake Turkana, Kenya in the past 15,000 years, and potential hydroclimate variability spanning the duration of the African Humid Period*

**Bloszies, CA**, & Forman, SL. Submitted. *Seasonal controls of equatorial sea surface temperatures on Lake Turkana water levels in the 20<sup>th</sup> and 21<sup>st</sup> centuries*. Journal of Hydrology

Forman, SL, Wright, DK, **Bloszies, CA**, Pierson, J.M., Mazzocco, J.G. Submitted. *Variations in water level for Lake Turkana in the past 8500 years near Mt. Porr, Kenya and the transition from the African Humid Period to Holocene aridity*. Quaternary Science Reviews.

### ABSTRACTS

**Bloszies, CA**, Forman, SL, Wright, DK; *Water level changes for Lake Turkana and climate variability during the African Humid Period*. Poster to be presented at the AGU Fall Meeting; 2013 Dec. 9-13; San Francisco, CA. (GC13A-1048)

**Bloszies, CA**, Forman, SL, Wright, DK; *Assessing Holocene water level changes of Lake Turkana, Kenya with potential linkages to monsoon variability*. Poster presented at the AGU Fall Meeting; 2012 Dec. 3-7; San Francisco, CA. (CAGC33A-1010)